

Doctorate Program in Molecular
Oncology and Endocrinology
Doctorate School in Molecular
Medicine

XXIV cycle - 2008–2011
Coordinator: Prof. Massimo Santoro

**“Role of Twist1 transcription
factor in thyroid tumor
progression”**

Tammaro Claudio Bencivenga

University of Naples Federico II
Dipartimento di Biologia e Patologia
Cellulare e Molecolare
“L. Califano”

Administrative Location

Dipartimento di Biologia e Patologia Cellulare e Molecolare
“L. Califano”
Università degli Studi di Napoli Federico II

Partner Institutions

Italian Institutions

Università degli Studi di Napoli “Federico II”, Naples, Italy
Istituto di Endocrinologia ed Oncologia Sperimentale “G. Salvatore”, CNR, Naples, Italy
Seconda Università di Napoli, Naples, Italy
Università degli Studi di Napoli “Parthenope”, Naples, Italy
Università degli Studi del Sannio, Benevento, Italy
Università degli Studi di Genova, Genova, Italy
Università degli Studi di Padova, Padova, Italy
Università degli Studi “Magna Graecia”, Catanzaro, Italy
Università degli Studi di Udine, Udine, Italy

Foreign Institutions

Université Libre de Bruxelles, Bruxelles, Belgium
Universidade Federal de Sao Paulo, Brazil
University of Turku, Turku, Finland
Université Paris Sud XI, Paris, France
University of Madras, Chennai, India
University Pavol Jozef Šafárik, Kosice, Slovakia
Universidad Autonoma de Madrid, Centro de Investigaciones Oncologicas (CNIO), Spain
Johns Hopkins School of Medicine, Baltimore, MD, USA
Johns Hopkins Krieger School of Arts and Sciences, Baltimore, MD, USA
National Institutes of Health, Bethesda, MD, USA
Ohio State University, Columbus, OH, USA
Albert Einstein College of Medicine of Yeshiva University, N.Y., USA

Supporting Institutions

Dipartimento di Biologia e Patologia Cellulare e Molecolare
“L. Califano”, Università degli Studi di Napoli “Federico II”,
Naples, Italy
Istituto di Endocrinologia ed Oncologia Sperimentale “G. Salvatore”, CNR, Naples, Italy
Istituto Superiore di Oncologia, Italy

Italian Faculty

Salvatore Maria Aloj	Paolo Emidio Macchia
Francesco Saverio	Barbara Majello
Ambesi Impiombato	Rosa Marina Melillo
Francesco Beguinot	Claudia Miele
Maria Teresa Berlingieri	Nunzia Montuori
Bernadette Biondi	Roberto Pacelli
Francesca Carlomagno	Giuseppe Palumbo
Gabriella Castoria	Silvio Parodi
Maria Domenica	Nicola Perrotti
Castellone	Maria Giovanna
Angela Celetti	Pierantoni
Lorenzo Chiariotti	Rosario Pivonello
Vincenzo Ciminale	Giuseppe Portella
Annamaria Cirafici	Giorgio Punzo
Annamaria Colao	Maria Fiammetta
Sabino De Placido	Romano
Gabriella De Vita	Antonio Rosato
Monica Fedele	Giuliana Salvatore
Pietro Formisano	Massimo Santoro
Alfredo Fusco	Giampaolo Tortora
Domenico Grieco	Donatella Tramontano
Michele Grieco	Giancarlo Troncione
Maddalena Illario	Giancarlo Vecchio,
Massimo Imbriaco	Giuseppe Viglietto
Paolo Laccetti	Mario Vitale
Antonio Leonardi	

**“Role of Twist1
transcription factor
in thyroid tumor
progression”**

TABLE OF CONTENTS

LIST OF PUBLICATIONS	3
ABBREVIATIONS.....	4
ABSTRACT.....	6
1. BACKGROUND	7
1.1 Thyroid tumors	7
1.1.1 Morphological and clinical features of thyroid tumors.....	7
1.1.2 Risk factors of thyroid carcinomas	8
1.1.3 Genetic alterations in thyroid carcinomas	9
1.2 The transcription factor Twist1	15
1.2.1 Structure of Twist1.....	15
1.2.2 The expression of Twist1 in normal tissues.....	18
1.2.3 Twist1 protein stability	20
1.2.4 Physiological functions of Twist1 protein.....	20
1.2.5 Overexpression of Twist1 in human cancers.....	21
1.2.6 Role of Twist1 in cancer cell survival, immortalization and acquired chemoresistance	22
2. AIMS OF THE STUDY	24
3. MATERIALS AND METHODS	25
3.1 Cell lines	25
3.2 Tissue samples	25
3.3 Immunohistochemistry	25
3.4 Reverse transcription and quantitative PCR	26
3.5 Protein studies	26
3.6 RNA silencing	26
3.7 Twist1 transfection	27
3.8 Cell viability measurement	27
3.9 Chemoinvasion Assay	27
3.10 Wound Healing Assay	28
3.11 Microarray Analysis	28
3.12 Statistical analysis.....	28
4. RESULTS	29
4.1 Up-regulation of Twist1 in ATC	29
4.2 Up-regulation of Twist1 in thyroid cancer cell lines	31
4.3 Knockdown of Twist1 induces apoptosis of ATC cells	31
4.4 Effects of stable silencing of Twist1 in CAL62 cells	33
4.5 Ectopic Twist1 promotes cell migration and invasion of PTC cells	34

4.6 Ectopic Twist1 protects PTC cells from apoptosis	35
4.7. Identification of Twist1 target genes	36
4.8 Expression of Twist1 target genes in CAL62 shTwist1 transfected cells	42
4.9 Silencing of Twist1 target genes in cells ectopically expressing Twist1 (TPC Twist1 mp 1)	44
4.10 Silencing of HS6ST2, ID4, PDZK1, PDZK1IP1 and TACSTD1 reduced cell viability in OCUT-2 cells	46
4.11 Silencing of genes HS6ST2, PDZK1, PDZK1IP1 and TACSTD1 reduced cell viability in CAL62 cells	48
5. DISCUSSION	48
6. CONCLUSIONS	54
7. ACKNOWLEDGEMENTS	55
8. REFERENCES	56

LIST OF PUBLICATIONS

This dissertation is based upon the following publications:

- I. **Bencivenga TC** *et al.* Identification of a set of genes that mediates Twist1 biological effects in thyroid carcinoma cell lines. Manuscript in preparation (main body of the dissertation).
- II. Salerno P, Garcia-Rostan G, Piccinin S, **Bencivenga TC**, Di Maro G, Doglioni C, Basolo F, Maestro R, Fusco A, Santoro M, Salvatore G. TWIST1 plays a pleiotropic role in determining the anaplastic thyroid cancer phenotype. *J Clin Endocrinol Metab.* 2011 May;96(5):E772-81.
- III. Salvatore G, Salerno P, Cirafici AM, **Bencivenga TC** *et al.* Cytostatic activity of monoclonal antibodies against RET tyrosine kinase receptor in medullary thyroid carcinoma cell lines. Manuscript in preparation.

ABBREVIATIONS

AKT	v-akt murine thymoma viral oncogene
ATC	anaplastic thyroid carcinoma
bHLH	basic helix-loop-helix
BRAF	B-type RAF
CBP	CREB-binding protein
CML	chronic myelogenous leukemia
CREB	cAMP-response element binding protein
CV-PTC	classic variant of papillary thyroid carcinoma
dNTPs	deoxyribonucleoside triphosphates
DMEM	Dulbecco's modified Eagle's medium
DMSO	dimethyl sulfoxide
EGFR	epidermal growth factor receptor
ERK	extracellular signal-regulated kinase
EMT	epithelial mesenchymal transition
FBS	fetal bovine serum
FDA	food and drug administration
FMTC	familial medullary thyroid carcinoma
FTC	follicular thyroid carcinoma
GDNF	glial-derived neurotrophic factor
GFR α	GDNF family receptor alpha
hIP	human prostacyclin receptor
mAb	monoclonal antibodies
MAPK	mitogen-activated protein kinase
MEN2	multiple endocrine neoplasia type 2
MTC	medullary thyroid carcinoma
NF-K β	nuclear factor-kappaB
NGF	nerve growth factor
NLS	nuclear localization signal
NT	normal thyroid
NTRK1	neurotrophic tyrosine kinase receptor type 1
PCAF	p300/CBP associated factor
PDC	poorly differentiated carcinoma
PI3KCA	phosphatidylinositol-3 kinase catalytic domain
PPAR γ	peroxisome proliferation activated receptor
PTC	papillary thyroid carcinoma
PTEN	phosphatase and tensin homolog
Rb	retinoblastoma
RET	rearranged during transfection
RPMI	Roswell Park Memorial Institute

SCS Saethre-Chotzen syndrome
siRNA small interference RNA
WDTC well differentiated thyroid carcinoma
WT wild type

ABSTRACT

Thyroid carcinomas are the most common endocrine tumors in humans, with a globally increasing incidence. Differentiated tumors, such as papillary (PTC) and follicular (FTC) thyroid cancers, are often curable with surgical resection and radiotherapy, whereas undifferentiated (anaplastic) thyroid carcinoma (ATC) is invariably lethal, due to the high invasiveness and insensitivity to radioiodine or chemotherapeutic treatment. Little is known about the molecular events that lead from the highly curable differentiated tumors to the very aggressive ATC. Through, a cDNA microarray analysis on different thyroid tumors we have isolated Twist1 as a gene upregulated in ATC. Twist1 is a highly conserved basic helix-loop-helix transcription factor that plays an important role in the development and progression of human cancer. Twist1 has been associated with epithelial-to-mesenchymal transition (EMT) a key step during embryonic morphogenesis and in the progression of primary tumors toward metastasis. In this dissertation, we have shown that approximately 50% of ATCs upregulate Twist1 with respect to normal thyroids as well as to poorly- and well-differentiated thyroid carcinomas. Knockdown of Twist1 by RNA interference in ATC cells reduced cell migration and invasion and increased sensitivity to apoptosis. The ectopic expression of Twist1 in thyroid cells induced resistance to apoptosis and increased cell migration and invasion. To understand the molecular mechanisms through which Twist1 exert is biological effects in thyroid cancer cells, we have performed a microarray analysis of thyroid cancer cells ectopically expressing Twist1 in comparison to vector control cells. We have identified a set of 20 genes involved in migration, invasion and apoptosis; expression levels of these genes changed upon Twist1 overexpression or knockdown. Silencing of 5 of the 20 target genes reduced viability of thyroid cancer cells overexpressing Twist1. Thus, our data suggest that Twist1 plays a key role in determining malignant features of the anaplastic phenotype and identifies a set of Twist1 target genes that could be used as molecular target for the therapy of ATC.

1. BACKGROUND

1.1 Thyroid tumors

1.1.1 Morphological and clinical features of thyroid tumors

Thyroid carcinoma accounts for about 1% of all human cancers. The incidence of thyroid cancer has been steadily increasing worldwide over the last few decades, predominantly due to the increased ability to detect small papillary carcinomas (Hodgson et al. 2004; Jemal et al. 2010).

Thyroid tumors represent an heterogeneous group of neoplasms with distinctive clinical and pathological features. It can originate from follicular cells (~ 95%) or from calcitonin-secreting C-cells (~ 5%). There are five major types of thyroid carcinoma divided in distinct classes: well-differentiated carcinomas, including papillary (PTC), follicular (FTC); poorly differentiated carcinomas (PDC); undifferentiated or anaplastic thyroid carcinoma (ATC) and medullary thyroid carcinoma (MTC). PTC and FTC account for about 80% and 10% of cases, respectively, PDC account for ~5%, ATC account for ~2% and MTC account for ~3% (DeLellis and Williams 2004; DeLellis 2006; Kondo et al. 2006). These tumors differ noticeably in aggressiveness, ranging from well differentiated to ATC.

PTC is characterized by a branching (papillary) architecture and peculiar nuclear features, several variants are known (DeLellis, 2006). PTC is more frequent in women than men and affects patients of 20-50 years old. PTC can also occur in childhood as consequence of accidental or therapeutic radiation exposure. PTC present an indolent behavior, tendency to form metastasis to local lymph nodes and survival rate greater than 90% (Schlumberger, 1998; Kondo et al. 2006). Sometimes the disease may show an aggressive behavior and lose the ability to concentrate radioiodine.

FTC is characterized by follicular cell differentiation in the absence of the diagnostic nuclear features of PTC. It mostly affects 40-60 years old patients with a female to male

ratio 3-4:1. Despite a higher frequency of distant haematogenous metastasis compared to PTC, most FTC patients can also be cured, with good long-term survival rate (Kondo et al. 2006).

PDC represent a small group of thyroid tumors. These tumors shows loss of structural and functional differentiation and, characteristically, show widely infiltrative growth, necrosis, vascular invasion and numerous mitotic figures (DeLellis, 2006; Pulcrano et al. 2007; Volante et al. 2007).

ATC is the most aggressive thyroid tumor, and it is described among the most lethal human malignancies, with a median survival from diagnosis of ~3-6 months (Perri et al. 2011). Despite accounting for only ~2 of all thyroid tumors, ATC is responsible for more than half of the deaths attributed to thyroid cancer. Clinically, these tumors usually present during the 6th to 7th decade of life as a rapidly enlarging neck mass that extends locally, compressing the adjacent structures and tends to disseminate both to regional nodes and to distant sites, including lung, pleura, bone and brain. Worse prognosis is associated with large tumor mass, distant metastases, and acute obstructive symptoms (Pierie et al. 2002, McIver et al. 2001). Current treatment of ATC has often only palliative purposes, particularly relief of airway compression, having little impact on patient's survival (De Crevoisier et al. 2004).

MTC derives from the neuroendocrine C-cells of the thyroid. Sporadic disease accounts for 80% of cases; the remainder 20% of patients inherit MTC in the context of autosomal dominant multiple endocrine neoplasia type 2 syndromes (MEN2A, MEN2B and FMTC). Sporadic MTC usually presents with palpable thyroid nodules in the 3rd-6th decades of life. Total thyroidectomy is recommended for MTC patients. Clinical recurrence in the neck or in mediastinum is a common problem for MTC patients (Leboulleux et al. 2004, Cote and Gagel 2003).

1.1.2 Risk factors of thyroid carcinomas

Thyroid neoplasms are related to several risk factors that influence the incidence and mortality, including geographical area, the inter-individual variability, reduced iodine uptake and hormonal factors.

Radiation exposure is an important exogenous risk

factor able to cause thyroid carcinoma. Indeed, after nuclear explosions of Hiroshima and Nagasaki and Chernobyl nuclear disaster, PTC frequency markedly increased in children exposed to radiations (Ciampi and Nikiforov 2005). It is still unclear whether this particular occurrence in children is because the thyroid is most susceptible to radiation-induced damage in childhood or because children were exposed to contaminated milk or both (Williams 2002). The radiation associated to PTC typically belong to the solid-follicular variant, and are frequently positive for chromosomal rearrangements involving the RET proto-oncogene, as well as being more aggressive than other cancers not linked to radiation exposure (Williams 2002).

Recently, Antico-Arciuch and co-workers revealed a role for estrogens using a transgenic model of thyroid carcinogenesis (Antico-Arciuch et al. 2010).

A deficient dietary intake of iodine can result in increased proliferation of thyroid cells in the goiter. The incidence of FTC in iodine-deficient areas is significantly increased (Kondo et al. 2006).

1.1.3 Genetic alterations in thyroid carcinomas

The genetic lesions associated to thyroid carcinomas can affect either proto-oncogenes (gain-of-function mutations) or tumor suppressor genes (loss-of-functions). These lesions are listed in Table 1.

Table 1: Genetic alterations in thyroid carcinomas.

Tumor Type	Cell Type	Molecular Lesion
PTC	Follicular cells	-RET/PTC rearrangements -NTRK1 rearrangements -BRAF point mutation
FTC	Follicular cells	-PAX8/PPAR γ rearrangements -RAS point mutation
PDC	Follicular cells	-RAS point mutation -PI3KCA point mutation or amplification
ATC	Follicular cells	-TP53 point mutation -BRAF point mutation -RAS point mutation -TP53 point mutation -CTNNB1 point mutation

Genetic alterations in PTC

Genetic alterations associated with PTC include chromosomal rearrangements targeting the RET or NTRK1 genes, and point mutations in the RAS or BRAF genes. Involved genes encode proteins that signal along the mitogen-activated protein kinase (MAPK) pathway, and the genetic alterations targeting them result in MAPK pathway activation.

The RET (Rearranged during Transfection) proto-oncogene is located on chromosome 10q11.2 and encodes for the tyrosine kinase receptor of growth factors belonging to the GDNF (Glial cell line-derived neurotrophic factor) family (Manié et al. 2001). Binding to the ligand in the presence of co-receptors of the GFR α (GDNF family receptors α) family causes RET dimerization and autophosphorylation of tyrosine residues within its intracellular domain. Phosphorylated tyrosines become binding sites for signaling molecules containing phosphotyrosine-binding motifs (Santoro et al. 2004). In the thyroid gland, RET is normally expressed at high levels in parafollicular C-cells, but not in follicular cells. By providing an active promoter, chromosomal rearrangements fusing the 3' kinase-encoding portion of the RET gene with the 5' portion of heterologous genes, enable thyroid expression of the chimeric RET/PTC oncoproteins (Fusco et al. 1987; Grieco et al. 1990). Moreover, fusion with partner genes encoding for proteins possessing protein-protein interaction motifs results in RET/PTC ligand-independent dimerization and autophosphorylation. Breakpoints in the RET gene leave an intact kinase domain, and 11 autophosphorylation sites are maintained in RET/PTC oncoproteins. Phosphorylated Y1062, RET/PTC is able to bind SHC and FRS2, which recruit Grb2-SOS complexes leading to the activation of the RAS-RAF-MAPK cascade (Asai et al. 1996). Through Y1062, RET is also able to activate the phosphatidylinositol 3-kinase (PI3K)/AKT pathway (Segouffin-Cariou and Billaud 2000; Pelicci et al. 2002; Frêche et al. 2005).

So far, at least 11 RET/PTC have been identified, formed by the RET fusion to different partners; RET/PTC1 and

RET/PTC3, resulting from fusion with the H4 (D10S170) (Grieco et al. 1990) and the RFG (NCOA4, ELE1 or ARA70) (Santoro et al. 1994; Borganzone et al. 1994) genes respectively, are the most prevalent variants. RET rearrangements are found in 20-40% of PTC, but the prevalence is significantly higher in patients with a history of accidental or therapeutic radiation exposure. RET/PTC1 is more frequently associated with classic PTCs and with the diffuse sclerosing variant; conversely, RET/PTC3 is more common in the solid variant and in PTC associated to ionizing radiations (Thomas et al. 1999). RET rearrangements appear to have a lower prevalence in the follicular variant compared to classic PTC. RET/PTC is able to induce transformation and dedifferentiation of cultured thyroid cells. RET/PTC-transgenics mice develop PTC, meaning RET/PTC oncogenes are able to initiate thyroid carcinogenesis (Powell et al. 1998). Moreover, RET/PTC is frequently detected in clinically silent papillary micro carcinomas, proving it can be an early event in thyroid tumorigenesis (Fusco et al. 2002).

Similar to RET, the NGF (Nerve Growth Factor) high affinity receptor NTRK1 (neurotrophic receptor-tyrosine kinase) gene may undergo oncogenic activation by chromosomal rearrangement. Such rearrangements are significantly less common in PTCs than the ones involving the RET gene (DeLellis 2006).

Activating point mutations in RAS, small GTPase, are quite uncommon in in the follicular variant of PTC (De Lellis 2006)

BRAF is a serine-threonine kinase belonging to the RAF family (ARAF, BRAF, CRAF) of intracellular effectors of the MAPK pathway (Davies et al. 2002). Recruitment to the cell surface and binding to RAS in its GTP- bound state triggers RAF activation, which in turn phosphorylates MEK, causing sequential activation of downstream effectors of the MAPK cascade. Among the RAF family members, BRAF appears to have the highest basal kinase activity and is the most potent activator of the MAPK pathway. Activating point mutations within the kinase domain of the BRAF gene have been found in several tumor types, including melanoma and colorectal cancer (Davies et al. 2002). A thymine to adenine substitution at nucleotide 1799 (T1799A), resulting in a substitution of a valine with a glutamic acid at residue 600 (V600E) of the protein, is the most common event; V600E and most other mutations within the kinase domain target either the activation loop or the ATP binding site (P loop). By disrupting the interactions between the activation loop and the P loop that hold the kinase in an inactive

conformation, these mutations cause BRAF constitutive activation. BRAF mutation represents the most common genetic event in PTC, occurring approximately in 45% of all cases (Xing 2007; Ciampi and Nikoiforov 2005). Virtually, all the mutations in these tumors are V600E; other rare mutations, like point mutation K601E, insertion V599Ins, and the inversion of chromosome 7q fusing the kinase domain encoding-region of the BRAF gene with the AKAP9 gene, have been described (Carta et al. 2006; Ciampi et al. 2005). BRAF mutations are highly prevalent in classic and tall-cell variant PTCs, but similar to RET rearrangements, they are rarely found in the follicular variant (Xing 2007), again underlining the association of different mutations with specific thyroid tumor subtypes. The presence of BRAF mutations has been found to correlate with aggressive tumor behavior, tumor recurrence, decreased radioiodine concentration ability, failure to treat recurrent disease. Furthermore, BRAF mutation proved to be able to predict tumor recurrence (Namba et al. 2003; Riesco-Eizaguirre et al. 2006; Lupi et al. 2007). Thyroid-specific BRAF V600E-transgenic mice develop papillary carcinomas that closely recapitulate the features of human PTC. These animals develop PTCs that not only share morphological features with their human counterpart, but also show characteristics of aggressive behavior and tendency towards progression to PDC. This suggests the involvement of BRAF mutation in PTC initiation and progression to PDC. Moreover, BRAF (V600E) mutation has been found in very early stages of PTC (Ugolini et al. 2007), further supporting its role in the initiation of these tumors.

Overall, genetic events involving RET, NTRK1, BRAF or RAS are found in the vast majority of PTC cases and rarely overlap in the same tumor (Kimura et al. 2003; Soares et al. 2003; Frattini et al. 2004), underlining the importance of MAPK pathway signaling-abnormalities in the pathogenesis of PTC.

Finally, point mutation or gene amplification of PI3KCA have been reported in a small fraction of PTC (Wu et al. 2005).

Genetic alterations in FTC

FTC may develop through at least two different pathways, involving either RAS or the peroxisome proliferation-activated receptor (PPAR) γ 1. RAS point mutations are detected in about 50% of follicular carcinomas. Another subset of FTC

(~30%) harbor the t(2:3)(q12-13;p24-25) chromosomal translocation, which causes the fusion of the region encoding the DNA binding domains of the thyroid transcription factor PAX8 to the one encoding domains A-F of PPAR γ steroid-hormone receptor; the resultant fusion protein displays dominant-negative activity on wild-type PPAR γ (Kroll et al. 2000). As in PTC, point mutation or gene amplification of PI3KCA have been reported in some FTC cases (Wu et al. 2005).

Genetic alterations in PDC

PDC share genetic lesions in common with well-differentiated carcinoma, consistent with the hypothesis of a multi-step model of thyroid carcinogenesis (Tallini 2002; Nikiforov, 2004). PDC are characterized by point mutations in RAS (Garcia-Rostan et al. 2005; Volante et al. 2007), amplification or point mutation in PI3KCA (Garcia-Rostan et al. 2005). Moreover a significant fraction of PDC show point mutations of TP53 (Nikiforov 2004; Kondo et al. 2006). About 30% of PDC harbor the V600E BRAF mutation, particularly those samples with morphological evidence of pre-existing PTC (Begum et al. 2004). Point mutations in exon 3 of CTNNB1 have been reported in PDC and more frequently in ATC, but not in well-differentiated (Garcia-Rostan et al. 2001), suggesting that they might play a direct role in the dedifferentiation and progression to ATC.

Genetic alterations in ATC

ATC may derive *de novo* or from pre-existing PTC or FTC. A small number of gene mutations have been identified, and there appears to be a progression in mutations acquired during dedifferentiation. Several mutations occurring in PTC (RAS and BRAF) are also seen in ATC, suggesting these are early events (Nikiforov 2004). Frequencies of RAS range from 6% to 50% of cases. Mutation of BRAF is highly variable in ATC, reaching up to 25%. When ATCs with a papillary component were examined, BRAF mutation was observed in both the differentiated and undifferentiated regions (Costa et al. 2008; Begum et al. 2004; Takano et al. 2007).

Late mutations include TP53, β -catenin 1 and PIK3CA, suggesting that one or more of these mutations

contribute to the extremely aggressive behavior of ATC (Santarpia et al. 2008; Hou et al. 2007). Mutations of TP53 occur in more than 70% of ATCs (Salvatore et al. 2007). By contrast, the RET/PTC rearrangements and the PAX8/PPAR γ fusion protein detected in well-differentiated, are not observed in ATCs (Nikiforov 2004). The β -catenin 1 is involved in WNT signaling and cell-adhesion. The mutation and abnormal nuclear localization of this protein was seen in malignancies. This cytoplasmic protein, encoded by the CTNNB1 gene, plays an important role in E-cadherin mediated cell-cell adhesion. In thyroid tumors, point mutations in exon 3 of CTNNB1 have been reported in ATC (Garcia Rostan et al. 1999). This mutation was detected in many ATC cases, from 50% to 60% (with nuclear localization in half with mutations), while abnormalities were detected also in poorly differentiated, in ~30% of cases (Garcia Rostan et al. 2001; Miyake et al. 2001). PIK3CA was mutated in 15-39% of ATC cases and copy gains occur in 38-61%. AKT1 was activated in most ATC cases (85-93%) (Hou et al. 2007; Liu et al. 2008; Santarpia et al. 2008), PTEN, (phosphatase and tensin homology encoding chromosome 10), negatively regulates the PI3K pathway and was found mutated in ~30% of ATC cases (Santarpia et al. 2008) (Table 1).

Genetic alterations in MTC

As previously mentioned, MTC can occur either sporadically or in the context of autosomal dominant MEN 2 syndromes (MEN 2A, MEN 2B and FMTC) (Mani \acute{e} et al. 2001). MEN 2 are caused by germ line point mutations that convert RET into a dominant oncogene. In all MEN2A cases, mutations target extracellular cysteine residues in RET. In more than 80% of the cases, MEN 2B is caused by the Met 918 Thr intracellular substitution in the P+1 loop of the kinase. FMTC (Familial Medullary Thyroid Carcinoma) is caused by mutations in the RET extracellular or kinase domains. Roughly 40% of sporadic MTC cases harbor similar point mutations in RET.

In the last years our laboratory has been launched a program to develop RET-directed targeted therapy for thyroid cancer. Thus, we generated roughly 50 monoclonal antibodies (mAbs) against the extracellular domain of RET and tested their therapeutic potential in MTC cell lines (attached manuscript III in preparation).

1.2 The transcription factor Twist1

1.2.1 Structure of Twist1

Little is known about the molecular events that lead from the highly curable differentiated tumors to the very aggressive ATC. Through, a cDNA microarray analysis on different thyroid tumors we have isolated Twist1 transcription factor as a gene upregulated in ATC (Salvatore et al. 2007).

Human Twist1 gene is mapped to 7q21.2 and contains two exons and one intron (Wang et al. 1997). The first exon contains an ATG site followed by an open reading frame encoding 202 amino-acid residues. The open reading frame is followed by a 45-bp untranslated portion in exon 1, a 536-bp intron and a second untranslated exon with two potential polyadenylation sites that are 65 and 415 bp from the 5' end of exon 2. The molecular mass calculated from the amino-acid sequence of human Twist1 is approximately 21 kDa, with a theoretical isoelectric point of ~9.6. The protein contains relatively more polar amino-acid residues in the region close to the NH₂-terminus and more non-polar residues at the COOH-terminus where the bHLH domain is located.

The Twist1 gene belongs to the family of basic helix-loop-helix (bHLH) transcription factors (Thisse et al. 1987). bHLH proteins are structurally and functionally characterized by a conserved domain containing a stretch of basic amino-acids adjacent to two amphipathic α -helices separated by an interhelical loop. The α -helices mediate dimerization with a second bHLH factor, leading to the formation of a bipartite DNA-binding domain that specifically binds to hexanucleotide sequences (CANNTG), known as E-boxes (Figure 1). The E-boxes are found in the regulatory elements of many lineage-specific genes. Consistently, bHLH are transcription factors acting in various differentiation processes, and play key roles in different developmental events like neurogenesis and myogenesis.

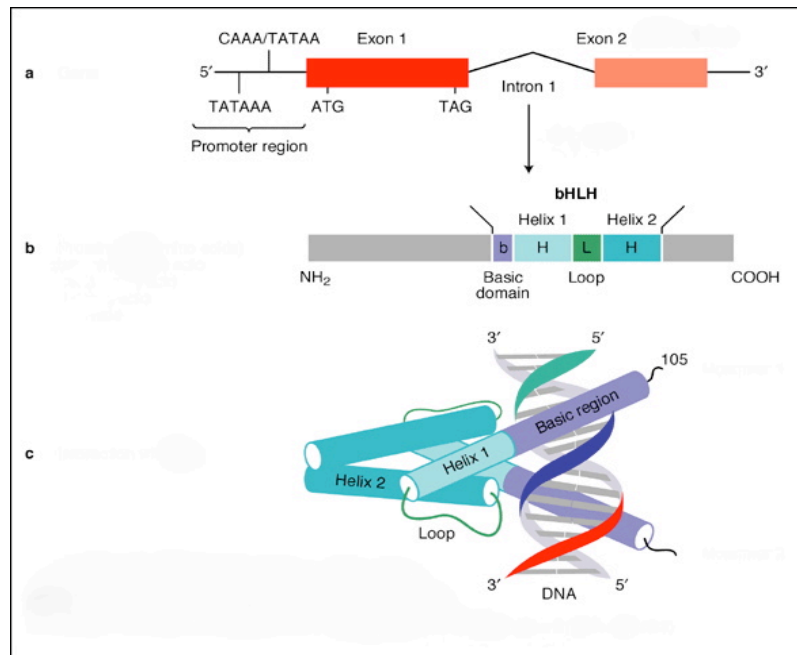


Figure 1. Structure and function of human-Twist1. a) The gene encoding human-Twist1 comprises two exons separated by a unique intron. b) The human-Twist1 protein is 202 amino acids with a basic helix-loop-helix (bHLH) domain. c) Interaction of Twist1 with DNA acting as dimers. (modified from Bonaventure and El Ghouzzi 2003).

The bHLH domains of Twist1 show a very high degree of conservation among a broad range of species, including human, mouse, frog, *Drosophila*, leech and *Caenorhabditis elegans*. The C-terminal part of the proteins comprises the WR motif also called “Twist box” (Spring et al. 2000; Bialek et al. 2004). The WR motif is located between 20 and 55 amino acids COOH terminal to the bHLH region, is highly conserved among vertebrates; the amino-acid sequences in this domain show 100% homology among human, mouse and *Xenopus* Twist1. The function of this WR region is unclear, it is postulated to be required for Twist1 protein folding and activity (Gripp et al. 2000).

Twist1 functions as a transcription factor in the cell nucleus. There are two nuclear localization signal (NLS) sequences, ³⁷RKRR⁴⁰ and ⁷³KRGKK⁷⁷, in the human Twist1 protein. Furthermore, the N-terminus of Twist1 can interact with p300, cAMP-response element binding protein (CREB), CREB-binding protein (CBP) and p300/CBP associated factor (PCAF),

resulting in inhibition of the acetyl transferase activities of these histone remodeling enzymes (Hamamori et al. 1999). Since histone acetylation is usually coupled with transcriptional activation, the inhibition of p300, CBP and PCAF activities by Twist1 should repress gene expressions mediated by transcription factors that recruit these histone acetyltransferases.

The C-terminus of Twist1 interacts with the DNA-binding domain of Runx2 to repress Runx2 function (Bialek et al. 2004). Runx2 is a necessary transcription factor for osteoblast differentiation. These findings suggest that Twist1 not only serves as a transcription factor to directly regulate its target genes, but also regulates other transcription factor/coregulator-mediated gene expression through interaction with other transcriptional regulators (Figure 2).

In addition, Twist1 protein directly interact with several other transcription factors, including MyoD, MEF2, RUNX1, PGC1- α , p53 and NF- κ B and inhibit their activities (Sosic et al. 2003; Bialek et al. 2004; Sharabi et al. 2008; Shiota et al. 2008; Pan et al. 2009).

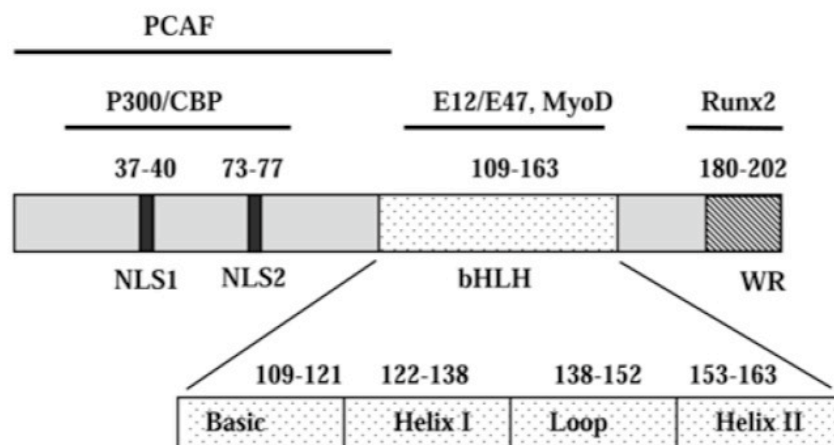


Figure 2. Molecular structure of the human Twist1 protein. The number of amino-acid residues for each structural domain is indicated. The regions that interact with other proteins are also indicated by solid lines. NLS1 and NLS2, nuclear localization signal sequences 1 and 2; bHLH, basic helix-loop-helix domain; WR, the tryptophan and arginine motif; CBP, cAMP-response element binding protein (CREB)-binding protein; PCAF, p300/CBP-associated factor, Runx2, Runt-related transcription factor.

Two Twist genes exist in vertebrates, Twist1 (Twist) and Twist2 (formerly known as *Dermo-1*). The human Twist2 protein contains 160 amino-acid residues and it shares 68% homology with human Twist1. The amino-acid sequences of their bHLH and Twist box domains are almost identical, which provides a structural base for their partially redundant biological functions. Indeed Twist proteins display more than 90% identity in the bHLH and carboxy-terminal domains. The N-terminal of Twist1 and Twist2 are more divergent, and Twist2 lacks a glycine-rich region that is present in Twist1 (Li et al. 1995) (Figure 3).

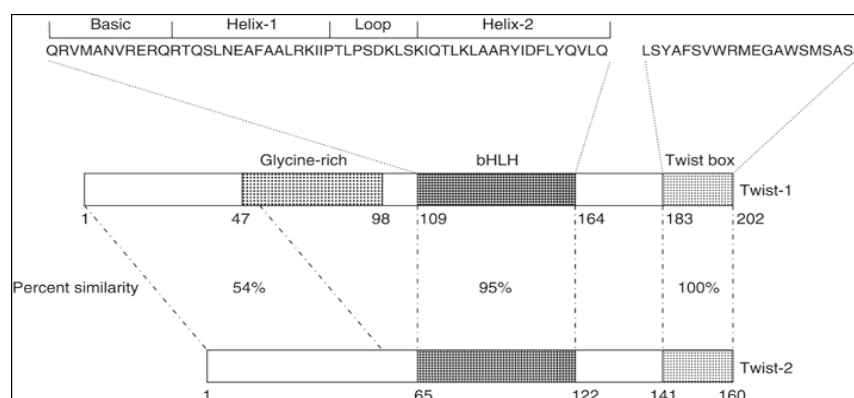


Figure 3. Functional domains of human Twist1 and Twist 2 proteins. The glycine-rich region is specific of Twist 1 (modified from Puisieux et al. 2006).

1.2.2 The expression of Twist1 in normal tissues

Twist1 expression was originally restricted to mesodermal-derived tissues, including: placenta, heart and skeletal muscles, presumably in precursor cells (Wang et al. 2004). While, Twist2 was additionally found to be expressed in granulocyte-macrophage progenitors, preventing their proliferation and differentiation into macrophages, neutrophils and basophils (Sharabi et al. 2008).

During *Drosophila* embryogenesis, Twist1 accumulates at early stages (from the beginning of cellular blastoderm to germ band extension) in all cells of the presumptive mesodermal

layer, but its expression decreases to relatively low levels in the mesodermal layer cells during later stages. This expression pattern is consistent with the critical roles of this zygotic gene in early embryogenesis.

During mouse embryogenesis, Twist1 transcripts are first seen at embryonic day 7.5 (E7.5) in the anterior lateral mesoderm underlying the head folds (Fuchtbauer et al. 1995), in the primitive streak epiblast, and in scattered cells in the amniotic cavity (Stoetzel et al. 1995). Then, Twist1 is predominantly and sequentially expressed in the somites, the neural crest derived head mesenchyme, the first aortic arches, the lateral mesoderm, the second, third and fourth branchial arches, the anterior limb buds, and finally, the posterior limb buds (Wolf et al. 1991; Fuchtbauer 1995; Gitelman 1997). A general tendency is that Twist1 expression in the mouse embryo occurs first along a dorsoventral gradient pattern until the headfold stage, and then moves along the rostro-caudal axis of the embryos as mesoderm cell layer- and neural crest cell-derived tissues develop.

After birth, Twist1 is expressed in the adult stem cells of the mesenchyme (Figeac et al. 2007; Zhao and Hoffman 2004). Twist1 mRNA has also been detected in primary osteoblastic cells derived from newborn mouse calvariae (Murray et al. 1992) and in mouse brown and white adipocytes (Pan et al. 2009; Pettersson et al. 2011).

While the expression patterns of Twist1 during embryonic development of *Drosophila* and mouse have been well studied, information regarding the expression profile of Twist1 during human embryogenesis is lacking. Twist1 mRNA expression pattern was examined in various adult human tissues, as well as several cell lines originated from different normal human tissues (Wang et al. 1997). Among the human tissues analyzed, the strongest signals for Twist1 mRNA were observed in the placenta, a tissue containing a large fetal portion and a small maternal portion. In particular, strong Twist1 signals were seen in the fetal portion of the placenta developed from the chorionic sac, which is mostly derived from the mesoderm. Intermediate strength signals were seen in the adult heart and skeletal muscle, which are also mostly derived from the mesoderm. Weak signals were found in the kidney and pancreas, while no signals were observed in the ectoderm-derived cells in the brain and endoderm-derived cells in the lung and liver. Additionally, Twist1 expression is also observed in human white adipocytes (Pettersson et al. 2011). Twist1 expression was not observed in human epithelial cells, although

its mRNA was detected in both fetal and adult human skin fibroblasts (Wang et al. 1997).

1.2.3 Twist1 protein stability

Regulation of protein stability is an important way to control Twist1 function. Recently, it was reported that Twist1 protein stability is largely regulated by mitogen-activated protein kinase (MAPK)-mediated phosphorylation on S68. The S68 in Twist1 can be phosphorylated by p38, JNK and ERK1/2 MAPKs, and this phosphorylation prevents Twist1 protein from ubiquitination-mediated degradation (Hong et al. 2011). Accordingly, activation of MAPKs by an active RAS protein or TGF β treatment significantly increases S68 phosphorylation and Twist1 protein levels without altering Twist1 mRNA expression, while blocking of MAPK activities by either specific inhibitors or dominant negative inhibitory mutants effectively reduces both S68 phosphorylation and Twist1 protein levels (Hong et al. 2011).

1.2.4 Physiological functions of Twist1 protein

Twist1, identified originally in *Drosophila* as a zygotic developmental gene, is considered crucial for the establishment of the ventral furrow, a prerequisite for the development of all mesoderm-derived internal organs (Thisse et al. 1987).

In mice Twist1^{-/-} have normal gastrulation but die at E10.5-11 displaying severe defects in closure of the cephalic neural tube, deficient cranial mesoderm, malformed branchial arches and facial primordium and retarded limb bud development (El Ghouzzi et al. 1997). Consistently, germ line mutations of the coding sequences of Twist1 gene, leading to haploinsufficiency, have been identified in Saethre-Chotzen syndrome (SCS), an human hereditary disorder transmitted as an autosomal dominant trait and characterized by abnormalities of the limbs, asymmetric head and face, and premature fusion of cranial sutures. Twist1^{-/-} mice also present a significant increase in apoptotic cells, especially in the developing sclerotome (Chen and Behringer 1995). This cell death could reflect Twist1 anti-

apoptotic properties as Twist1 protein also behave as key regulators of the p53 oncosuppressive protein and as major effectors of the NF- κ B survival pathway (Puiseux et al. 2006; Doreau et al. 2009). Heterozygosis for Twist1 null mutation results in a moderate phenotype including minor skull and limb abnormalities. Instead, Twist2^{-/-} do not present abnormalities of embryogenesis but show high levels of inflammatory cytokines with high perinatal mortality (Sosic et al. 2003).

1.2.5 Overexpression of Twist1 in human cancers

In addition to its essential role in modulating mesenchymal tissues critical for organogenesis, Twist1 is also expressed in and associated with many types of aggressive tumors, including breast cancer (Yang et al. 2004), hepatocellular carcinoma (Lee et al. 2006; Yang et al. 2009), prostate cancer (Yuen et al. 2007), esophageal squamous cell carcinoma, bladder cancer (Zhang et al. 2007; Wallerand et al. 2009) and pancreatic cancer.

Twist1 plays multiple roles in cancer initiation, progression and metastasis. Importantly, Twist1 has been identified as a master regulator of Epithelial-Mesenchymal Transition (EMT) the process in which adherent epithelial cells lose their epithelial characteristics and acquire mesenchymal properties (Ansieau et al. 2010). EMT is a critical mechanism of migration and invasion during development and in the case of cancer cells is a mechanism of increased invasion, metastasis, and resistance to chemotherapy. Recent studies have linked EMT with acquisition of stem-cell characteristics. Typical features of EMT are loss of expression of epithelial markers, mainly E-cadherin, with gain of mesenchymal markers such as Vimentin and sm-actin. E-cadherin, encoded by the CDH1 gene, is generally defined as a guardian of the epithelial phenotype and loss of its expression is associated with tumor invasiveness, metastatic dissemination and poor patient prognosis (Umbas et al. 1994). Repression of CDH1 gene by Twist1 is either direct (Vesuna et al. 2008) or mediated by SNAI1 (Smit et al. 2009). Together with Twist1 other transcription factors are capable, on its own, of inducing an EMT. These transcription factors include Twist2, Goosecoid, Hoxb7, Snai1 (Snail), Snai2 (Slug), Foxc1, Foxc2, Zeb1 and Zeb2 (Sip1). In addition, members of the miR-200 family of micro RNAs are down regulated during an EMT (Kalluri 2009).

Some microRNAs may be involved in mediating cancer metastasis. The microRNA-10b (miR-10b) is highly expressed in metastatic breast cancer cells, and it positively regulates cell migration and invasion (Ma et al. 2007). The miR-10b transcription is directly regulated by Twist1, and miR-10b in turn inhibits translation of the mRNA encoding homeobox D10, resulting in increased expression of the pro-metastatic gene RhoC. Moreover, the level of miR-10b expression in primary breast carcinomas is associated with clinical cancer progression. These findings suggest that Twist1 indirectly upregulates RhoC expression to increase breast cancer, cell invasion and metastasis.

1.2.6 Role of Twist1 in cancer cell survival, immortalization and acquired chemoresistance

Oncogenic mutations usually induce p53 and/or retinoblastoma (Rb) expression and result in cell apoptosis or senescence, which is a defensive barrier against cell transformation and tumor progression. Thus, tumorigenesis needs to protect cells from apoptosis or immortalize cells from senescence. Interestingly, both Twist1 and Twist2 were shown to inhibit oncogene-induced and p53- dependent cell death (Ansieau et al. 2008). Further analysis revealed that Twist1 might affect p53 indirectly through inhibition of ARF expression to modulate the ARF/MDM2/p53 pathway (Maestro et al. 1999). Twist1 promote chromosomal instability and consequently tumor progression. Accordingly ectopic expression of Twist1 in the MCF7 breast cell line induces chromosomal instability and frequencies of chromosomal amplifications are significantly higher in Twist1 -expressing breast carcinomas (Mironchik et al. 2005).

Twist1 also plays a role in the acquired resistance of cancer cells to chemotherapy. Twist1 upregulation is associated with cellular resistance to taxol and vincristine, two microtubule-targeting anticancer drugs in nasopharyngeal, bladder, ovarian, and prostate cancers (Wang et al. 2004) On the other hand, the chemotherapy-induced cancer cell apoptosis is counter-regulated by a subset of NF- κ B regulated genes. Twist1 is one of the major targets of NF- κ B responsible for antagonizing chemotherapy-induced apoptosis, suggesting an important role of Twist1 in NF- κ B-mediated cell survival and chemoresistance (Pham et al. 2007).

Multiple lines of evidence have demonstrated a link between Twist1-induced EMT and stem-like cells. It was demonstrated that induction of EMT by expressing Twist1 or Snail in mammary epithelial cells increases stem-like cell population with high CD44 and low CD24 expression, while isolated mammary epithelial stem-like cells express endogenous EMT-inducing factors including Twist1, Snail, SIP1, Slug and FOXC2, and EMT marker genes (Mani et al. 2008).

2. AIMS OF THE STUDY

The aim of this study was to analyze the role of Twist1 transcription factor in thyroid cancer progression. The specific aims were as follow:

1. Study the expression of Twist1 in normal human thyroids, PTC, PDC and ATC samples by quantitative RT-PCR and immunohistochemistry.
2. Study the functional consequences of Twist1 knockdown (in endogenously overexpressing cells) and of ectopic expression (in negative cells) on cell growth, survival, migration and invasion.
3. Identify a transcriptional profile of genes that mediates Twist1 biological effects in thyroid cancer cells.

3. MATERIALS AND METHODS

3.1 Cell lines

Normal thyroid primary S11N and P5 4N cells were grown in RPMI (Roswell Park Memorial Institute) supplemented with 20% FBS (Fetal Bovine Serum), L-glutamine and penicillin/streptomycin. Human papillary (TPC-1, BCPAP and NIM) and anaplastic (8505C, CAL62, OCUT-2) thyroid cancer cell lines were grown in DMEM (Dulbecco's Modified Eagle Medium), supplemented with 10% FBS, L-glutamine and penicillin/streptomycin. All the cells were SNP genotyped to ensure correct identity. The Fischer rat-derived differentiated thyroid follicular cell line PC Cl 3 (here after named "PC") and PC adoptively expressing several oncogenes (PC RET/PTC1, PC RET/PTC3, PC v-HRAS, PC-BRAF-V600E, PC-TRK-T1, PC v-RAF, PC v-MOS, PC E1A and PC E1A-v-RAF) have been cultured as described in the attached manuscript II.

3.2 Tissue samples

Tumors and normal thyroid tissue samples for immunohistochemical analysis were retrieved from the files of the Pathology Department of the Hospital Central de Asturias (Oviedo University, Asturias, Spain) and of the Hospital Clinico Universitario de Santiago de Compostela (Santiago de Compostela University, Galicia, Spain). Tumors and normal thyroid tissue samples for RNA extraction and Q-RT-PCR were retrieved from the files of the Department of Surgery, University of Pisa (Italy). Detailed of the histological diagnosis is described in the attached manuscript II.

3.3 Immunohistochemistry

The experimental procedure is discussed in detail in the attached publication II. A brief description is provided here. Slides of tumor sections deparaffinized were incubated with mouse monoclonal antibody against Twist1 (sc-81417, Santa

Cruz Biotechnology, USA) and processed according to standard procedures. Cases were scored as positive when unequivocal brown staining was observed in the nuclei of tumor cells. Immunoreactivity was expressed as the percentage of positively stained target cells in four intensity categories [-, no staining; +, low/weak; ++ moderate/distinct; +++, high/ intense].

3.4 Reverse transcription and quantitative PCR

Total RNA was isolated with the RNeasy Kit (Qiagen, Crawley, West Sussex, UK). The quality and concentration of the RNA was verified by the NanoDrop 2005 (Thermo Scientific). One μg of total RNA from each sample was reverse-transcribed with the QuantiTect [®] Reverse Transcription (Qiagen) according to manufacturer's instructions. The expression level of each gene was measured by quantitative PCR assay, using the Universal ProbeLibrary Set, Human (Roche). PCR reactions were performed in triplicate and fold changes were calculated with the formula: $2^{(\text{sample 1 } \Delta\text{Ct} - \text{sample 2 } \Delta\text{Ct})}$, where ΔCt is the difference between the amplification fluorescent thresholds of the mRNA of interest and the mRNA of RNA polymerase 2 used as an internal reference.

3.5 Protein studies

Immunoblotting was carried out according to standard procedures. Anti- α -Twist1 (sc-81417) monoclonal antibody was from Santa Cruz Biotechnology and anti- α -tubulin antibody was from Sigma-Aldrich. Secondary anti-mouse and anti-rabbit antibodies coupled to horseradish peroxidase were from Santa Cruz Biotechnology.

3.6 RNA silencing

The procedure to silence Twist1 is described in detail in the attached manuscript II.

To silence Twist1 target genes (i.e. HS6ST2, ID4, PDZK1, PDZK1IP1 and TACSTD1), the TPC-1 Twist1 mp or the

OCUT-2 or the CAL62 cells were transfected with the specific siRNA (Qiagen) in 6-well plate in triplicate. For each transfection, 5 μ l of 100 micromolar siRNA (25 nM) were mixed with 20 μ l of HyPerfect Transfection reagent (Qiagen) and 300 μ l of Optimem medium (Invitrogen). Following 10 minutes of incubation, the transfection mix was delivered to each well and incubated at 37°C for 72 hours.

3.7 Twist1 transfection

To generate a cell line stably expressing Twist1 we used TPC-1 cells in which we transfected the vector pcDNA 3-Twist1 (described in Demontis et al. 2006). Protocol procedure is detailed in attached manuscript II.

To generate stable shTwist1-expressing cell line, CAL62 cells were transfected with shTwist1 and shLUC vectors by using the Lipofectamine Reagent (Invitrogen) according to the instructions of the manufacturer. Protocol procedure is detailed in attached manuscript II.

3.8 Cell viability measurement

Cells were collected by trypsinization, stained for 10 minutes with 0.4% trypan-blue (Sigma) according to manufacturer's instructions, and counted in triplicate.

3.9 Chemoinvasion Assay

Cell invasion was examined using a reconstituted extracellular matrix (Matrigel, BD Biosciences, San Jose, CA). The cell suspension (1×10^5 cells per well) was added to the upper chamber of trans well cell culture chambers on a prehydrated polycarbonate membrane filter of 8 μ m pore size (Costar, Cambridge, MA) coated with 35 μ g of Matrigel (BD Biosciences). The lower chamber was filled with 2.5% medium. After 12 hours incubation at 37°C, non migrating cells on the upper side of the filter were wiped-off. Invading cells were mounted on glass slides using mounting medium and stained with Hoechst (Sigma). Cell migration was quantified by

counting the number of stained nuclei in five individual fields in each Transwell membrane, by fluorescence microscopy, in triplicate.

3.10 Wound Healing Assay

A wound was induced on the confluent monolayer cells by scraping a gap using a micropipette tip. Photographs were taken at 10 X magnification using phase-contrast microscopy immediately after wound incision and 24 hours later. Pixel densities in the wound areas was measured using the Cell^a software (Olympus Biosystem Gmb) and expressed as percentage of wound closure where 100 % is the value obtained at 10 hours for control cells.

3.11 Microarray Analysis

10 μ g purified total RNA from 3 Twist1 TPC-1 transfectants (Twist1 mp1, Twist1 mp2, Twist1 Cl2) and pcDNA mp2 control was transcribed into cDNA using Superscript RT (Invitrogen), in the presence of T7-oligo (dT) 24 primer, deoxyribonucleoside triphosphates (dNTPs), and T7 RNA polymerase promoter (Invitrogen). An *in vitro* transcription reaction was then performed to generate biotinylated cRNA which, after fragmentation, was used in a hybridization assay on Affymetrix U133 plus 2.0 GeneChip microarrays, according to manufacturer's protocol (GeneChip 3' ivt Express Kit, Affymetrix). Normalization was performed by global scaling and analysis of differential expression was performed by Microarray Suite software 5.0 (Affymetrix). The final results were imported into Microsoft Excel (Microsoft).

3.12 Statistical analysis

Statistical analyses were carried out using the GraphPad InStat software program (version 3.06.3, San Diego, CA). All *p* values were two-sided and differences were significant when *p* < 0.05.

4. RESULTS

4.1 Up-regulation of Twist1 in ATC

We evaluated Twist1 expression levels by immunohistochemistry in 157 human tissues including: 15 normal thyroids (NT), 13 PTC, 88 PDC, and 41 ATC samples. The data are detailed in the attached manuscript II. Twist1 was virtually undetectable in NT, PTC, and PDC samples. In contrast, 49% of the ATC samples were positive for Twist1 expression (Figure 4).

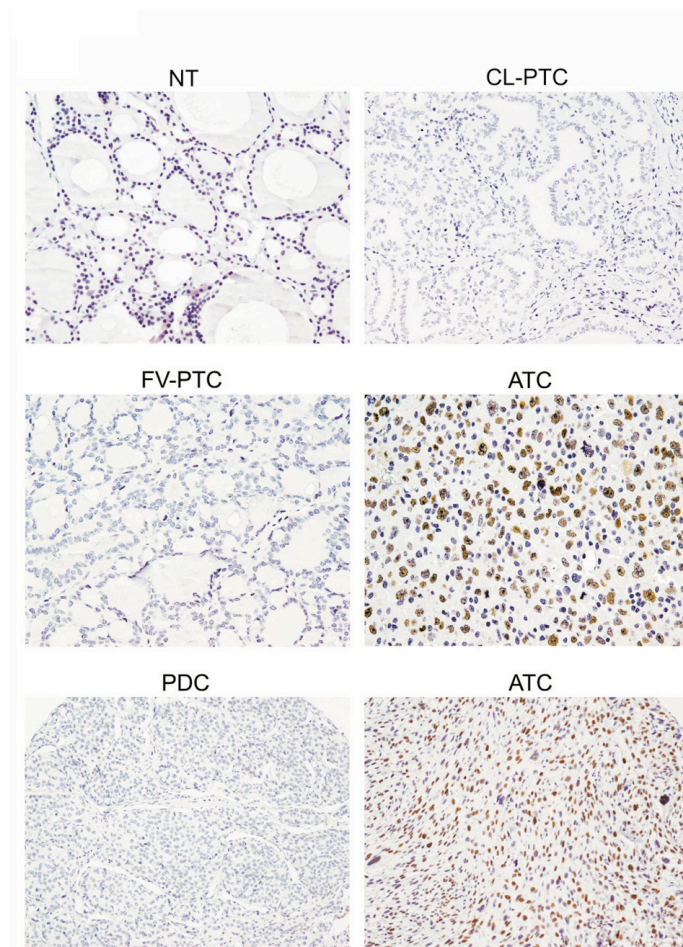


Figure 4. Immunohistochemical analysis of Twist1 protein expression in normal and malignant thyroid tissues. Representative histological sections from NT, classical PTC, follicular variant PTC, PDC, and ATC stained with a mouse monoclonal anti-Twist1 antibody are shown.

Twist1 positivity correlated with moderate/high proliferation rate assessed by Ki67/MIB1 immunoreactivity. Twist1 expression correlated with the fusocellular ATC phenotype and inversely correlated with the epithelioid ATC phenotype, suggesting that Twist1 is involved in mesenchymal transition of ATC cells. Accordingly, there was a trend toward a correlation between Twist1 upregulation and lack of β -catenin staining at the plasma membrane (data not shown).

To determine whether Twist1 up-regulation also occurred at the RNA level, we examined an independent set of ATC, PDC, PTC, and NT samples by quantitative RT-PCR. Twist1 mRNA was up-regulated by more than 5-fold in about 50% of the ATC samples (data are described in detail in the attached manuscript II). NT, PTC, and PDC samples express lower Twist1 levels compared with ATC (Figure 5).

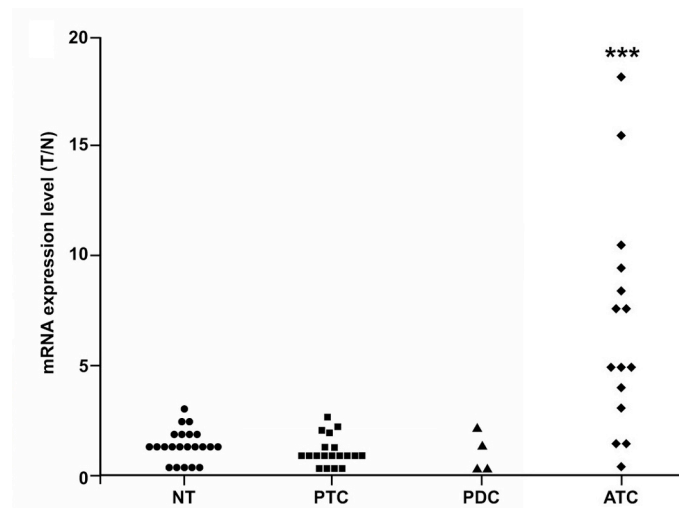


Figure 5. Quantitative RT-PCR of Twist1 mRNA in NT, PDC and ATC snap-frozen tissue samples. The level of Twist1 expression in each sample was measured by comparing its fluorescence threshold with the average fluorescence threshold of the NT samples.

Furthermore, we measured Twist2 expression by quantitative RT-PCR in thyroid tissue samples. Twist2 was overexpressed in some cases, but at a lower extent with respect to Twist1. No PTC sample up-regulate Twist2 (data are shown in the supplemental information of the attached manuscript II).

4.2 Up-regulation of Twist1 in thyroid cancer cell lines

We analyzed Twist1 expression in cultured human thyroid cells. To this aim, we used primary cultures of normal follicular cells (P5 4N and S11N) and a panel of PTC (TPC-1, NIM, BCPAP) and ATC (ACT-1, OCUT-2, 8505C, SW1736, CAL62) cell lines. Western blot analysis showed up-regulation of a band at approximately 26 kDa, which corresponded to the Twist1 protein only in the ATC cell lines OCUT-2, 8505C, and CAL62 (Figure 6). Twist1 expression was lower in the other ATC cells and in all the PTC cell lines analyzed, whereas it was undetectable in normal cells.

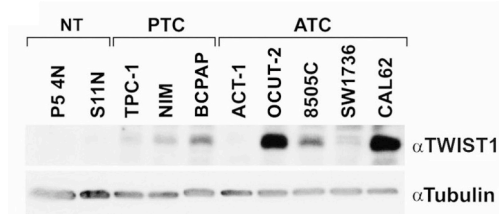


Figure 6. NT follicular cells (P5 4N and S11N), PTC (TPC-1, NIM, and BCPAP), and ATC (ACT- 1, OCUT-2, 8505C, SW1736, and CAL62) cell lines were analyzed by immunoblot using a mouse monoclonal anti-Twist1 antibody. Anti α -tubulin monoclonal antibody was used as a control for equal protein loading.

4.3 Knockdown of Twist1 induces apoptosis of ATC cells

We evaluated the effects of Twist1 ablation in ATC cells by RNA interference. We initially tested, by Western blot

in CAL62 cells, the efficiency of Twist1 ablation using three different siRNA (# 3, 5, and 7). Twist1 siRNA 3 (hereafter named Twist1 siRNA) reduced Twist1 protein levels of about 60% and therefore was selected for further experiments (data are shown in the supplemental information of the attached manuscript II). Then, we knocked down Twist1 by transient siRNA Twist1 transfection in CAL62, 8505C, and OCUT-2 cells. The Twist1 siRNA silenced the Twist1 protein starting at 24 h after transfection, and the effect lasted up to 72 h, whereas a scrambled siRNA control had no effect (the data are shown in attached manuscript II). At 48 and 72 h, siRNA Twist1 induced apoptosis of CAL62 and 8505C cells as measured by immunoblot with an antibody for the cleaved products of caspase 3 (the data are described in attached manuscript II).

Accordingly, the percentages of trypan blue excluding (viable) cells, of CAL62 transfected with Twist1 siRNA 48 and 72 hours after transfection, were of 69 and 32%, respectively, with respect to scrambled control, confirming that Twist1 depletion reduced thyroid cancer cell viability (Figure 7).

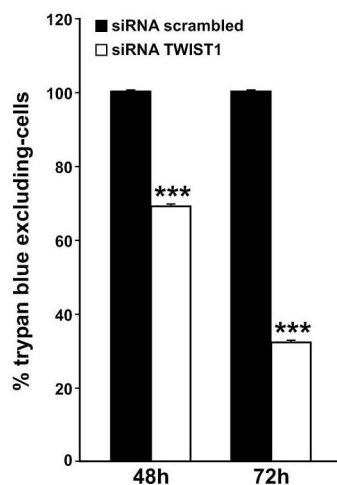


Figure 7. CAL62 cell line was transfected with Twist1 siRNA or scrambled siRNA; after 48 and 72 h, cells were collected by trypsinization and counted in triplicate.

We evaluated the migration by Wound-Healing assay and invasion (the data are detailed in attached manuscript II)

ability of Twist1 siRNA-transfected cells compared with scrambled siRNA-transfected cells. 8505C and OCUT-2 cells transfected with the scrambled control efficiently migrated into the wound; in contrast, cells transfected with Twist1 siRNA had a greatly reduced migrating ability (Figure 8).

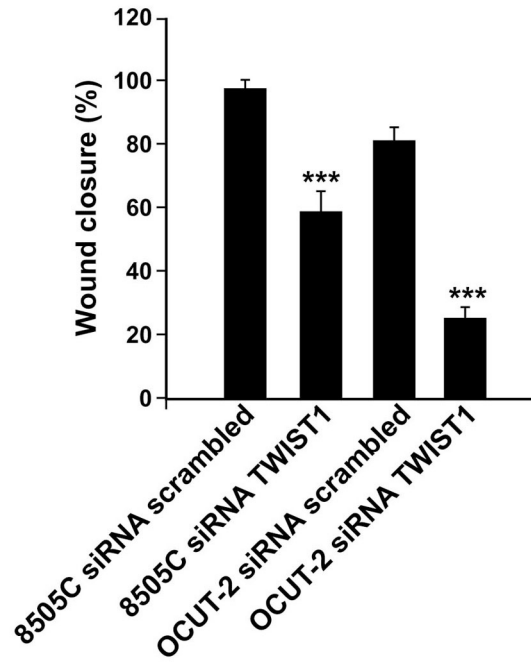


Figure 8. Cells were transfected with Twist1 siRNA or scrambled siRNA; a scraped wound was introduced and cell migration into the wound was monitored at 24 hours. Wound closure was measured by calculating pixel densities in the wound area and expressed as percentage of wound closure of triplicate areas \pm SD.

4.4 Effects of stable silencing of Twist1 in CAL62 cells

We stably transfected CAL62 cells with an shTwist1 plasmid or with shLUC control. After antibiotic selection, cells were screened by Western blot for Twist1 expression. A mass population (mp) (shTwist1 mp) with a Twist1 knockdown of approximately 50% was used for further study. Consistent with data obtained upon transient Twist1 silencing, shTwist1 mp

cells showed decreased migration and invasion ability and a decreased viability compared to control (the data are detailed in attached manuscript II).

4.5 Ectopic Twist1 promotes cell migration and invasion of PTC cells

PTC cells, TPC-1, which have low endogenous levels of Twist1, were transfected with a Twist1-expressing plasmid (pcDNA-Twist1) or with the empty vector (pcDNA). Mass populations and cell clones were selected. Twist1 expression was increased (4- to 13- fold) in all the cell lines transfected with Twist1 compared with the controls (the data are shown in attached manuscript). Growth rate was similar in Twist1- and vector-transfected control cell lines.

Therefore, we studied cell migration using the wound closure assay. As shown in Figure 9, the migration rate was higher in Twist1-transfected cells than in control cells.

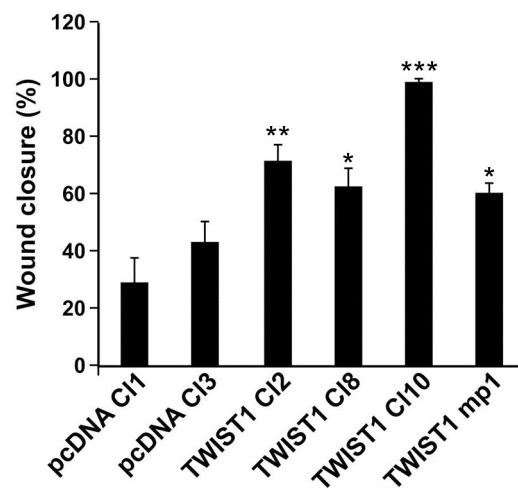


Figure 9. Cells were transfected with Twist1 siRNA or scrambled siRNA; a scraped wound was introduced and cell migration into the wound was monitored at 24 hours. Wound closure was measured by calculating pixel densities in the wound area and expressed as percentage of wound closure of triplicate areas \pm SD.

We next evaluated Twist1- transfected and control cells

for their ability to invade Matrigel. Twist1 transfectants had a greater ability to invade Matrigel (data are shown and detailed in attached manuscript II).

4.6 Ectopic Twist1 protects PTC cells from apoptosis

We treated TPC-1 cells transfected with Twist1 or control vector with different concentrations of Cisplatin (200, 1000, and 2000 nM) and counted cells 24 hours upon treatment. As shown in Figure 10, cell viability was higher in Twist1-transfected than in control cells upon treatment with the highest dose of Cisplatin.

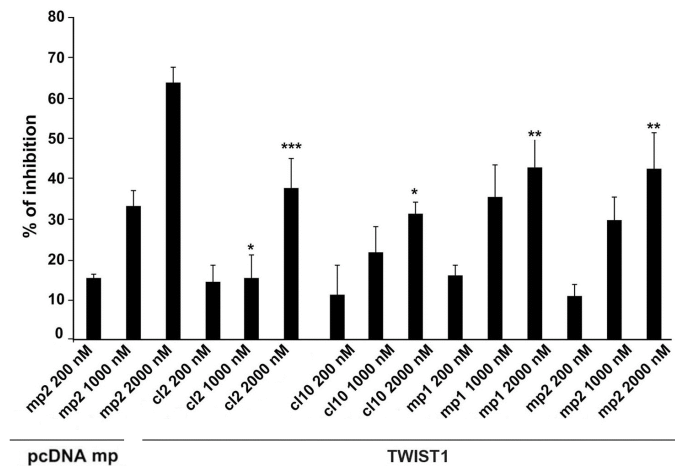


Figure 10. The indicated cells were treated with increasing doses of Cisplatin and counted 24 h after treatment. Data are shown as percentage of inhibition of cell viability.

Moreover, the amount of caspase 3 cleaved products was lower in Twist1-transfected than in control cells (data are shown and detailed in attached manuscript II). Thus, Twist1 overexpression protected thyroid cancer cells from cell death induced by Cisplatin. This data suggests that Twist1 may be exploited as a molecular marker of the response of thyroid cancer to chemotherapy.

4.7. Identification of Twist1 target genes

To determine the molecular mechanisms by which Twist1 regulates anaplastic thyroid cancer phenotype, we analyzed gene expression profiles in TPC-1 Twist1 transfected cells. Total RNA extracted from three TPC Twist1 stable transfectants (Twist1 mp1, Twist1 mp2 and Twist1 C12) was used to examine their gene expression profile in comparison to vector control transfected cells. The screening was conducted in collaboration with Aarhus Biotechnology (Aarhus, Denmark) using the human Genome U133 Plus 2.0 Array GeneChips (Affymetrix) containing > 47.000 gene transcripts. We analyzed only the genes that were changed in all the three Twist1 transfectant compared to vector control cells. Genes were analyzed only if the signal intensity was ≥ 50 . We found 37 genes upregulated more than ~ 3 fold and 42 downregulated more than ~ 5 fold in TPC Twist1 transfectant compared to vector control cells. In Table 2 and 3 are shown, respectively, the list of the genes upregulated and downregulated.

Table 2: List of genes upregulated more than ~3 fold in Twist1 overexpressing TPC cells (Twist1 mp1, Twist1 mp2, Twist1 C12) versus vector (pcDNA mp) transfected cells (n=37).

Gene Name	Gene Symbol	Fold Change (average of fold change in Twist1 mp1, Twist1 mp2, Twist1 C12 versus pcDNA mp)	SD
heparan sulfate 6-O-sulfotransferase 2*	HS6ST2	10.28	0.35
CD24 molecule*	CD24	8.66	1.82
collagen type I alpha 1	COL1A1	7.22	1.41
GDNF family receptor alpha 1	GFRA1	6.92	0.61
keratin 7	KRT7	5.57	0.83
vang-like 2 (van gogh. Drosophila)	VANGL2	5.48	0.31
matrix-remodelling associated 8	MXRA8	5.42	0.58
plakophilin 2*	PKP2	5.34	0.87
coagulation factor II (thrombin) receptor-like 1	F2RL1	5.31	0.95
leprecan-like 1	LEPREL1	4.99	0.47
thyroid hormone receptor, beta (erythroblastic leukemia viral (v-erb-a) oncogene homolog 2, avian)	THRB	4.88	0.87

zinc finger, BED-type containing 2	ZBED2	4.60	0.66
ADAM metalloproteinase with thrombospondin type 1 motif. 5 (aggrecanase-2)*	ADAMTS5	4.37	0.85
inhibitor of DNA binding 4. dominant negative helix-loop- helix protein*	ID4	4.34	0.26
ras homolog gene family, member B*	RHOB	4.14	0.61
PDZ domain containing 1*	PDZK1	3.99	0.55
netrin 4	NTN4	3.98	0.75
papilin, proteoglycan-like sulfated glycoprotein*	PAPLN	3.95	0.70
cytochrome P450, family 24. subfamily A, polypeptide 1	CYP24A1	3.90	0.97
filaggrin	FLG	3.73	0.69
AKIP1	A kinase (PRKA) interacting protein 1 (AKIP1)	3.64	0.52
coiled-coil domain containing 80	CCDC80	3.59	0.86
transforming growth factor, beta- induced	TGFBI	3.50	0.20
Suppression of tumorigenicity 7 like	ST7L	3.45	0.87
prostaglandin I2 (prostacyclin) synthase	PTGIS	3.43	0.78
transgelin	TAGLN	3.41	1.01
mal. T-cell differentiation protein 2	MAL2	3.38	0.52
EGF-like repeats and discoidin I- like domains 3	EDIL3	3.29	0.64
tumor-associated calcium signal transducer 1*	TACSTD1	3.24	0.95
death-associated protein kinase 1*	DAPK1	3.21	0.62
LIM and cysteine-rich domains 1	LMCD1	3.20	0.46
WAS protein family, member 3 microphthalmia-associated transcription factor*	WASF3 MITF	3.12 2.95	0.59 0.85
phospholipase C, beta 4	PLCB4	2.93	0.79
ADAM metalloproteinase with thrombospondin type 1 motif, 1*	ADAMTS1	2.93	0.78
chromosome 10 open reading frame 65	C10orf65	2.92	0.61
PDZK1 interacting protein 1*	PDZK1IP1	2.90	0.57

* Genes that were further studied.

Table 3: List of genes downregulated more than 5 fold in Twist1 overexpressing TPC cells (Twist1 mp1, Twist1 mp2, Twist1 C12) versus vector (pcDNA mp) transfected cells (n=42).

Gene Name	Gene Symbol	Fold Change (average of fold change in Twist1 mp1, Twist1 mp2, Twist1 C12 versus pcDNA mp)	SD
peroxisomal biogenesis factor 5-like	PEX5L	-32.00	3.25
NADPH oxidase. EF-hand calcium binding domain 5	NOX5	-25.62	2.82
hydroxysteroid (11-beta) dehydrogenase 1	HSD11B1	-24.56	2.21
chromosome 10 open reading frame 116	C10orf116	-24.37	2.72
protocadherin 7*	PCDH7	-23.27	2.57
interleukin 13 receptor. alpha 2	IL13RA2	-23.06	2.65
granzyme A (granzyme 1. cytotoxic T-lymphocyte-associated serine esterase 3)	GZMA	-19.47	1.37
Rho GTPase activating protein 9*	ARHGAP9	-15.03	1.86
hematopoietic cell-specific Lyn substrate 1	HCLS1	-12.84	2.03
G protein-coupled receptor 65	GPR65	-11.25	1.44
FAT tumor suppressor homolog 3 (Drosophila)	FAT3	-9.70	2.02
solute carrier family 22 (organic cation transporter). member 18 antisense	SLC22A18AS	-9.63	1.64
BCL2-related protein A1	BCL2A1	-9.27	1.66
linker for activation of T cells family. member 2	LAT2	-8.22	1.40
serpin peptidase inhibitor. clade D (heparin cofactor). member 1	SERPIND1	-8.15	1.61
heat shock 70kDa protein 1A	HSPA1A	-7.85	1.47
myeloma overexpressed gene (in a subset of t(11;14) positive multiple myelomas)	MYEOV	-7.78	0.68
gap junction protein. beta 2. 26kDa	GJB2	-7.68	1.70
protease. serine. 3 (mesotrypsin)	PRSS3	-7.64	1.26
growth hormone receptor	GHR	-7.38	1.01
interleukin 1. alpha	IL1A	-7.08	1.11
synaptotagmin-like 3	SYTL3	-6.86	1.47
vanin 1	VNN1	-6.59	0.92
SLAIN motif family. member 1	SLAIN1	-6.30	1.05
keratin 15*	KRT15	-6.15	1.14
baculoviral IAP repeat-containing 3	BIRC3	-6.13	1.27
podoplanin	PDPN	-6.12	1.31
tissue factor pathway inhibitor 2	TFPI2	-6.02	1.39

chemokine (C-X-C motif) ligand 3	CXCL3	-5.69	0.68
interleukin 7	IL7	-5.62	0.97
hypothetical protein LOC339400	LOC339400	-5.57	1.05
phosphatidylinositol 3,4,5- trisphosphate-dependent RAC exchanger 1*	PREX1	-5.47	1.12
epithelial membrane protein 1	EMP1	-5.47	1.70
sorbin and SH3 domain containing 1	SORBS1	-5.36	1.27
neurotrimin	HNT	-5.31	1.01
absent in melanoma 1	AIM1	-5.18	1.08
signal-regulatory protein beta 1	SIRPB1	-5.17	1.25
thrombomodulin	THBD	-5.13	0.38
Rho GDP dissociation inhibitor (GDI) beta*	ARHGDI3	-4.98	1.15
sorbin and SH3 domain containing 1	SORBS1	-4.8	1.19
G0/G1switch 2	GOS2	-4.8	1.18
solute carrier family 7 (cationic amino acid transporter, y+ system), member 7	SLC7A7	-4.80	0.85
carbohydrate (keratan sulfate Gal-6) sulfotransferase 1	CHST1	-4.76	1.28
metastasis suppressor 1*	MTSS1	-4.70	0.60

* Genes that were further studied.

We used the Ingenuity pathways Analysis (Ingenuity Systems, www.ingenuity.com) to classify the genes in pathway. Molecules from the dataset were associated with Ingenuity's Knowledge Base. Signal pathways that were mostly changed in Twist1 transfected cells were: RhoA Signaling, Death Receptor Signaling, Wnt/ β -catenin Signaling, Hepatic Stellate Cell Activation, Apoptosis Signaling.

Among these top changed genes we further selected 13 genes upregulated and 7 genes downregulated for further validation. The genes upregulated further studied were: ADAMTS1 (ADAM metalloproteinase with thrombospondin type 1 motif, 1), ADAMTS5 (ADAM metalloproteinase with thrombospondin type 1 motif 5), CD24 (CD24 molecule), DAPK1 (death-associated protein kinase 1), HS6ST2 (heparan sulfate 6-O-sulfotransferase 2), ID4 (inhibitor of DNA binding 4 dominant negative helix-loop-helix protein), PAPLN (papilin, proteoglycan-like sulfated glycoprotein), PDZK1 (PDZ domain containing 1), PDZK1IP1 (PDZK1 interacting protein 1), PKP2 (plakophilin 2), RHOB (ras homolog gene family, member B), TACTSD1 (tumor-associated calcium

signal transducer and WASF3 (WAS protein family member 3 microphthalmia-associated transcription factor). The genes downregulated further studied were: ARHGDIB (Rho GDP dissociation inhibitor (GDI) beta), ARGHPA9 (Rho GTPase activating protein 9), GPR65 (G protein-coupled receptor 65), KRT15 (keratin 15), PCDH7 (protocadherin 7), MTSS1 (metastasis suppressor 1) and PREX1 (phosphatidylinositol 3.4.5-trisphosphate-dependent RAC exchanger 1) cells. We chose these genes on the basis of their fold change and on what is known of their role in the literature.

Initially, we confirmed the microarray data by performing quantitative RT-PCR in the cell lines used for the screening: TPC Twist1 mp1, Twist1 mp2 and Twist1 C12 in comparison to vector control transfected cells, furthermore we used also Twist1 C110 (see attached manuscript II). As shown in the Figure 11, all the 13 genes upregulated were confirmed (with some degree of variability among the clones) in all cells transfected with Twist1 compared to control ($p < 0.01$).

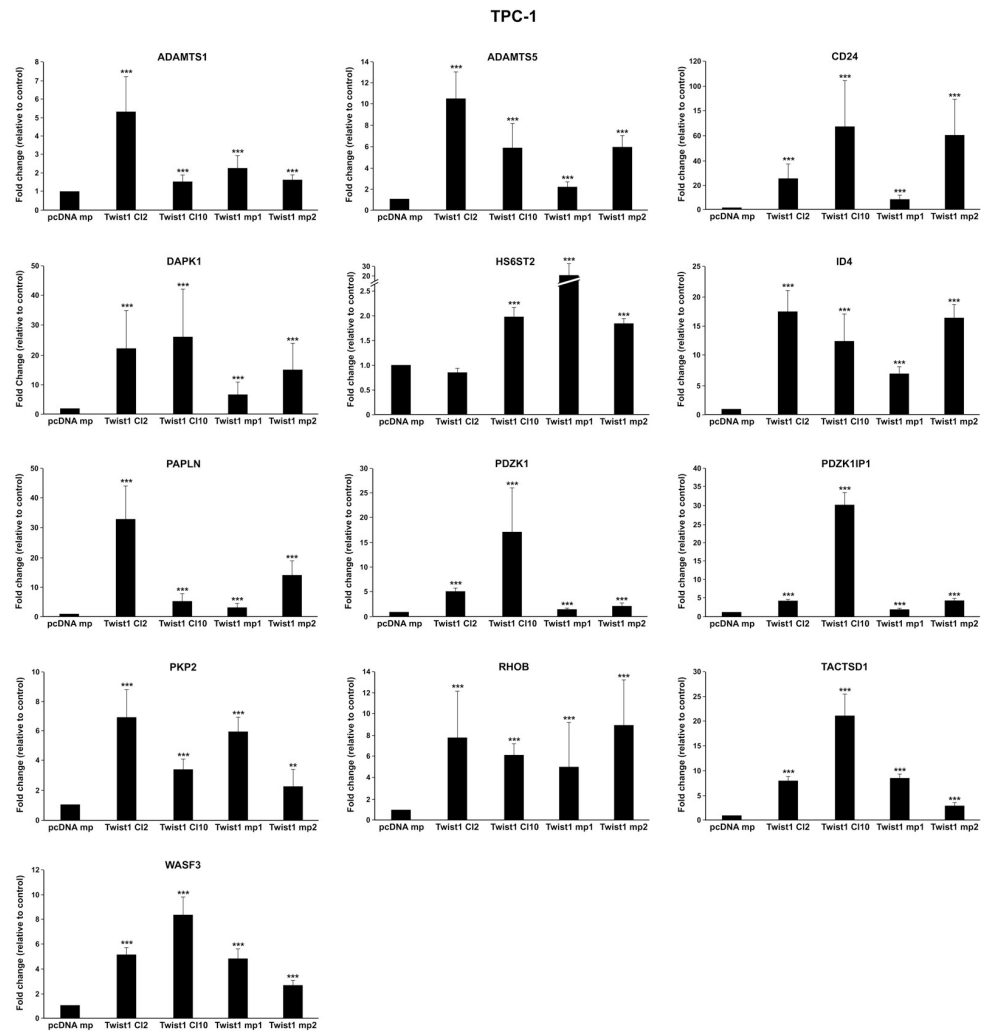


Figure 11. Quantitative RT-PCR of the indicated genes in TPC Twist1 transfectant cells in comparison to vector control. Asterisks indicate: $p < 0.01$ (**) and $p < 0.001$ (***)

Similar results were obtained for the genes downregulated (Figure 12).

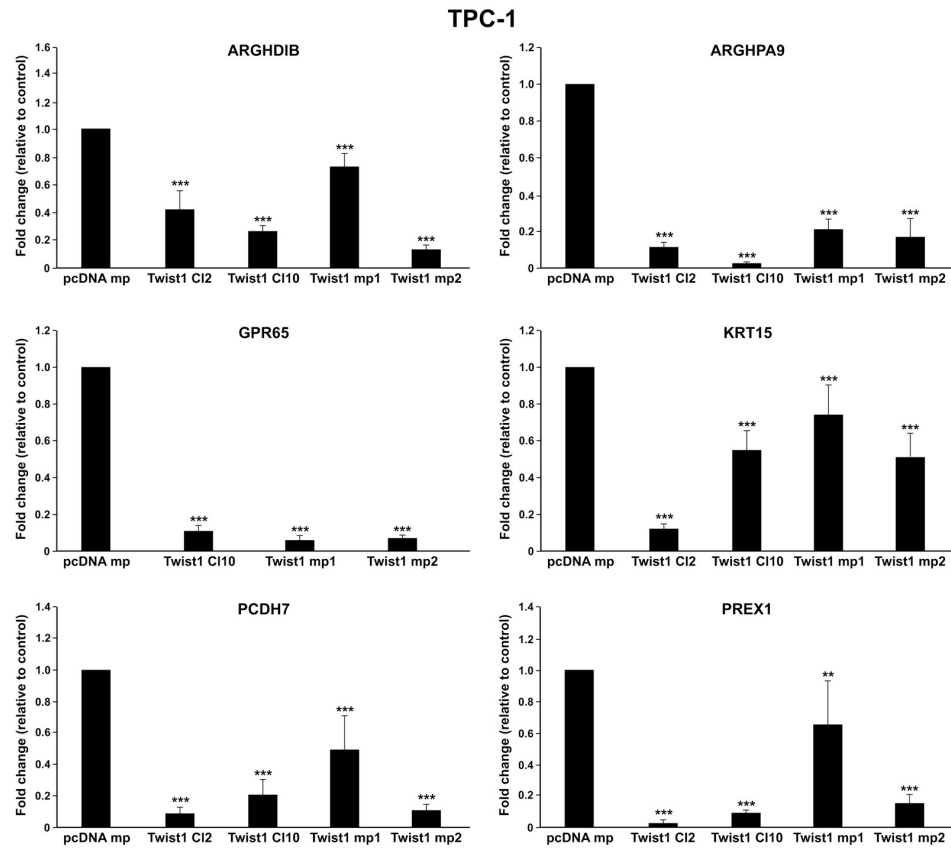


Figure 12. Quantitative RT-PCR of the indicated genes in TPC Twist1 transfectant cells in comparison to vector control. Asterisks indicate: $p < 0.01$ (**) and $p < 0.001$ (***)

4.8 Expression of Twist1 target genes in CAL62 shTwist1 transfected cells

To further confirm that Twist1 transcriptionally regulates this set of genes, we studied whether the suppression of Twist1 affect the expression levels of the 20 genes. Thus, we performed quantitative RT-PCR for the 13 upregulated genes and 7 downregulated in the ATC, CAL62 cell line stably transfected with an shTwist1 plasmid. As shown in Figure 13, transfection of CAL62 cell line with a Twist1 shRNA promoted a severe downregulation of ADAMTS1, CD24, HS6ST2, ID4, PAPLN, PDZK1, PDZK1IP1, PKP2, RHOB, TACTSD1 and WASF3 mRNA with respect to the control cells transfected with an irrelevant shRNA (shLUC) ($p < 0.01$).

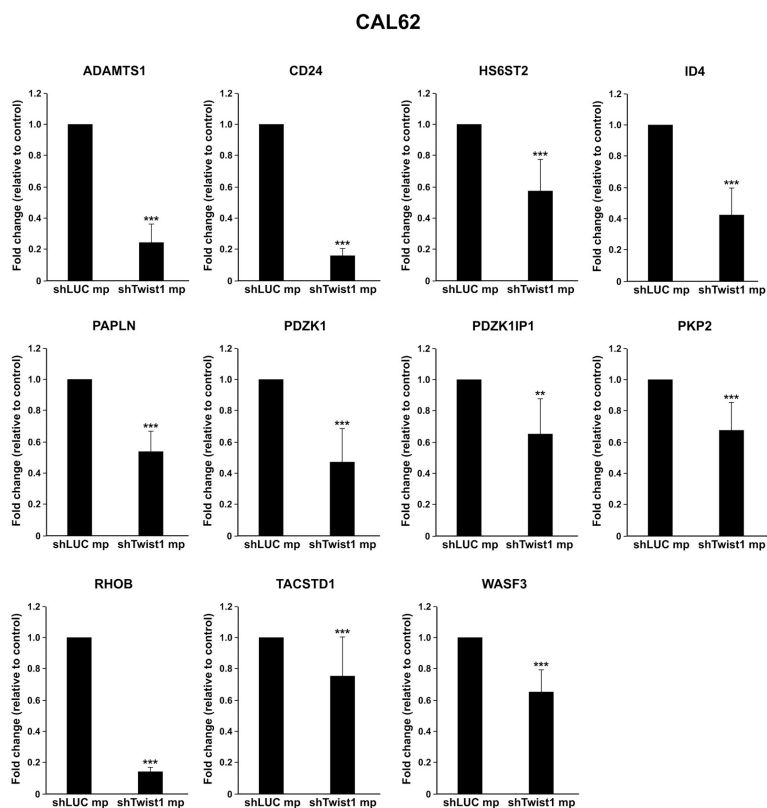


Figure 13. Quantitative RT-PCR of the indicated genes in CAL62 shTwist1 transfectant cells in comparison to vector control. Asterisks indicate: $p < 0.01$ (**) and $p < 0.001$ (***).

On the contrary, Twist1 downregulated genes i.e. ARHGDI1B, GPR65, KRT15, PCDH7 and MTSS1 were upregulated upon Twist1 silencing (Figure 14).

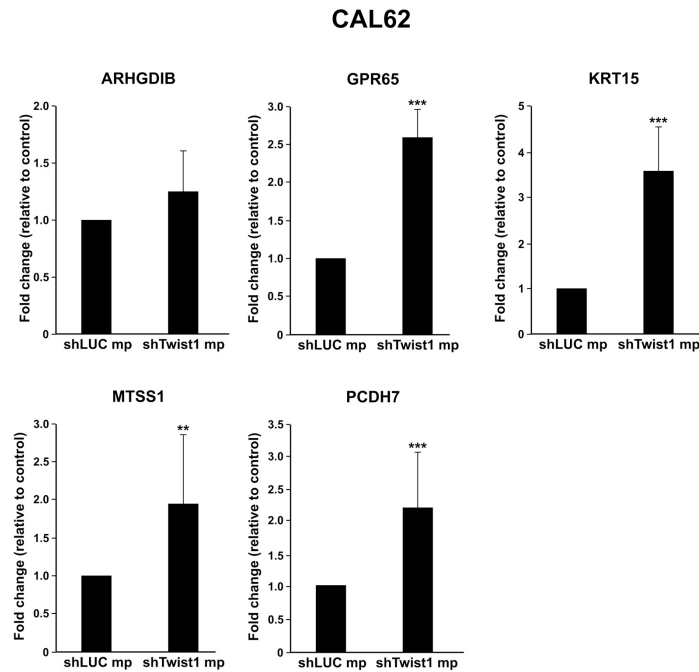


Figure 14. Quantitative RT-PCR of the indicated genes in CAL62 shTwist1 transfectant cells in comparison to vector control. Asterisks indicate: $p < 0.01$ (**) and $p < 0.001$ (***).

4.9 Silencing of Twist1 target genes in cells ectopically expressing Twist1 (TPC Twist1 mp 1)

To further study the functional significance of our findings we transfected siRNA specific for the genes HS6ST2, ID4, PDZK1, PDZK1IP1 and TACSTD1 in the TPC cells overexpressing Twist1 (TPC Twist1 mp1). We choose to start from these genes because they were significantly changed in the quantitative RT-PCR.

TPC Twist1 mp cells were transiently transfected with siRNA for HS6ST2, ID4, PDZK1, PDZK1IP1 and TACSTD1 or a scrambled siRNA and examined 72 hours post-transfection. We initially verified by quantitative RT-PCR that the specific siRNA silenced the corresponding gene. As shown in the Figure 15, siRNA for HS6ST2, ID4, PDZK1, PDZK1IP1 and TACSTD1 efficiently downregulated the specific gene in TPC Twist1 mp transfected cells ($p < 0.001$).

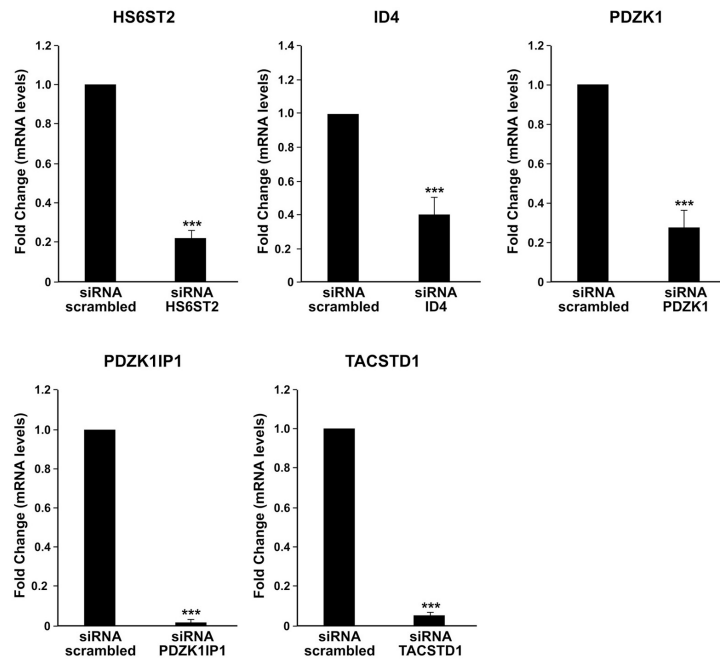


Figure 15. Cells were transiently transfected with the indicated siRNA. After 72 hours RNA was extracted and mRNA expression levels were measured by quantitative RT-PCR. Results are reported as fold change in comparison to the scrambled control. Asterisks indicate: $p < 0.001$ (***)

Then, we measured cell viability using trypan blue assay. TPC Twist1 mp1 cells were transfected in transient with siRNA for HS6ST2, ID4, PDZK1, PDZK1IP1 and TACSTD1, 72 hours after transfection cells were stained with trypan blue and counted. As shown in Figure 16, transient silencing of HS6ST2, ID4, PDZK1, PDZK1IP1 and TACSTD1 impaired viability of TPC Twist1 mp cells ($p < 0.001$).

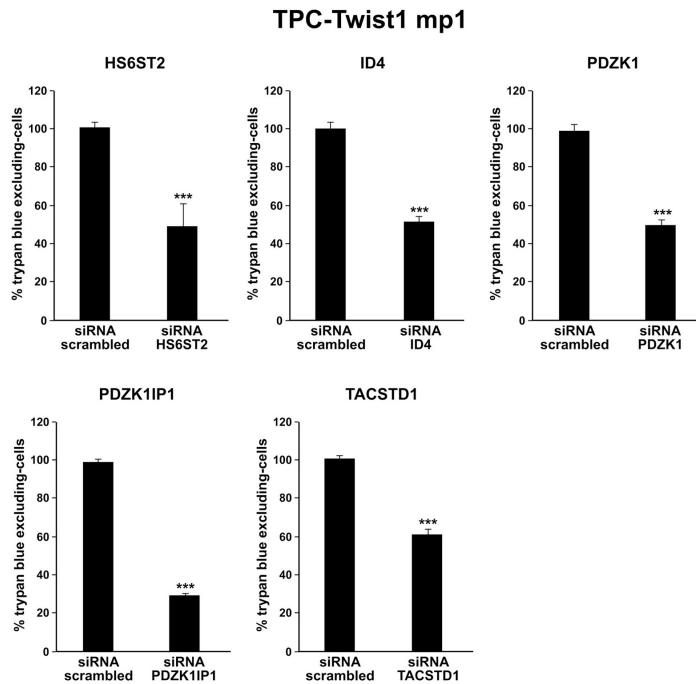


Figure 16. TPC- Twist1 mp cell line was transfected with HS6ST2, ID4, PDZK1, PDZK1IP1 and TACSTD1 siRNA or scrambled siRNA; after 72 hours, cells were collected by trypsinization, stained for 10 min with trypan-blue and counted in triplicate. The percentage of trypan blue excluding cells compared to cells transfected with siRNA scrambled is reported \pm SD. Asterisks indicate $p < 0.001$ (***)

4.10 Silencing of HS6ST2, ID4, PDZK1, PDZK1IP1 and TACSTD1 reduced cell viability in OCUT-2 cells

To confirm the data obtained we also used the ATC cell line OCUT-2 that endogenously express high levels of Twist1 (shown in the manuscript attached II). OCUT-2 cells were transiently transfected with siRNA specific for HS6ST2, ID4, PDZK1, PDZK1IP1 and TACSTD1 or scrambled siRNA and examined 72 hours post- transfection. As shown in the Figure 17, silencing of HS6ST2, ID4, PDZK1, PDZK1IP1 and TACSTD1 was effective with a reduction of mRNA levels from 2 to more than 10 fold.

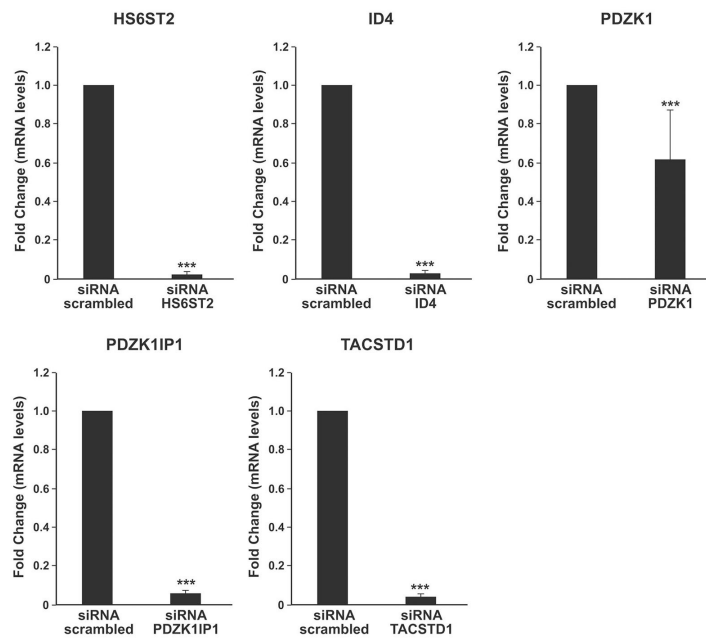


Figure 17. Cells were transiently transfected with the indicated siRNA. After 72 hours RNA was extracted and mRNA expression levels were measured by quantitative RT-PCR. Results are reported as fold change in comparison to the scrambled control. Asterisks indicate: $p < 0.001$ (***)

Then, we measured cell viability using trypan blue assay. OCUT-2 cells were transfected in transient with siRNA for HS6ST2, ID4, PDZK1, PDZK1IP1 and TACSTD1; 72 hours after transfection cells were stained with trypan blue and counted. As shown in Figure 18, cells viability was significantly impaired in cells transfected with siRNA for HS6ST2, ID4, PDZK1, PDZK1IP1 and TACSTD1 compared to control ($p < 0.001$).

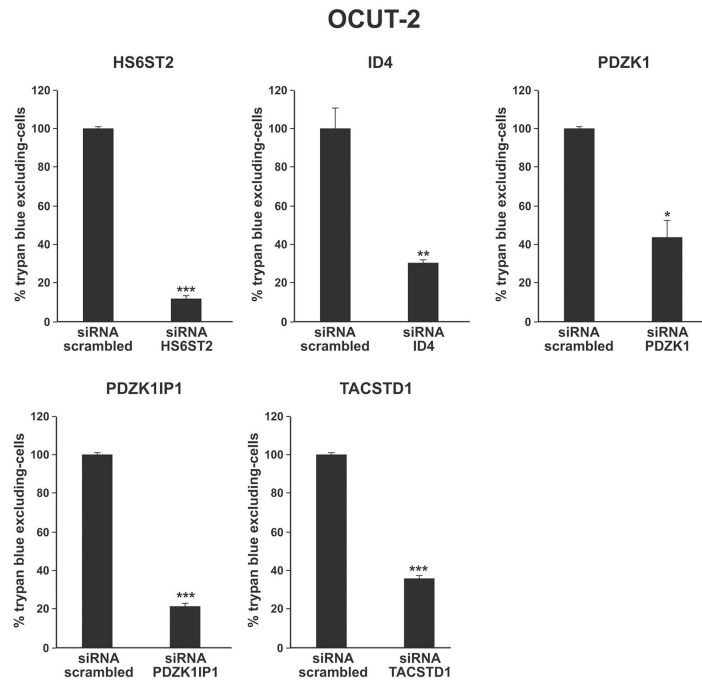


Figure 18: OCUT-2 cell line was transfected with HS6ST2, ID4, PDZK1, PDZK1IP1 and TACSTD1 siRNA or scrambled siRNA; after 72 hours, cells were collected by trypsinization, stained for 10 min with trypan-blue and counted in triplicate. The percentage of trypan blue excluding cells compared to cells transfected with siRNA scrambled is reported \pm SD. Asterisks indicate: $p < 0.01$ (**) and $p < 0.001$ (***).

4.11 Silencing of genes HS6ST2, PDZK1, PDZK1IP1 and TACSTD1 reduced cell viability in CAL62 cells

Finally, we have used another ATC cell line CAL62 in which we showed that Twist1 depletion affected several hallmarks of malignancy, including anchorage independent proliferation, survival, and invasion (see attached manuscript II). As shown in Figure 19, HS6ST2, PDZK1, PDZK1IP1 and TACSTD1 mRNA were significantly downregulated upon respective siRNA transfection in CAL62 cells ($p < 0.001$).

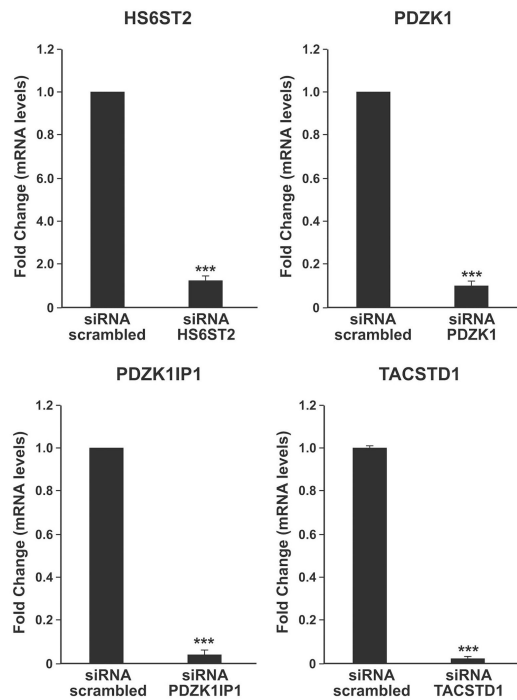


Figure 19. Cells were transiently transfected with the indicated siRNA. After 72 hours RNA was extracted and mRNA expression levels were measured by quantitative RT-PCR. Results are reported as fold change in comparison to the scrambled control. Asterisks indicate: $p < 0.001$ (***)

Furthermore, in agreement with the data obtained in the other Twist1 overexpressing cells (TPC Twist1 mp and OCUT-2), cells viability in CAL62 transfected with siRNA for HS6ST2, PDZK1, PDZK1IP1 and TACSTD1 was greatly impaired compared to cells transfected with siRNA scrambled (Figure 20).

CAL62

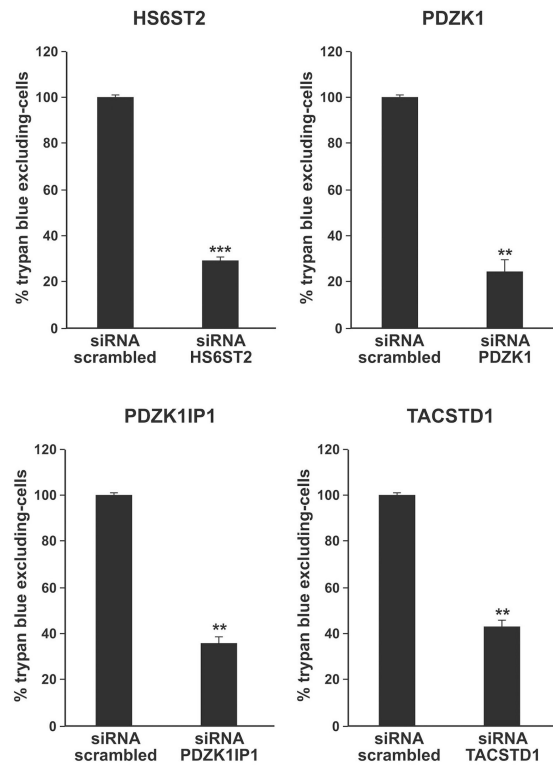


Figure 20. CAL62 cell line was transfected with HS6ST2, PDZK1, PDZK1IP1 and TACSTD1 siRNA or scrambled siRNA; after 72 hours, cells were collected by trypsinization, stained for 10 min with trypan-blue and counted in triplicate. The percentage of trypan blue excluding cells compared to cells transfected with siRNA scrambled is reported \pm SD. Asterisks indicate: $p < 0.01$ (**) and $p < 0.001$ (***).

Further experiments on cell migration (by wound closure assay) and cell invasion (by matrigel assay) upon knockdown of HS6ST2, ID4, PDZK1, PDZK1IP1 and TACSTD1, in TPC Twist1 mp1, OCUT-2 and CAL62 cells are ongoing in our laboratory.

5. DISCUSSION

Thyroid cancer includes tumor types as different as well differentiated carcinomas that have a very good prognosis and undifferentiated carcinomas or ATC that are among the most aggressive human cancers. As yet, the molecular players sustaining such different behavior are largely unknown. In this dissertation, we have demonstrated that Twist1 is up-regulated in ATC samples. Overall Twist1 up-regulation in ATC is more prominent at the RNA than at the protein level. It is possible that Twist1 overexpression is affected not only at the transcriptional level but also at the post-transcriptional level.

Twist1 up-regulation was associated with mitotic index, as determined by Ki67/MIB1. However, the fact that Twist1 did not influence cell proliferation in cultured cells suggests that it is not directly involved in controlling cell proliferation.

In ATC samples, Twist1 positivity also correlated with markers of mesenchymal transition (fusocellular phenotype) and malignancy (p53 positivity); however, correlation with p53 expression was not demonstrated in cultured thyroid cancer cells because Twist1-positive (OCUT-2, 8505C, and CAL62) and Twist1-negative (TPC-1, BCPAP, NIM, ACT-1, SW1736) cells both had either high (8505C, ACT-1) or low/undetectable (CAL62, OCUT-2, TPC-1, BCPAP, NIM, SW1736) p53 expression (data not shown).

Twist1 expression is responsive to Wnt-1, IGF-I, and nuclear factor B (NF- κ B) signaling. Elements of the Wnt pathway, particularly CTNNB1 (the gene coding β -catenin), were found to be mutated in PDC and ATC. Moreover, NF- κ B is activated in human thyroid cancer cells, in particular in ATC. Therefore, both the Wnt-1/ β -catenin and NF- κ B pathways are good candidates as mediators of Twist1 up-regulation in ATC.

Although a number of direct and indirect targets have been identified in recent years, the exact mechanisms through which Twist1 contributes to tumorigenesis are still largely unknown. To uncover the molecular mechanisms underlying Twist1 biological effects in thyroid cancer cells, we have performed a gene expression profile of Twist1 overexpressing cells. Gene signature obtained enriched for genes involved in invasion, migration and apoptosis consistent with the role of Twist1 in anaplastic thyroid cancer cells. Indeed the genes further studied were: ADAMTS1, ADAMTS5, ARHGDIB, ARGHPA9, CD24, DAPK1, GPR65, HS6ST2, KRT15, ID4,

MTSS1, PAPLN, PDZK1, PDZK1IP1, PCDH7, PKP2, PREX1, RHOB, TACTSD1 and WASF3.

In particular several genes studied (i.e. ARHGDIB, ARGHPA9, PREX1, RHOB) are members of the Rho pathway. Overexpression of Rho GTPases in human tumors often correlates with a poor prognosis. Furthermore, coordinated Rho GTPase signaling is considered to be part of mechanism underlying tumor cell invasion (Street et al. 2011).

One of the highly upregulated gene in TPC Twist1 transfected cells is HS6ST2, a member of the heparan sulfate (HS) sulfotransferase gene family. Heparan sulfate proteoglycans are ubiquitous components of the cell surface, extracellular matrix, and basement membranes, and interact with various ligands to influence cell growth, differentiation, adhesion, and migration. HS6ST2, catalyze the transfer of sulfate to HS (Song et al. 2011).

Another gene of particular interest is ID4. ID proteins (ID-1 to 4) are dominant negative regulators of basic helix-loop-helix transcription factors. They play a key role during development, preventing cell differentiation while inducing cell proliferation. They are poorly expressed in adult life but can be reactivated in tumorigenesis. Several evidences indicate that ID proteins are associated with loss of differentiation, unrestricted proliferation and neoangiogenesis in diverse human cancers (Dell'Orso et al. 2010).

Among the genes overexpressed in TPC Twist1 transfected cells we have isolated PDZK1 and its interacting protein PDZK1IP1 (MAP17). PDZK1IP1 is a small 17 kDa non-glycosylated membrane protein found overexpressed in a great variety of human carcinomas. Immunohistochemical analysis of PDZK1IP1 during cancer progression shows, at least in prostate and ovarian carcinomas, that overexpression of the protein strongly correlates with tumoral progression. Moreover, it was described that PDZK1IP1 promoter is activated by different oncogenes (Guijarro et al. 2007).

Another gene upregulated in TPC Twist1 transfected cells is the epithelial cell adhesion molecule TACSTD1 (EpCAM). TACSTD1 is a membrane glycoprotein that is highly expressed on most carcinomas and therefore of potential use as a diagnostic and prognostic marker for a variety of carcinomas. Recently, TACSTD1 has been identified as an additional marker of cancer-initiating cells. Furthermore, TACSTD1 abrogates E-cadherin mediated cell-cell adhesion thereby promoting metastasis (van der Gun et al. 2010).

Twist1 upregulated CD24 mRNA. CD24 is an antigen

overexpressed in various tumor types and has been shown to be involved in tumor cell migration, invasion, and metastasis. CD24 has been shown to recruit adhesion molecules to lipid rafts, thereby contributing to tumor cell migration, dissemination and metastasis (Bretz, 2011).

Consistent with the biological role of Twist1 in ATC, we found upregulated in TPC Twist1 transfectants compared to control cells, WASF3. This gene encodes a member of the Wiskott-Aldrich syndrome protein family. The gene product is a protein that forms a multiprotein complex that links receptor kinases and actin. Binding to actin occurs through a C-terminal verprolin homology domain in all family members. The multiprotein complex serves to transduce signals that involve changes in cell shape, motility or function. Inactivation of the WASF3 gene in prostate cancer cells leads to suppression of tumorigenicity and metastases (Teng et al. 2010).

In conclusion, we have identified a set of 20 genes that mediates Twist1 biological effects in thyroid cancer. Further studies are on going in our laboratory to test the expression of the set of 20 Twist1 target genes in thyroid carcinoma samples. Based on the results obtained, for selected genes, when commercially antibodies are available, we will further perform western blot and immunohistochemistry studies. Other, studies are on going in our laboratory to investigate the effects of the silencing of HS6ST2, ID4, PDZK1 PDZK1IP1 and TACSTD1 genes on cell migration and invasion of TPC Twist1, OCUT-2 and CAL62 cells. Finally, a future direction of our work will be to verify if Twist1 binds to the promoter of selected genes. Possible binding sites for Twist1 are E-box (5'-CANNTG-3') sequence motif. We will search in the promoter of the genes isolated in the screening, E-boxes sites using Match program (www.gene-regulation.com). We envisage the possibility for selected genes to perform chromatin immunoprecipitation.

Identification of genes downstream transcription factor is important for clinical translation of basic research. Indeed, despite the growing evidences linking EMT to metastasis in various human cancers, therapeutically targeting EMT may be difficult. Directly inhibiting the transcription factors that drive EMT is currently infeasible, as targeting large binding interfaces is not amenable to small-molecule inhibition. Instead, downstream targets of these transcription factors essential for their role in invasion and metastasis are more realistic targets of therapeutic intervention.

6. CONCLUSIONS

Anaplastic thyroid carcinoma (ATC) ranks among the most lethal human malignancies. Here, we showed that ATCs up-regulate Twist1 with respect to normal thyroids as well as to poorly and well differentiated thyroid carcinomas. Knockdown of Twist1 by RNA interference in ATC cells reduced cell migration and invasion and increased sensitivity to apoptosis. The ectopic expression of Twist1 in thyroid cells induced resistance to apoptosis and increased cell migration and invasion. Finally, we have identified a set of 20 genes that mediates Twist1 biological effects. Further studies of each of these genes and of the pathway activated could lead to the discoveries of novel therapeutic target for ATC.

ACKNOWLEDGEMENTS

I would like to express my gratitude to all those who shared with me these three years. First and foremost, I wish to thank the Coordinator of the School of Doctorate in Molecular Oncology and Endocrinology, prof. Massimo Santoro, and my tutor, prof. Giuliana Salvatore, who gave me the opportunity to work in his laboratory, being always helpful for suggestions and advices. I want to express my sincere gratitude to prof. Giuliana Salvatore and Dr. Paolo Salerno: since my first day on lab, they were my direct supervisors and from them I learned most of “secrets” of this work. I would also to thank all the researchers, Dr. Annamaria Cirafici, Valentina De Falco, Dr. Nello Cerrato and Dr. Donatella Vitagliano, because from each I learned something and they help me whenever I needed. Thanks also to all the other colleagues and students: Mara Cantisani, Gennaro Di Maro, Magesh Muthu and Francesca Orlandella for their support and help.

Finally, a special thank is for my parents, Antonio and Carmela, my brothers and my girlfriend Ivana. Thank you because with your love, your patience and support, I would not have it. To you I dedicate this work.

7. REFERENCES

Ansieau S, Bastid J, Doreau A, Morel AP, Bouchet BP, Thomas C, Fauvet F, Puisieux I, Doglioni C, Piccinin S, Maestro R, Voeltzel T, Selmi A, Valsesia-Wittmann S, Caron de Fromental C, Puisieux A. Induction of EMT by twist proteins as a collateral effect of tumor-promoting inactivation of premature senescence. *Cancer Cell* 2008; 14: 79-89.

Ansieau S, Caron de Fromental C, Bastid J, Morel AP, Puisieux A. Role of the epithelial-mesenchymal transition during tumor progression. *Bull Cancer*. 2010; 97(1): 7-15.

Ansieau S, Hinkal G, Thomas C, Bastid J, Puisieux A. Early origin of cancer metastases: dissemination and evolution of premalignant cells. *Cell Cycle* 2008; 7: 3659-63.

Antico-Arciuch VG, Dima M, Liao XH, Refetoff S, Di Cristofano A. Cross-talk between PI3K and estrogen in the mouse thyroid predisposes to the development of follicular carcinomas with a higher incidence in females. *Oncogene* 2010; 29:5678-86.

Asai N, Murakami H, Iwashita T, Takahashi M. A mutation at tyrosine 1062 in MEN2A-Ret and MEN2B-Ret impairs their transforming activity and association with shc adaptor proteins. *J Biol Chem* 1996;271:17644-9.

Begum S, Rosenbaum E, Henrique R, Cohen Y, Sidransky D, Westra WH. BRAF mutations in anaplastic thyroid carcinoma: implications for tumor origin, diagnosis and treatment. *Mod Pathol*. 2004; 17(11): 1359-63.

Bialek P, Kern B, Yang X, Schrock M, Sosic D, Hong N, Wu H, Yu K, Ornitz DM, Olson EN, Justice MJ, Karsenty G. A twist code determines the onset of osteoblast differentiation. *Dev Cell* 2004; 6: 423-35.

Borganzone I, Butti MG, Coronelli S, Borrello MG, Santoro M, Mondellini P, Pilotti S, Fusco A, Della Porta G, Pierotti MA. Frequent activation of ret protooncogene by fusion with a new activating gene in papillary thyroid carcinomas. *Cancer Res* 1994; 54: 2979-85.

Bretz N, Noske A, Keller S, Erbe-Hofmann N, Schlange T, Salnikov AV, Moldenhauer G, Kristiansen G, Altevogt P. CD24 promotes tumor cell invasion by suppressing tissue factor pathway inhibitor-2 (TFPI-2) in a c-Src-dependent fashion. *Clin Exp Metastasis*. 2011 Oct 8. [Epub ahead of print].

Carta C, Moretti S, Passeri L, Barbi F, Avenia N, Cavaliere A, Monacelli M, Macchiarulo A, Santeusano F, Tartaglia M, Puxeddu E. Genotyping of an Italian papillary thyroid carcinoma cohort revealed high prevalence of BRAF mutations, absence of RAS mutations and allowed the detection of a new mutation of BRAF oncoprotein (BRAF(V599Ins)). *Clin Endocrinol (Oxf)* 2006; 64: 105-9.

Chen ZF, Behringer RR. twist is required in head mesenchyme for cranial neural tube morphogenesis. *Genes Dev* 1995; 9: 686-99.

Ciampi R, Knauf JA, Kerler R, Gandhi M, Zhu Z, Nikiforova MN, Rabes HM, Fagin JA, Nikiforov YE. Oncogenic AKAP9-BRAF fusion is a novel mechanism of MAPK pathway activation in thyroid cancer. *J Clin Invest*. 2005; 115(1): 94-101.

Ciampi R, Nikiforov YE. Alterations of the BRAF gene in thyroid tumors. *Endocr Pathol* 2005; 16: 163-72.

Costa AM, Herrero A, Fresno MF, Heymann J, Alvarez JA, Cameselle-Teijeiro J, Garcia-Rostan G. BRAF mutation associated with other genetic events identifies a subset of aggressive papillary thyroid carcinoma. *Clinical Endocrinology* 2008; 68: 618-34.

Cote GJ, Gagel RF. Lessons learned from the management of a rare genetic cancer. *N Engl J Med*. 2003; 349(16): 1566-8.

Davies H, Bignell GR, Cox C, Stephens P, Edkins S, Clegg S, Teague J, Woffendin H, Garnett MJ, Bottomley W, Davis N, Dicks E, Ewing R, Floyd Y, Gray K, Hall S, Hawes R, Hughes J, Kosmidou V, Menzies A, Mould C, Parker A, Stevens C, Watt S, Hooper S, Wilson R, Jayatilake H, Gusterson BA, Cooper C, Shipley J, Hargrave D, Pritchard-Jones K, Maitland N, Chenevix-Trench G, Riggins GJ, Bigner DD, Palmieri G, Cossu A, Flanagan A, Nicholson A, Ho JW, Leung SY, Yuen

ST, Weber BL, Seigler HF, Darrow TL, Paterson H, Marais R, Marshall CJ, Wooster R, Stratton MR, Futreal PA. Mutations of the BRAF gene in human cancer. *Nature* 2002; 417:949-54.

De Crevoisier R, Baudin E, Bachelot A, Leboulleux S, Travagli JP, Caillou B, Schlumberger M. Combined treatment of anaplastic thyroid carcinoma with surgery, chemotherapy, and hyperfractionated accelerated external radiotherapy. *Int J Radiat Oncol Biol Phys.* 2004; 60(4): 1137-43.

DeLellis RA, Williams ED. Thyroid and parathyroid tumors. In *Tumors of Endocrine Organs, World Health Organization Classification of Tumors.* DeLellis RA, Lloyd RV, Heitz PU and Eng C. 2004 . p. 51-6.

DeLellis RA. Pathology and genetics of thyroid carcinoma. *J Surg Oncol* 2006; 94: 662-9.

Dell'Orso S, Ganci F, Strano S, Blandino G, Fontemaggi G. ID4: a new player in the cancer arena. *Oncotarget* 2010;1:48-58.

Doreau A, Belot A, Bastid J, Riche B, Trescol-Biemont MC, Ranchin B, Fabien N, Cochat P, Pouteil-Noble C, Trolliet P, Durieu I, Tebib J, Kassai B, Ansieau S, Puisieux A, Eliaou JF, Bonnefoy-Bérard N. Interleukin 17 acts in synergy with B cell-activating factor to influence B cell biology and the pathophysiology of systemic lupus erythematosus. *Nat Immunol* 2009; 10: 778-85.

El Ghouzzi V, Le Merrier M, Perrin-Schmitt F, Lajeunie E, Benit P, Renier D et al. Mutations of the TWIST gene in the Saethre-Chotzen syndrome. *Nat Genet* 1997; 15: 42-46.

Figeac N, Daczewska M, Marcelle C, Jagla K. Muscle stem cells and model systems for their investigation. *Dev Dyn* 2007; 236: 3332-42.

Frattini M, Ferrario C, Bressan P, Balestra D, De Cecco L, Mondellini P, Bongarzone I, Collini P, Gariboldi M, Pilotti S, Pierotti MA, Greco A. Alternative mutations of BRAF, RET and NTRK1 are associated with similar but distinct gene expression patterns in papillary thyroid cancer. *Oncogene* 2004 ; 23: 7436-40.

Frêche B, Guillaumot P, Charmetant J, Pelletier L, Luquain C, Christiansen D, Billaud M, Mani SN. Inducible dimerization of RET reveals a specific AKT deregulation in oncogenic signaling. *J Biol Chem* 2005; 280: 36584-91.

Fuchtbauer EM. Expression of M-twist during postimplantation development of the mouse. *Dev Dyn* 1995; 204:316-22.

Fusco A, Chiappetta G, Hui P, Garcia-Rostan G, Golden L, Kinder BK, Dillon DA, Giuliano A, Cirafici AM, Santoro M, Rosai J, Tallini G. Assessment of RET/PTC oncogene activation and clonality in thyroid nodules with incomplete morphological evidence of papillary carcinoma: a search for the early precursors of papillary thyroid cancer. *Am J Pathol* 2002; 160: 2157-67.

Fusco A, Grieco M, Santoro M, Berlingieri MT, Pilotti S, Pierotti MA, Della Porta G, Vecchio G. A new oncogene in human thyroid papillary carcinomas and their lymph-nodal metastases. *Nature* 1987; 328: 170-72.

Garcia-Rostan G, Tallini G, Herrero A, D'Aquila TG, Carcangiu ML, Rimm DL. Frequent mutation and nuclear localization of beta-catenin in anaplastic thyroid carcinoma. *Cancer Research* 1999; 59: 1811-15.

Garcia-Rostan G, Camp RL, Herrero A, Carcangiu ML, Rimm DL, Tallini G. Beta-catenin dysregulation in thyroid neoplasms: down-regulation, aberrant nuclear expression, and CTNNB1 exon 3 mutations are markers for aggressive tumor phenotypes and poor prognosis. *Am J Pathol* 2001; 158: 987-96.

Garcia-Rostan G, Costa AM, Pereira-Castro I, Salvatore G, Hernandez R, Hermsem MJ, Herrero A, Fusco A, Cameselle-Teijeiro J, Santoro M. Mutation of the PIK3CA gene in anaplastic thyroid cancer. *Cancer Res* 2005; 65: 10199-207.

Gitelman I. Twist protein in mouse embryogenesis. *Dev Biol* 1997; 189: 205-14.

Grieco M, Santoro M, Berlingieri MT, Melillo RM, Donghi R, Borganzone I, Pierotti MA, Della Porta G, Fusco A, Vecchio G. PTC is a novel rearranged form of the ret proto-oncogene and is frequently detected in vivo in human thyroid papillary carcinomas. *Cell* 1990; 60: 557-63.

Gripp KW, Zackai EH, Stolle CA. Mutations in the human TWIST gene. *Hum Mutat* 2000; 15: 150-5.

Guijarro MV, Leal JF, Fominaya J, Blanco-Aparicio C, Alonso S, Leonart M, Castellvi J, Ruiz L, Ramon Y Cajal S, Carnero A. MAP17 overexpression is a common characteristic of carcinomas. *Carcinogenesis* 2007; 28: 1646-52.

Hamamori Y, Sartorelli V, Ogryzko V, Puri PL, Wu HY, Wang JY, Nakatani Y, Kedes L. Regulation of histone acetyltransferases p300 and PCAF by the bHLH protein twist and adenoviral oncoprotein E1A. *Cell* 1999; 96: 405-13.

Hodgson NC, Button J, Solorzano CC. Thyroid cancer: is the incidence still increasing? *Ann Surg Oncol* 2004; 11(12):1093-7.

Hong J, Zhou J, Fu J, He T, Qin J, Wang L, Liao L, Xu Phosphorylation of serine 68 of Twist 1 by MAPKs stabilizes Twist 1 protein and promotes breast cancer cell invasiveness. *J.Cancer Res.* 2011; 71(11): 3980-90.

Hou P, Liu D, Shan Y, Hu S, Studeman K, Condouris S, Wang Y, Trink A, El-Naggar AK, Tallini G, et al. Genetic alterations and their relationship in the phosphatidylinositol 3-kinase/Akt pathway in thyroid cancer. *Clinical Cancer Research* 2007; 13:1161-70.

Jemal A, Siegel R, Xu J, Ward E. Cancer statistics, 2010. *CA Cancer J Clin* 2010; 60(5):277-300.

Kalluri R. EMT: when epithelial cells decide to become mesenchymal-like cells. *J Clin Invest.* 2009; 119(6): 1417-9.

Kimura ET, Nikiforova MN, Zhu Z, KnaufJA, Nikiforov YE, Fagin JA. High prevalence of BRAF mutations in thyroid cancer: genetic evidence for constitutive activation of the RET/PTC-RAS-BRAF signaling pathway in papillary thyroid carcinoma. *Cancer Res* 2003; 63: 1454-7.

Kondo T, Ezzat S, Asa SL. Pathogenetic mechanisms in thyroid follicular-cell neoplasia. *Nat Rev Cancer* 2006; 6:292–306.

Kroll TG, Sarraf P, Pecciarini L, Chen CJ, Mueller E,

Spiegelman BM, Fletcher JA. PAX8-PPARgamma1 fusion oncogene in human thyroid carcinoma. *Science* 2000; 289: 1357-60.

Leboulleux S, Baudin E, Travagli JP, Schlumberger M. Medullary thyroid carcinoma. *Clin Endocrinol (Oxf)*. 2004; 61(3):299-310.

Lee ML, Chen GG, Vlantis AC, Tse GM, Leung BC, van Hasselt CA. Induction of thyroid papillary carcinoma cell proliferation by estrogen is associated with an altered expression of Bcl-xL. *Cancer J* 2005; 11: 113-21.

Lee TK, Man K, Poon RT, Lo CM, Yuen AP, Ng IO, Ng KT, Leonard W, Fan ST. Twist overexpression correlates with hepatocellular carcinoma metastasis through induction of epithelial-mesenchymal transition. *Clin Cancer Res* 2006; 12: 5369-76.

Li L, Cserjesi P, Olson EN. Dermo-1: a novel twist-related bHLH protein expressed in the developing dermis. *Dev Biol* 1995; 172: 280-92.

Liu Z, Hou P, Ji M, Guan H, Studeman K, Jensen K, Vasko V, El-Naggar AK, Xing M. Highly prevalent genetic alterations in receptor tyrosine kinases and phosphatidylinositol 3-kinase/akt and mitogenactivated protein kinase pathways in anaplastic and follicular thyroid cancers. *Journal of Clinical Endocrinology and Metabolism* 2008; 93: 3106-16.

Lupi C, Giannini R, Ugolini C, Proietti A, Berti P, Minuto M, Materazzi G, Elisei R, Santoro M, Miccoli P, Basolo F. Association of BRAF V600E Mutation with Poor Clinicopathological Outcomes in 500 Consecutive Cases of Papillary Thyroid Carcinoma. *J Clin Endocrinol Metab* 2007; 92: 4085-90.

Ma L, Teruya-Feldstein J, Weinberg RA. Tumour invasion and metastasis initiated by microRNA-10b in breast cancer. *Nature* 2007; 449: 682-8.

Maestro R, Dei Tos AP, Hamamori Y, Krasnokutsky S, Sartorelli V, Kedes L, Doglioni C, Beach DH, Hannon GJ. Twist is a potential oncogene that inhibits apoptosis. *Genes Dev* 1999; 13: 2207-17.

Mani SA, Guo W, Liao MJ, Eaton EN, Ayyanan A, Zhou AY, Brooks M, Reinhard F, Zhang CC, Shipitsin M, Campbell LL, Polyak K, Briskin C, Yang J, Weinberg RA. The epithelial-mesenchymal transition generates cells with properties of stem cells. *Cell* 2008; 133: 704-15.

Maniè S, Santoro M, Fusco A, Billaud M. The RET receptor: function in development and dysfunction in congenital malformation. *Trends Genet.* 2001; 17(10): 580-9.

McIver B, Hay ID, Giuffrida DF, Dvorak CE, Grant CS, Thompson GB, van Heerden JA, Goellner JR. Anaplastic thyroid carcinoma: a 50-year experience at a single institution. *Surgery* 2001; 130(6): 1028-34.

Mironchik Y, Winnard PT Jr, Vesuna F, Kato Y, Wildes F, Pathak AP, Kominsky S, Artemov D, Bhujwala Z, Van Diest P, Burger H, Glackin C, Raman V. Twist over expression induces in vivo angiogenesis and correlates with chromosomal instability in breast cancer. *Cancer Res* 2005: 10801-9.

Miyake N, Maeta H, Horie S, Kitamura Y, Nanba E, Kobayashi K, Terada T. Absence of mutations in the beta-catenin and adenomatous polyposis coli genes in papillary and follicular thyroid carcinomas. *Pathol Int* 2001; 51: 680-5.

Murray SS, Glackin CA, Winters KA, Gazit D, Kahn AJ, Murray EJ. Expression of helix-loop-helix regulatory genes during differentiation of mouse osteoblastic cells. *J Bone Miner Res* 1992; 7: 1131-8.

Namba H, Nakashima M, Hayashi T, Hayashida N, Maeda S, Rogounovitch TI, Ohtsuru A, Saenko VA, Kanematsu T, Yamashita S. Clinical implication of hot spot BRAF mutation, V599E, in papillary thyroid cancers. *J Clin Endocrinol Metab* 2003; 88: 4393-7.

Nikiforov YE. Genetic alterations involved in the transition from well-differentiated to poorly differentiated and anaplastic thyroid carcinomas. *Endocr Pathol.* 2004; 15(4): 319-27.

Pan D, Fujimoto M, Lopes A, Wang YX. Twist-1 is a PPARdelta-inducible, negative-feedback regulator of PGC-1alpha in brown fat metabolism. *Cell* 2009; 137: 73-86.

Pan DJ, Huang JD, Courey AJ. Functional analysis of the *Drosophila* twist promoter reveals a dorsal-binding ventral activator region. *Genes Dev* 1991; 5: 1892-901.

Pelicci G, Troglio F, Bodini A, Melillo RM, Pettirossi V, Coda L, De Giuseppe A, Santoro M, Pelicci PG. The neuron-specific Rai (ShcC) adaptor protein inhibits apoptosis by coupling Ret to the phosphatidylinositol 3-kinase/Akt signaling pathway. *Mol Cell Biol* 2002; 20: 7351-63.

Perri F, Lorenzo GD, Scarpati GD, Buonerba. Anaplastic thyroid carcinoma: A comprehensive review of current and future therapeutic options. *World J Clin Oncol*. 2011; 2(3):150-7.

Pettersson AT, Mejhert N, Jernås M, Carlsson LM, Dahlman I, Laurencikiene J, Arner P, Rydén M. Twist 1 in human white adipose tissue and obesity. *J Clin Endocrinol Metab*. 2011; 96(1): 133-41.

Pham CG, Bubici C, Zazzeroni F, Knabb JR, Papa S, Kuntzen C, Franzoso G. Upregulation of Twist-1 by NF-kappaB blocks cytotoxicity induced by chemotherapeutic drugs. *Mol Cell Biol* 2007; 27: 3920-35.

Pierie JP, Muzikansky A, Gaz RD, Faquin WC, Ott MJ. The effect of surgery and radiotherapy on outcome of anaplastic thyroid carcinoma. *Ann Surg Oncol*. 2002; 9(1): 57-64.

Powell DJ Jr. Russell J, Nibu K, Li G, Rhee E, Liao M, Goldstein M, Keane WM, Santoro M, Fusco A, Rothstein JL. The RET/PTC3 oncogene: metastatic solidtype papillary carcinomas in murine thyroids. *Cancer Res* 1998; 58: 5523-8.

Puisieux A, Valsesia-Wittmann S, Ansieau S. A twist for survival and cancer progression. *Br J Cancer* 2006; 94: 13-17.

Pulcrano M, Boukheris H, Talbot M, Caillou B, Dupuy C, Virion A, De Vathaire F, Schlumberger M. Poorly differentiated follicular thyroid carcinoma: prognostic factors and relevance of histological classification. *Thyroid* 2007; 17: 639-46.

Riesco-Eizaguirre G, Gutierrez-Martinez P, Garcia-Cabezas

MA, Nistal M, Santisteban P. The oncogene BRAF V600E is associated with a high risk of recurrence and less differentiated papillary thyroid carcinoma due to the impairment of Na⁺/I⁻-targeting to the membrane. *Endocr Relat Cancer* 2006; 13: 257-69.

Salvatore G, Nappi TC, Salerno P, Jiang Y, Garbi C, Ugolini C, Miccoli P, Basolo F, Castellone MD, Cirafici AM, Melillo RM, Fusco A, Bittner ML, Santoro M. A cell proliferation and chromosomal instability signature in anaplastic thyroid carcinoma. *Cancer Res* 2007; 67(21):10148-58.

Santarpia L, El-Naggar AK, Cote GJ, Myers JN, Sherman SI. Phosphatidylinositol 3-kinase/akt and ras/ raf-mitogen-activated protein kinase pathway mutations in anaplastic thyroid cancer. *Journal of Clinical Endocrinology and Metabolism* 2008; 93: 278-84.

Santoro M, Dathan NA, Berlingieri MT, Borganzone I, Paulin C, Grieco M, Pierotti MA, Vecchio G, Fusco A. Molecular characterization of RET/PTC3; a novel rearranged version of the RET proto-oncogene in human thyroid papillary carcinoma. *Oncogene* 1994; 9: 509-16.

Santoro M, Melillo RM, Carlomagno F, Vecchio G, Fusco A. Minireview: RET: normal and abnormal functions. *Endocrinology* 2004; 145: 5448-51.

Schlumberger MJ. Papillary and follicular thyroid carcinoma. *N Engl J Med* 1998; 338: 297-306.

Segouffin-Cariou C, Billaud M. Transforming ability of MEN2A-RET requires activation of the phosphatidylinositol 3-kinase/AKT signaling pathway. *J Biol Chem* 2000; 275(5): 3568-76.

Sharabi AB, Aldrich M, Sosic D, Olson EN, Friedman AD, Lee SH et al. Twist-2 controls myeloid lineage development and function. *PLoS Biol* 2008; 6: e316.

Shiota M, Izumi H, Onitsuka T, Miyamoto N, Kashiwagi E, Kidani A, Hirano G, Takahashi M, Naito S, Kohno K. Twist and p53 reciprocally regulate target genes via direct interaction. *Oncogene* 2008. 27: 5543-53.

Smit MA, Geiger TR, Song JY, Gitelman I, Peeper DS. A Twist-Snail axis critical for TrkN-induced epithelial-mesenchymal transition-like transformation, anoikis resistance and metastasis. *Mol Cell Biol* 2009; 29: 3722-29.

Soares P, Trovisco V, Rocha AS, Lima J, Castro P, Preto A, Maximo V, Botelho T, Seruca R, Sobrinho-Simoes M. BRAF mutations and RET/PTC rearrangements are alternative events in the etiopathogenesis of papillary thyroid carcinoma. *Oncogene* 2003; 22: 4578-80.

Song K, Li Q, Peng YB, Li J, Ding K, Chen LJ, Shao CH, Zhang LJ, Li P. Silencing of hHS6ST2 inhibits progression of pancreatic cancer through inhibition of Notch signalling. *Biochem J* 2011; 436 :271-82.

Sosic D, Olson EN. A new twist on twist--modulation of the NF-kappa B pathway. *Cell Cycle*; 2003; 2(2):76-8.

Spring J, Yanze N, Middel AM, Stierwald M, Groger H, Schmid V. The mesoderm specification factor twist in the life cycle of jellyfish. *Dev Biol* 2000; 228: 363-75.

Stoetzel C, Weber B, Bourgeois P, Bolcato-Bellemin AL, Perrin-Schmitt F. Dorso-ventral and rostro-caudal sequential expression of M-twist in the postimplantation murine embryo. *Mech Dev* 1995; 51: 251-63.

Street CA, Bryan BA. Rho kinase proteins--pleiotropic modulators of cell survival and apoptosis. *Anticancer Res* 2011; 31(11) :3645-57.

Takano T, Ito Y, Hirokawa M, Yoshida H, Miyauchi A. BRAFV600E mutation in anaplastic thyroid carcinomas and their accompanying differentiated carcinomas. *British Journal of Cancer* 2007; 96: 1549-53.

Tallini G. Molecular pathobiology of thyroid neoplasms. *Endocr Pathol.* 2002; 13(4): 271-88.

Teng Y, Ren MQ, Cheney R, Sharma S, Cowell JK. Inactivation of the WASF3 gene in prostate cancer cells leads to suppression of tumorigenicity and metastases. *Br J Cancer.* 2010;103(7):1066-75.

Thisse B, el MM, Perrin-Schmitt F. The twist gene: isolation of a *Drosophila* zygotic gene necessary for the establishment of dorsoventral pattern. *Nucleic Acids Res* 1987; 15: 3439-53.

Thomas GA, Bunnell H, Cook HA, Williams ED, Nerovnya A, Cherstvoy ED, Tronko ND, Bogdanova TI, Chiappetta G, Viglietto G, Pentimalli F, Salvatore G, Fusco A, Santoro M, Vecchio G. High prevalence of RET/PTC rearrangements in Ukrainian and Belarussian post-Chernobyl thyroid papillary carcinomas: a strong correlation between RET/PTC3 and the solid-follicular variant. *J Clin Endocrinol Metab* 1999; 84: 4232-8.

Ugolini C, Giannini R, Lupi C, Salvatore G, Miccoli P, Proietti A, Elisei R, Santoro M, Basolo F. Presence of BRAF V600E in very early stages of papillary thyroid carcinoma. *Thyroid* 2007; 17: 381-8.

Umbas R, Isaacs WB, Bringuier PP, Schaafsma HE, Karthaus HF, Oosterhof GO, Debruyne FM, Schalken JA. Decreased E-cadherin expression is associated with poor prognosis in patients with prostate cancer. *Cancer Res* 1994; 54: 3929-33.

Valsesia-Wittmann S, Magdeleine M, Dupasquier S, Garin E, Jallas AC, Combaret V et al. Oncogenic cooperation between Htwist and N-Myc overrides failsafe programs in cancer cells. *Cancer Cell* 2004; 6: 625-30.

van der Gun BT, Melchers LJ, Ruiters MH, de Leij LF, McLaughlin PM, Rots MG. EpCAM in carcinogenesis: the good, the bad or the ugly. *Carcinogenesis* 2010; 31:1913-21.

Vesuna F, van Dienst P, Chen JH, Raman V. Twist is a transcriptional repressor of E-cadherin gene expression in breast cancer. *Biochem Biophys Res Commun* 2008; 367: 235-41.

Volante M, Collini P, Nikiforov YE, Sakamoto A, Kakudo K, Katoh R, Lloyd RV, LiVolsi VA, Papotti M, Sobrinho-Simoes M, Bussolati G, Rosai J. Poorly differentiated thyroid carcinoma: the Turin proposal for the use of uniform diagnostic criteria and an algorithmic diagnostic approach. *Am J Surg Pathol*. 2007; 31(8): 1256-64.

Wallerand H, Robert G, Pasticier G, Ravaud A, Ballanger P, Reiter RE, Ferrière JM. The epithelial-mesenchymal transition-

inducing factor TWIST is an attractive target in advanced and/or metastatic bladder and prostate cancers. *Urol Oncol* 2009; 28: 473-9.

Wang SM, Coljee VW, Pignolo RJ, Rotenberg MO, Cristofalo VJ, Sierra F. Cloning of the human twist gene: its expression is retained in adult mesodermally-derived tissues. *Gene* 1997; 187: 83-92.

Wang X, Ling MT, Guan XY, Tsao SW, Cheung HW, Lee DT, Wong YC. Identification of a novel function of TWIST, a bHLH protein, in the development of acquired taxol resistance in human cancer cells. *Oncogene*. 2004; 23(2): 474-82.

Welch DR, Steeg PS, Rinker-Schaeffer CW. Molecular biology of breast cancer metastasis. Genetic regulation of human breast carcinoma metastasis. *Breast Cancer Res* 2000; 2: 408-16.

Williams D. Cancer after nuclear fallout: lessons from the Chernobyl accident. *Nat Rev Cancer*. 2002; 2(7): 543-9.

Wolf C, Thisse C, Stoetzel C, Thisse B, Gerlinger P, Perrin-Schmitt F. The M-twist gene of *Mus* is expressed in subsets of mesodermal cells and is closely related to the *Xenopus* X-twi and the *Drosophila* twist genes. *Dev Biol* 1991; 143:363-73.

Wu G, Mambo E, Guo Z, Hu S, Huang X, Gollin SM, Trink B, Ladenson PW, Sidransky D, Xing M. Uncommon mutation, but common amplifications, of the PIK3CA gene in thyroid tumors. *J Clin Endocrinol Metab* 2005; 90: 4688-93.

Xing M. BRAF Mutation in Papillary Thyroid Cancer: Pathogenic Role, Molecular Bases, and Clinical Implications. *Endocr Rev* 2007; 28(7): 742-62.

Yang J, Mani SA, Donaher JL, Ramaswamy S, Itzykson RA, Come C, Savagner P, Gitelman I, Richardson A, Weinberg RA. Twist, a master regulator of morphogenesis, plays an essential role in tumor metastasis. *Cell*. 2004; 117(7):927-39.

Yang MH, Chen CL, Chau GY, Chiou SH, Su CW, Chou TY, Peng WL, Wu JC. Comprehensive analysis of the independent effect of twist and snail in promoting metastasis of hepatocellular carcinoma. *Hepatology* 2009; 50: 1464-74.

Yuen HF, Chua CW, Chan YP, Wong YC, Wang X, Chan KW. Significance of TWIST and E-cadherin expression in the metastatic progression of prostatic cancer. *Histopathology* 2007; 50: 648-58.

Zhang Z, Xie D, Li X, Wong YC, Xin D, Guan XY, Chua CW, Leung SC, Na Y, Wang X. Significance of TWIST expression and its association with E-cadherin in bladder cancer. *Hum Pathol* 2007; 38: 598-606.

Zhao P, Hoffman EP. Embryonic myogenesis pathways in muscle regeneration. *Dev Dyn* 2004; 229:380-92.

Attached manuscript II

Salerno P, Garcia-Rostan G, Piccinin S, **Bencivenga TC**, Di Maro G, Doglioni C, Basolo F, Maestro R, Fusco A, Santoro M, Salvatore G. TWIST1 plays a pleiotropic role in determining the anaplastic thyroid cancer phenotype. *J Clin Endocrinol Metab.* 2011 May;96(5):E772-81.

TWIST1 Plays a Pleiotropic Role in Determining the Anaplastic Thyroid Cancer Phenotype

Paolo Salerno, Ginesa Garcia-Rostan, Sara Piccinin, Tammaro Claudio Bencivenga, Gennaro Di Maro, Claudio Doglioni, Fulvio Basolo, Roberta Maestro, Alfredo Fusco, Massimo Santoro, and Giuliana Salvatore

Dipartimento di Biologia e Patologia Cellulare e Molecolare c/o Istituto di Endocrinologia ed Oncologia Sperimentale del Consiglio Nazionale delle Ricerche (P.S., T.C.B., G.D.M., A.F., M.S.), Università di Napoli "Federico II," 80131 Naples, Italy; Institute of Molecular Pathology and Immunology (G.G.-R.), University of Porto, 4200-465 Porto, Portugal; Instituto de Biología y Genética Molecular (G.G.-R.), Universidad Valladolid–Consejo Superior de Investigaciones Científicas, 47003 Valladolid, Spain; Experimental Oncology 1 (S.P., R.M.), Centro di Riferimento Oncologico, Istituto di Ricovero e Cura a Carattere Scientifico, Aviano National Cancer Institute, 33081 Aviano (Pordenone), Italy; Università Vita-Salute San Raffaele (C.D.), Istituto Scientifico San Raffaele, 20132 Milan, Italy; Division of Pathology (F.B.), Department of Surgery, University of Pisa, 56126 Pisa, Italy; and Dipartimento di Studi delle Istituzioni e dei Sistemi Territoriali (G.S.), Università "Parthenope," 80133 Naples, Italy

Context: Anaplastic thyroid carcinoma (ATC) is one of the most aggressive human tumors; it is characterized by chemoresistance, local invasion, and distant metastases. ATC is invariably fatal.

Objective: The aim was to study the role of TWIST1, a basic helix-loop-helix transcription factor, in ATC.

Design: Expression of TWIST1 was studied by immunohistochemistry and real-time PCR in normal thyroids and well-differentiated, poorly differentiated, and ATC. The function of TWIST1 was studied by RNA interference in ATC cells and by ectopic expression in well-differentiated thyroid carcinoma cells.

Results: ATCs up-regulate TWIST1 with respect to normal thyroids as well as to poorly and well-differentiated thyroid carcinomas. Knockdown of TWIST1 by RNA interference in ATC cells reduced cell migration and invasion and increased sensitivity to apoptosis. The ectopic expression of TWIST1 in thyroid cells induced resistance to apoptosis and increased cell migration and invasion.

Conclusions: TWIST1 plays a key role in determining malignant features of the anaplastic phenotype *in vitro*. (*J Clin Endocrinol Metab* 96: E772–E781, 2011)

Thyroid neoplasms include a broad spectrum of histotypes, ranging from benign adenomas to differentiated papillary and follicular, poorly differentiated, and rapidly growing anaplastic carcinomas (1, 2). Papillary thyroid carcinoma (PTC) far outnumbers the other morphological subtypes and is characterized, in general, by an indolent phenotype with a 10-yr survival rate of up to 90% (1, 2). Poorly differentiated carcinomas (PDC) include a heterogeneous group of neoplasms with morphological

features and clinical characteristics intermediate between those of well-differentiated and anaplastic carcinomas (1, 2). Anaplastic thyroid carcinomas (ATC) represent less than 2% of all thyroid cancers but are responsible for more than 50% of thyroid cancer mortality, with a mean survival time from diagnosis of 4–12 months (3). ATC is highly invasive, and the majority of ATC patients die from suffocation due to locoregional disease extension or because of overwhelming distant metastatic disease. Surgical

treatment, radiotherapy, and chemotherapy, based primarily on doxorubicin and cisplatin, show little efficacy in ATC patients (3, 4). ATC cells feature a highly mitogenic and motile phenotype and epithelial-mesenchymal transition and are refractory to apoptotic cell death (3, 4). ATC features genetic lesions that are typical of a well-differentiated carcinoma, namely BRAF or RAS point mutations. Only a few genetic lesions have been identified exclusively in ATC, *i.e.* p53, PI3KCA, or β -catenin mutations (5–8). Therefore, the molecular mechanisms driving the establishment of the highly aggressive anaplastic phenotype are still largely unknown (2–5).

We have recently identified, through a cDNA microarray analysis, a gene expression signature that is associated with the highly proliferative and aneuploid ATC phenotype (9). Among the genes highly up-regulated in ATC *vs.* normal tissue and PTC, we have isolated TWIST1. TWIST1 is a highly conserved basic helix-loop-helix transcription factor that plays a key role in mesodermal, myoblast, and osteoblast differentiation (10, 11). Mutational inactivation of TWIST1 is responsible for the Saethre-Chotzen syndrome, an autosomal dominant disorder characterized by premature fusion of the cranial sutures, skull deformations, limb abnormalities, and facial dysmorphism (12). TWIST1 plays an important role in the development and progression of human cancer. TWIST1 overexpression is reported in many human tumors, including rhabdomyosarcoma, glioma, melanoma, breast, gastric, and prostate carcinomas (13, 14). Elevated TWIST1 protein levels are associated with advanced tumor stage and poor prognosis in several cancer types (14, 15). TWIST1 promotes epithelial-mesenchymal transition (16, 17). TWIST1 gene amplification is associated with resistance to chemotherapeutic agents (18, 19). Finally, TWIST1 inhibits premature senescence in cancer cells (20).

Here we report that TWIST1 plays a key role in the ATC phenotype *in vitro* and suggest that it may mediate chemoresistance of ATC cells.

Materials and Methods

Reagents

Staurosporine and cisplatin were obtained from Sigma-Aldrich (St. Louis, MO).

Cell cultures

Human cell lines (S11N, P5 4N, 8505C, CAL62, SW1736, OCUT-2, ACT-1, TPC-1, BCPAP) (21–23), rat cell lines (PC RET/PTC1, PC RET/PTC3, PC *v*-HRAS, PC-BRAF-V600E, PC-TRK-T1, PC *v*-RAF, PC *v*-MOS, PC E1A, and PC E1A-*v*-RAF) (24, 25), and culture conditions are detailed in the Supplemental Data (published on The Endocrine Society's Journals Online web site at <http://jcem.endojournals.org>).

Tissue samples

Tumors and normal thyroid (NT) tissue samples for immunohistochemical analysis were retrieved from the files of the Pathology Department of the Hospital Central de Asturias (Oviedo University, Asturias, Spain) and of the Hospital Clinico Universitario de Santiago de Compostela (Santiago de Compostela University, Galicia, Spain). Tumors and NT tissue samples for RNA extraction and quantitative RT-PCR were retrieved from the files of the Department of Surgery, University of Pisa (Pisa, Italy). Case selection was based on the histological findings and on the availability of adequate material for RNA extraction. All histological diagnoses were reviewed by two blinded pathologists (G.G.-R. and C.D.) according to the latest recommendations about diagnostic features of PTC, PDC, and ATC (26–28). PDC were defined as malignant tumors of follicular cells displaying predominant solid/trabecular/insular growth patterns, high-grade features such as mitoses (more than three to five mitoses \times 10 high power field) and/or necrosis and convoluted nuclei, with or without concurrent differentiated components of the follicular or papillary type. ATC were defined as tumors displaying admixtures of spindle, pleomorphic giant, and epithelioid cells; high mitotic activity; extensive coagulative necrosis with irregular borders; and infiltration of vascular walls often accompanied by obliteration of the vascular lumina. After microscopic examination of exhaustively sampled specimens, 32 tumors were classified as PTC, 93 as PDC, and 56 as ATC. Processing of samples and of patient information proceeded in agreement with review board-approved protocols.

Immunohistochemistry

Formalin-fixed and paraffin-embedded 3- to 5- μ m-thick tumor sections were deparaffinized, placed in a solution of absolute methanol and 0.3% hydrogen peroxide for 30 min, and treated with blocking serum for 20 min. The slides were incubated with mouse monoclonal antibodies against TWIST1 (sc-81417; Santa Cruz Biotechnology, Santa Cruz, CA) and processed according to standard procedures. Negative controls by omitting the primary antibody were included in the assay. Cases were scored as positive when unequivocal brown staining was observed in the nuclei of tumor cells. Immunoreactivity was expressed as the percentage of positively stained target cells in four intensity categories (–, no staining; +, low/weak; ++, moderate/distinct; +++, high/intense). Twist1 score values were independently assigned by two blinded investigators (G.G.-R. and C.D.), and a consensus was reached on all scores used for computation.

RNA extraction and expression studies

Total RNA was isolated with the RNeasy Kit (QIAGEN, Crawley, West Sussex, UK). The quality of the RNAs was verified by the 2100 Bioanalyzer (Agilent Technologies, Waldbronn, Germany); only samples with an RNA integrity number value above 7 were used for further analysis. Real-time PCR was performed as detailed in the Supplemental Data: for the calculation of expression fold changes, sample 1 represented each single tumor sample, and sample 2 was the average of all ($n = 22$) NTs. Microarray methods are also reported in the Supplemental Data.

Protein studies

Immunoblotting was carried out according to standard procedures. Anti-TWIST1 (sc-81417) and anti-p53 (Pab 240) monoclonal antibodies were from Santa Cruz Biotechnology; monoclonal anti- α -tubulin antibody was from Sigma-Aldrich; anti-cleaved (Asp175) caspase-3 p17 and p19 fragments polyclonal (5A1) antibody was from Cell Signaling Technology, Inc. (Beverly, MA). Secondary antimouse and antirabbit antibodies coupled to horseradish peroxidase were from Santa Cruz Biotechnology.

RNA silencing

Small inhibitor duplex RNA targeting TWIST1 (no. 3, 5, and 7) and the scrambled control [nonspecific small interfering RNA (siRNA) duplex containing the same nucleotides but in irregular sequence] have been described previously (16) and were chemically synthesized by Sigma-Aldrich. Based on its higher silencing efficiency, TWIST1 siRNA 3 (hereafter referred to as TWIST1 siRNA) was selected and used throughout the paper. The day of transfection, 1×10^5 cells were incubated with 50 nM siRNA and electroporated using MicroPorator (MP-100, Digital Bio; Euroclone, Milan, Italy) according to the manufacturer's instructions. Cells were harvested 24, 48, and 72 h after transfection, counted, and analyzed for protein expression. Methods used to determine cell viability, motility, and invasion are detailed in the Supplemental Data.

TWIST1 transfection

The pcDNA 3-TWIST1 vector is described elsewhere (29). TPC-1 cells were transfected by using the Lipofectamine Reagent (Invitrogen, Carlsbad, CA) according to the instructions of the manufacturer. Two days later, G418 (Invitrogen) was added at a concentration of 1.2 mg/ml. Two mass populations of several clones and three independent cell clones were isolated, expanded, and screened for TWIST1 expression by Western blot and RT-PCR analysis. One mass population and two cell clones transfected with the control pcDNA 3 vector were expanded. To generate stable shRNA (short hairpin RNA)-expressing cell line, CAL62 cells were transfected with shTWIST1 and shLUC vectors (20) by using the Lipofectamine reagent (Invitrogen) according to the instructions of the manufacturer. Two days later, puromycin (Invitrogen) was added at a concentration of 0.5 mg/ml. Mass populations and several cell clones were isolated, expanded, and screened for TWIST1 knockdown by Western blot and RT-PCR analysis. Methods used to determine cell viability, motility, and invasion are detailed in the Supplemental Data.

Statistical analysis

Statistical analyses were carried out using the GraphPad In-Stat software program (version 3.06.3; GraphPad Software, Inc., San Diego, CA). All *P* values were two-sided, and differences were significant when *P* < 0.05.

Results

Up-regulation of TWIST1 in ATC

We evaluated TWIST1 expression levels by immunohistochemistry in 157 human tissues including: 15 NT, 13

PTC, 88 PDC, and 41 ATC samples. Representative immunohistochemical staining is shown in Fig. 1A, and the entire dataset is reported in Table 1. TWIST1 was virtually undetectable in NT, PTC, and PDC samples. In contrast, 49% of the ATC samples (20 of 41) were positive for TWIST1 expression. Positivity ranged between at least 5 and no more than 25% (+) to at least 60% (+++) of cells (Fig. 1A and Table 1); no staining was observed in the absence of the primary antibody (data not shown). TWIST1 positivity correlated with moderate/high proliferation rate assessed by Ki67/MIB1 immunoreactivity (Freeman-Halton extension of the Fisher exact probability test, *P* = 0.048) (Supplemental Table 1). There was also a trend for a significant association with up-regulation of the cell cycle regulated minichromosome maintenance 5 protein (Freeman-Halton extension of the Fisher exact probability test, *P* = 0.11) (data not shown). TWIST1 expression correlated with the fusocellular ATC phenotype and inversely correlated with the epithelioid ATC phenotype (χ^2 test, *P* = 0.0002; Freeman-Halton extension of the Fisher exact probability test, *P* = 0.0001) (Supplemental Table 1), suggesting that TWIST1 is involved in mesenchymal transition of ATC cells. Accordingly, there was a trend toward a correlation between TWIST1 up-regulation and lack of β -catenin staining at the plasma membrane (Freeman-Halton extension of the Fisher exact probability test, *P* = 0.119) (data not shown). Finally, TWIST1 positivity correlated with p53 positivity (Freeman-Halton extension of the Fisher exact probability test, *P* = 0.030) (Supplemental Table 1).

To determine whether TWIST1 up-regulation also occurred at the RNA level, we examined an independent set of ATC (*n* = 15), PDC (*n* = 4), PTC (*n* = 19), and NT (*n* = 22) samples by quantitative RT-PCR. As shown in Fig. 1B, TWIST1 mRNA was up-regulated by more than 5-fold in about 50% (seven of 15) of the ATC samples, with values greater than 10-fold in 13% (two of 15) of them. NT, PTC, and PDC samples expressed lower TWIST1 levels compared with ATC (*P* < 0.001) (Fig. 1B).

In vertebrates, there are two TWIST genes, TWIST1 and TWIST2 (also known as Dermo1), and their encoded proteins show an identity in the basic helix-loop-helix domain of more than 90% (20). Therefore, we also measured TWIST2 expression by quantitative RT-PCR in thyroid tissue samples. TWIST2 was overexpressed in some cases, but at a lower extent with respect to TWIST1 (Supplemental Fig. 1). Indeed, TWIST2 was up-regulated by more than 2-fold in only about half of the ATC samples (four of nine), with values greater than 5-fold in only one of nine ATC samples. No PTC sample up-regulated TWIST2 (Supplemental Fig. 1A).

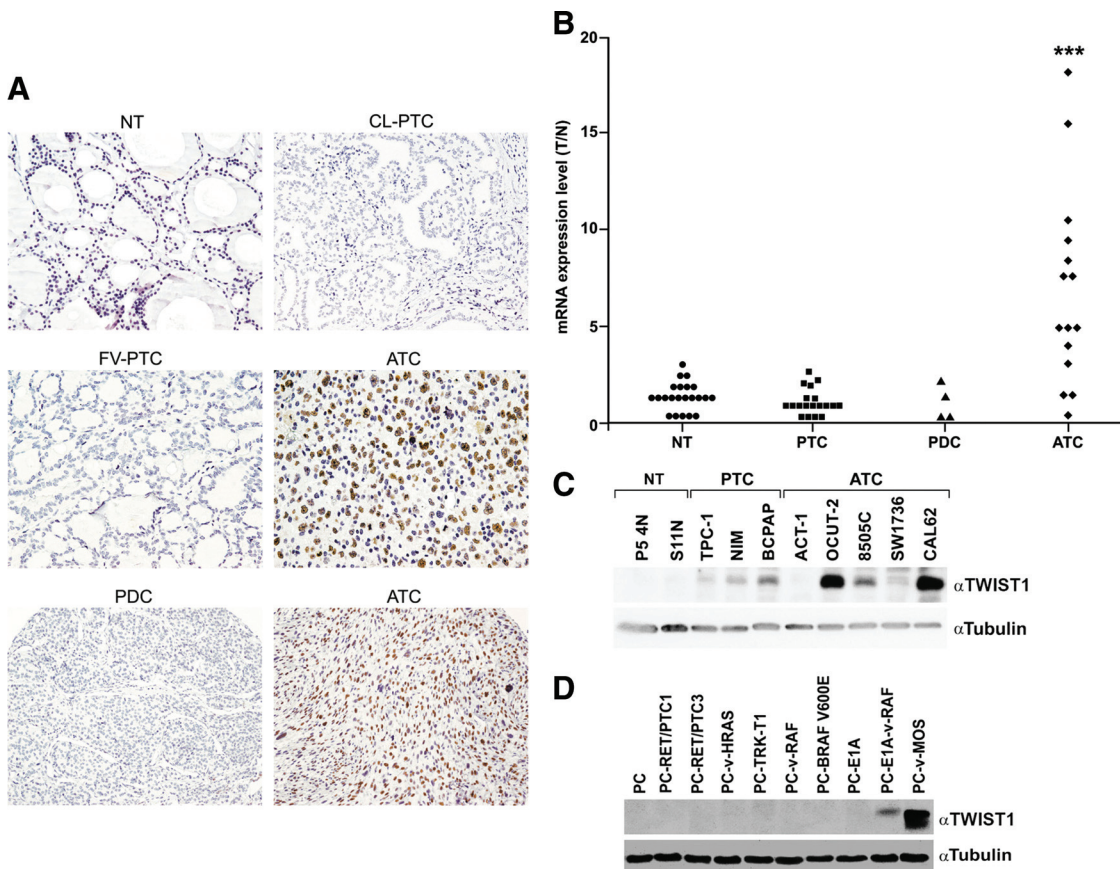


FIG. 1. Expression of TWIST1 in thyroid tissue samples and in cell lines. A, Immunohistochemical analysis of TWIST1 protein expression in normal and malignant thyroid tissues. Representative histological sections from NT (20× magnification), classical PTC (CL-PTC; 10× magnification), follicular variant PTC (FV-PTC; 20× magnification), PDC (4× magnification), and ATC (20× and 4× magnification) stained with a mouse monoclonal anti-TWIST1 antibody are shown. The NT, CL-PTC, FV-PTC, and PDC sections were negative for TWIST1, whereas the two ATC cases featured high/intense immunoreactivity levels (+++, e.g. ≥60% of cells); in particular, the ATC sample at 20× magnification showed 65% of positive cells, whereas the ATC at 4× magnification showed 85% of positive cells. B, Quantitative RT-PCR of TWIST1 mRNA in NT (n = 22), PTC (n = 19), PDC (n = 4) and ATC (n = 15) snap-frozen tissue samples. The level of TWIST1 expression in each sample was measured by comparing its fluorescence threshold with the average fluorescence threshold of the NT samples. The average results of triplicate samples are plotted. C, NT follicular cells (P5 4N and S11N), PTC (TPC-1, NIM, and BCPAP), and ATC (ACT-1, OCUT-2, 8505C, SW1736, and CAL62) cell lines were analyzed by immunoblot using a mouse monoclonal anti-TWIST1 antibody. Anti α -tubulin monoclonal antibody was used as a control for equal protein loading. D, Immunoblot of TWIST1 expression in rat thyroid PC cells expressing the indicated oncogenes. ***, $P < 0.001$.

Up-regulation of TWIST1 in thyroid cancer cell lines

We analyzed TWIST1 expression in cultured human thyroid cells. To this aim, we used primary cultures of NT follicular cells (P5 4N and S11N) and a panel of PTC

TABLE 1. TWIST1 expression in thyroid samples (n = 157)

Tissue	TWIST1 positivity, % of positive samples (positive/total samples)		
NT	0% (0/15)		
PTC	0% (0/13)		
PDC	0% (0/88)		
ATC	49% (20/41)	+	17% (7/41)
		++	15% (6/41)
		+++	17% (7/41)

+, ≥5 to ≤25% of positive cells; ++, >25 to <60% of positive cells; +++, ≥60% of positive cells.

(TPC-1, NIM, BCPAP) and ATC (ACT-1, OCUT-2, 8505C, SW1736, CAL62) cell lines. Western blot analysis showed up-regulation of a band at approximately 26 kDa, which corresponded to the TWIST1 protein only in the ATC cell lines OCUT-2, 8505C, and CAL62 (Fig. 1C). TWIST1 expression was lower in the other ATC cells and in all the PTC cell lines analyzed, whereas it was undetectable in NT cells (Fig. 1C). RT-PCR analysis confirmed the Western blot results (data not shown). Finally, CAL62 and BCPAP also up-regulated TWIST2 mRNA by more than 2-fold with respect to NT cells (Supplemental Fig. 1B).

To confirm TWIST1 expression in a model cell system and to start exploring whether TWIST1 up-regulation correlated with loss of differentiation or with an aggressive tumor phenotype, we used a panel of rat thyroid follicular Fischer rat-derived thyroid follicular cell

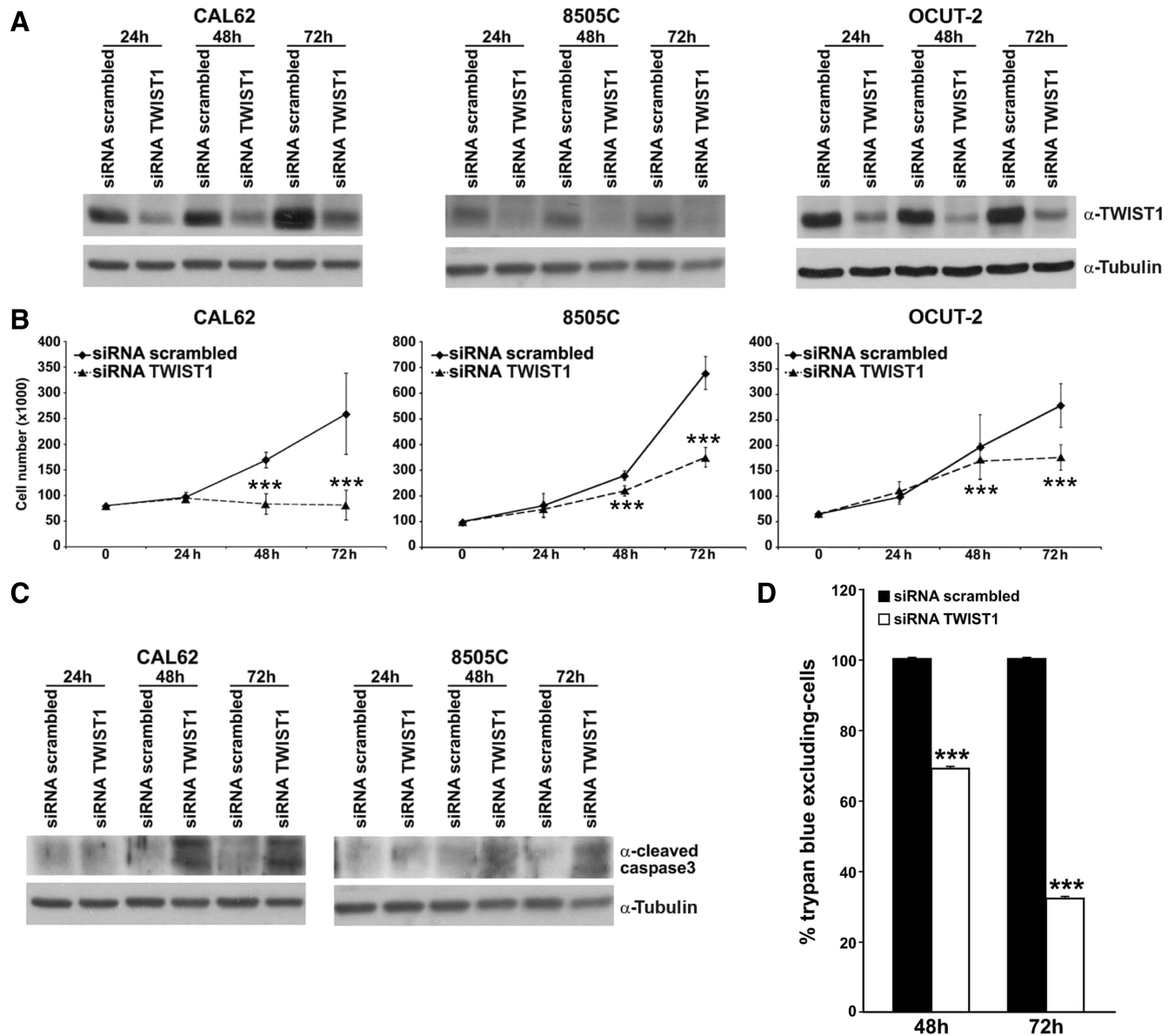


FIG. 2. Effects of TWIST1 knockdown in ATC cells. A, CAL62, 8505C, and OCUT-2 cells were transfected with TWIST1 siRNA or with scrambled siRNA. Cells were harvested at different time points, and protein lysates were subjected to immunoblotting with the indicated antibodies. B, CAL62, 8505C, and OCUT-2 cells were transfected with TWIST1 siRNA or with scrambled siRNA and counted at different time points. Values represent the average of triplicate experiments \pm 95% confidence intervals. C, CAL62 and 8505C cells were transfected with TWIST1 siRNA or with scrambled siRNA. Cells were harvested at different time points, and protein lysates were subjected to immunoblotting with the indicated antibodies. D, The indicated cell lines were transfected with TWIST1 siRNA or scrambled siRNA; after 48 and 72 h, cells were collected by trypsinization, stained for 10 min with trypan blue, and counted in triplicate. The percentage of trypan blue excluding cells compared with cells transfected with siRNA scrambled is reported \pm sd. ***, $P < 0.001$.

line PC CI 3 (PC) cells adoptively expressing various oncogenes (PC-RET/PTC1, PC-RET/PTC3, PC-v-HRAS, PC-TRK-T1, PC-v-RAF, PC-BRAF V600E, PC-E1A, PC-E1A-v-RAF, and PC-v-MOS). Although the expression of v-MOS and of the E1A/v-RAF combination enabled PC cells to grow in semisolid medium and to induce tumors in athymic mice, the expression of the RET/PTC1/3, HRAS, TRK, RAF (v-RAF and BRAF) and E1A oncogenes only caused loss of differentiation without fostering a tumorigenic phenotype (24, 25). Figure 1D shows that TWIST1 was only expressed in the PC cells

transformed by v-MOS, and at lower levels by E1A + v-RAF. Therefore, TWIST1 up-regulation correlated with malignant phenotype rather than loss of differentiation of rat thyroid cells.

Knockdown of TWIST1 induces apoptosis of ATC cells

We evaluated the effects of TWIST1 ablation in ATC cells by RNA interference. We initially tested, by Western blot in CAL62 cells, the efficiency of TWIST1 ablation using three different siRNA (no. 3, 5, and 7) (16). TWIST1

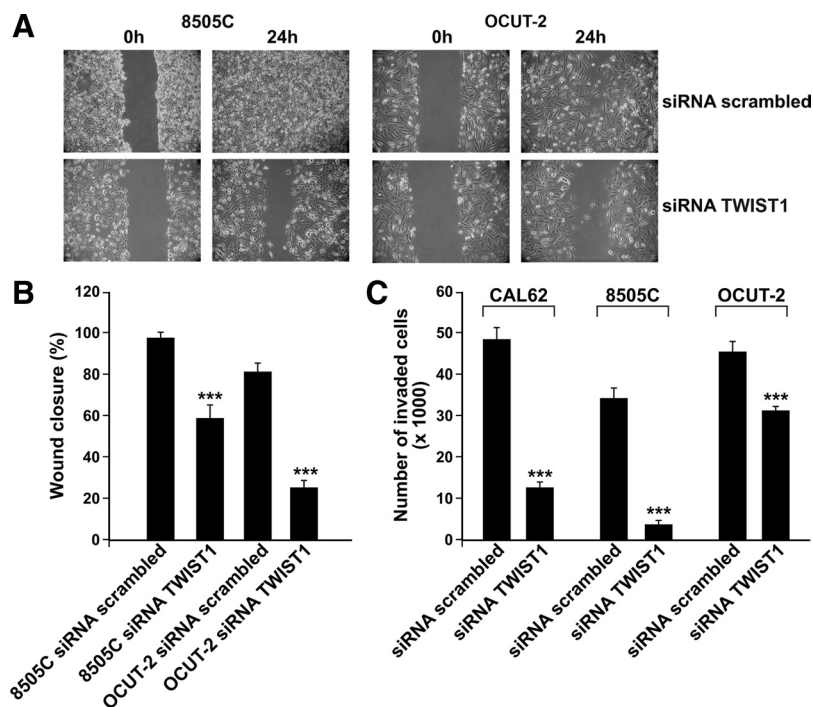


FIG. 3. Effects of TWIST1 knockdown on ATC cell migration and invasion. A, Cells were transfected with TWIST1 siRNA or scrambled siRNA; a scraped wound was introduced, and cell migration into the wound was monitored at 24 h. B, Wound closure was measured by calculating pixel densities in the wound area and expressed as percentage of wound closure of triplicate areas \pm SD. C, Cells were transfected with TWIST1 siRNA or scrambled siRNA; after transfection, cells were seeded in the upper chamber of transwells and incubated for 12 h; the upper surface of the filter was wiped clean, and cells on the lower surface were stained and counted. Invasive ability was expressed as number of invaded cells. Values represent the average of triplicate experiments \pm SD. ***, $P < 0.001$.

siRNA 3 (hereafter named TWIST1 siRNA) reduced TWIST1 protein levels of about 60% (Fig. 2A) and therefore was selected for further experiments, whereas the other two siRNAs (5 and 7) were less effective, with siRNA 5 being practically devoid of any effect and siRNA 7 depleting TWIST1 protein by less than 30% (Supplemental Fig. 2).

We knocked down TWIST1 by transient siRNA TWIST1 transfection in CAL62, 8505C, and OCUT-2 cells. As shown in Fig. 2A, a TWIST siRNA silenced the TWIST1 protein starting at 24 h after transfection, and the effect lasted up to 72 h, whereas a scrambled siRNA control had no effect (Fig. 2A). Thus, cells were transfected with TWIST1 siRNA or with scrambled siRNA and counted at different time points (24, 48, and 72 h) (Fig. 2B). Seventy-two hours after transfection, CAL62 cells transfected with scrambled siRNA numbered 259×10^3 , whereas those transfected with TWIST1 siRNA numbered 81×10^3 ($P = 0.0008$); 8505C cells transfected with scrambled siRNA numbered 679×10^3 , whereas those transfected with TWIST1 siRNA numbered 351×10^3 ($P < 0.0001$); OCUT-2 cells transfected with scrambled siRNA numbered 278×10^3 , and those transfected with

TWIST1 siRNA numbered 176×10^3 ($P = 0.0009$) (Fig. 2B). It should be noted that CAL62, but not 8505C and OCUT-2, expressed detectable levels of TWIST2 (Supplemental Fig. 1B). Thus, it is feasible, because of the high degree of homology between TWIST1 and TWIST2, that the effects of TWIST1 siRNA observed in CAL62 cells were due to the combined inhibition of TWIST1 and TWIST2. Accordingly, at 24 h after siRNA transfection, TWIST2 mRNA was down-regulated by 1.8-fold in CAL62 (data not shown).

At 48 and 72 h, siRNA TWIST1 induced cell apoptosis of CAL62 and 8505C cells as measured by immunoblot with an antibody for the cleaved products of caspase 3 (Fig. 2C). Accordingly, the percentages of trypan blue excluding (viable) cells, of CAL62 transfected with TWIST1 siRNA 48 and 72 h after transfection, were of 69 and 32%, respectively, with respect to scrambled control, confirming that TWIST1 depletion reduced thyroid cancer cell viability ($P < 0.001$) (Fig. 2D).

Because TWIST1 has been associated with premature senescence of cancer cells (20), we performed a senescence-associated β -galactosidase (SA- β -gal) staining assay on siRNA TWIST1-treated cells. Seventy-two hours after transfection with TWIST1 siRNA, the percentage of SA- β -gal-positive cells was 1.3%, whereas it was 0.7% in scrambled siRNA transfected cells. As a positive control, the percentage of SA- β -gal-positive cells was 38% in normal human diploid fibroblasts treated with Etoposide (Sigma-Aldrich) (data not shown). Thus, although significant, senescence induced by TWIST1 knockdown involved only a minor fraction of ATC cells.

Knockdown of TWIST1 impairs cell migration and invasion of ATC cells

We evaluated the migration (by a wound-healing assay) and invasion (by a Matrigel invasion assay) ability of TWIST1 siRNA-transfected cells compared with scrambled siRNA-transfected cells. As shown in Fig. 3A, 8505C and OCUT-2 cells transfected with the scrambled control efficiently migrated into the wound; in contrast, cells transfected with TWIST1 siRNA had a greatly reduced migrating ability ($P < 0.001$). Furthermore, cells transfected with TWIST1 siRNA had a reduced ability to invade Matrigel compared with control cells ($P < 0.001$) (Fig. 3B).

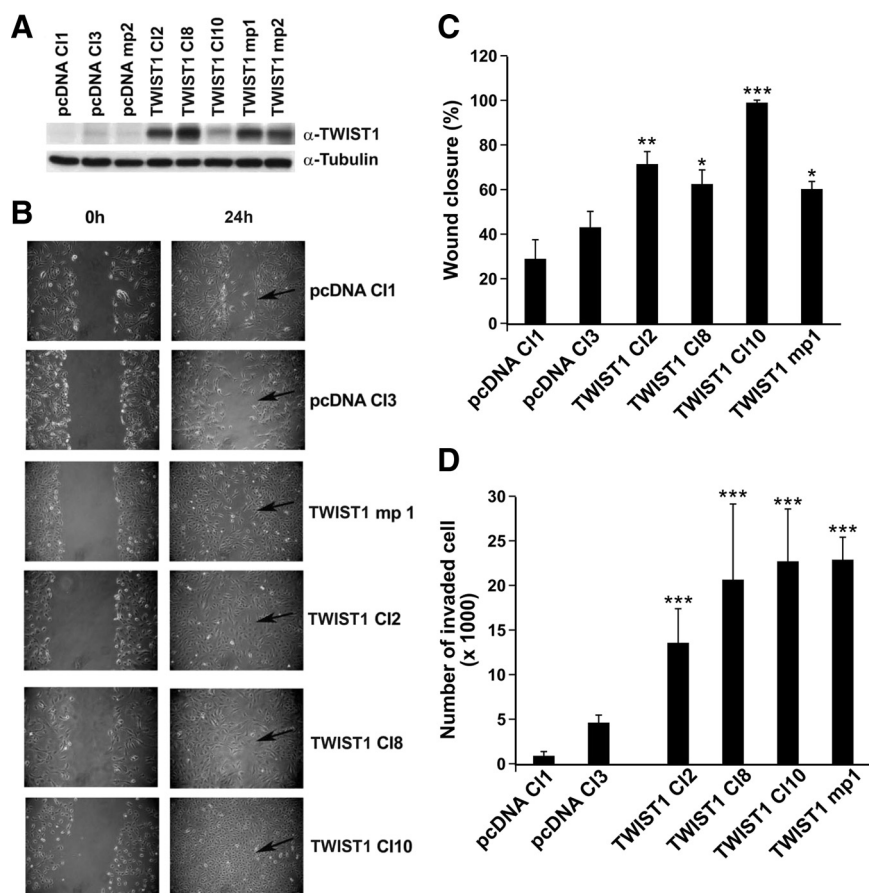


FIG. 4. Effects of TWIST1 overexpression on TPC-1 cell migration and invasion. A, Expression levels of TWIST1 in TPC-1-transfected cells. After G418 selection, cells were lysed and blotted with the indicated antibodies. B, A scraped wound was placed on the confluent monolayer of TPC-1 transfected with TWIST1 or the empty vector, and the cell migration into the wound was monitored at 24 h. Arrows indicate the site of wound closure. C, Wound closure was measured by calculating pixel densities in the wound area and expressed as percentage of wound closure of triplicate areas \pm SD. D, Cells were seeded in the upper chamber of transwells and incubated for 12 h; the upper surface of the filter was wiped clean, and cells on the lower surface were stained and counted. Invasive ability was expressed as number of invaded cells. Values represent the average of triplicate experiments \pm SD. *, $P < 0.05$; **, $P < 0.01$; and ***, $P < 0.001$.

Effects of stable silencing of TWIST1 in CAL62 cells

We stably transfected CAL62 cells with an shTWIST1 plasmid or with shLUC control (20). After antibiotic selection, cells were screened by Western blot for TWIST1 expression. A mass population (mp) (shTWIST1 mp) with a TWIST1 knockdown of approximately 52% was used for further study (Supplemental Fig. 3A). Consistent with data obtained upon transient TWIST1 silencing (Fig. 2), shTWIST1 mp cells showed decreased migration and invasion ability with respect to shLUC-transfected cells ($P < 0.001$) (Supplemental Fig. 3, B–D). To address effects of TWIST1 knockdown on chemosensitivity, cells were treated with cisplatin (200 or 1000 nM) or staurosporine (300 or 500 nM) and counted at 24 h. Upon treatment with cisplatin (1000 nM) or staurosporine (300–500 nM), shTWIST1 mp cells had a decreased viability compared with control cells ($P < 0.001$) (Supplemental Fig. 3E).

Finally, the number of colonies formed in semisolid medium (soft agar) was also reduced by 2-fold compared with the shLUC mp control ($P < 0.05$) (Supplemental Fig. 3F). Thus, TWIST1 ablation *in vitro* affected several hallmarks of malignancy of CAL62 cells, including anchorage-independent proliferation, survival, and invasion.

Ectopic TWIST1 promotes cell migration and invasion of PTC cells

PTC cells, TPC-1, which have low endogenous levels of TWIST1, were transfected with a TWIST1-expressing plasmid (pcDNA-TWIST1) or with the empty vector (pcDNA). Mass populations and cell clones were selected in G418 (1.2 mg/ml). TWIST1 expression was increased (~4- to 13-fold) in all the cell lines transfected with TWIST1 compared with the controls (Fig. 4A). Growth rate was similar in TWIST1- and vector-transfected control cell lines (data not shown). Therefore, we studied cell migration using the wound closure assay. As shown in Fig. 4, B and C, migration rate was higher in TWIST1-transfected cells than in control cells ($P < 0.05$). We next seeded TWIST1-transfected and control cells into the top chamber of transwells and evaluated their ability to invade Matrigel.

TPC-1 cells had basal levels of invasiveness, and TWIST1 overexpression further increased this ability by 4- to 6-fold ($P < 0.001$) (Fig. 4D). Thus, TWIST1 stimulated cell motility and invasion, although wound closure and Matrigel invasion extent were not directly proportional to the TWIST1 expression levels (Fig. 4). These findings suggest that the TWIST1 expression level is not the only molecular determinant of thyroid cancer cell invasive phenotype.

Ectopic TWIST1 protects PTC cells from apoptosis

We treated TPC-1 cells transfected with TWIST1 or control vector with different concentrations of cisplatin (200, 1000, and 2000 nM) and counted cell number at 24 h. As shown in Fig. 5A, cell viability was higher in TWIST1-transfected than in control cells upon treatment with the highest drug dose ($P < 0.05$). Moreover,

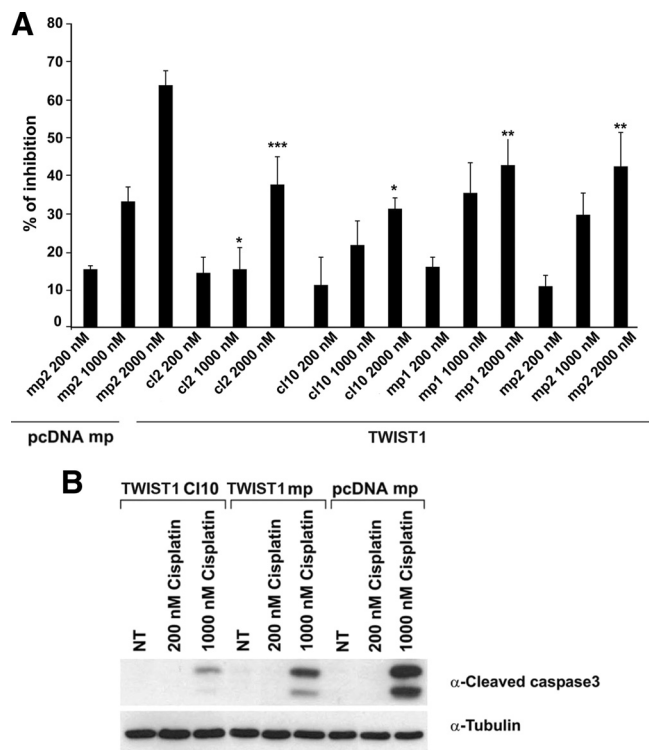


FIG. 5. Effects of TWIST1 overexpression on TPC-1 cell apoptosis. A, The cells were treated with increasing doses of cisplatin and counted 24 h after treatment. Data are shown as percentage of inhibition of cell viability. Values represent the average of three independent experiments \pm SD. *, $P < 0.05$; **, $P < 0.01$; and ***, $P < 0.001$. B, The indicated cell lines were treated with increasing doses of cisplatin, lysed, and blotted with the indicated antibodies.

the amount of caspase 3 cleaved product was lower in TWIST1-transfected than in control cells (Fig. 5B).

Finally, we searched an Affymetrix microarray-based data set for genes that were previously reported to be TWIST1 targets and related to cell cycle and apoptosis control (30). TWIST1-overexpressing cells (TPC-1 TWIST1 mp1, TWIST1 mp2, and TWIST1 Cl2) up-regulated ($P < 0.05$), with respect to pcDNAmp control, the expression of AKT2 (average fold change \pm SD, 2 ± 0.5) and BCL-2 (average fold change \pm SD, 1.67 ± 0.2), whereas they down-regulated the expression of p21CIP/WAF1 (average fold change \pm SD, 0.7 ± 0.3). TWIST1 overexpression, instead, did not significantly change the expression of p14ARF, BAX, and TIMP1 in our system (data not shown).

Discussion

Thyroid cancer includes tumor types as different as well-differentiated carcinomas that have a very good prognosis and undifferentiated carcinomas or ATC that are among the most aggressive human cancers. As yet, the molecular players sustaining such different behavior are largely un-

known. Here, we demonstrate that TWIST1 is up-regulated in ATC samples. Overall TWIST1 up-regulation in ATC is more prominent at the RNA than at the protein level. It is possible that TWIST1 overexpression is affected not only at the transcriptional level but also at the post-transcriptional level. TWIST1 up-regulation was associated with mitotic index, as determined by Ki67/MIB1. However, the fact that TWIST1 did not influence cell proliferation in cultured cells suggests that it is not directly involved in controlling cell proliferation. In ATC samples, TWIST1 positivity also correlated with markers of mesenchymal transition (fusocellular phenotype) and malignancy (p53 positivity); however, correlation with p53 expression was not demonstrated in cultured thyroid cancer cells because TWIST1-positive (OCUT-2, 8505C, and CAL62) and TWIST1-negative (TPC-1, BCPAP, NIM, ACT-1, SW1736) cells both had either high (8505C, ACT-1) or low/undetectable (CAL62, OCUT-2, TPC-1, BCPAP, NIM, SW1736) p53 expression (Supplemental Fig. 4).

In vitro cellular models confirmed the role of TWIST1 in determining the ATC phenotype and identified the ATC features that were sustained by TWIST1 up-regulation. TWIST1 up-regulation did not correlate with loss of differentiation; indeed, it did not occur in PC cells that lost differentiation secondary to the expression of various oncogenes. Rather, TWIST1 overexpression correlated with a malignant phenotype being present in tumorigenic PC-v-MOS and PC-E1A+v-RAF cells (24). Moreover, TWIST1 expression was necessary to counteract spontaneous ATC cell apoptosis and to sustain the invasive and motile phenotype of ATC cells. Accordingly, when overexpressed in PTC cells, TWIST1 promoted cell migration and protected cells from apoptosis. Given the high homology between TWIST1 and -2, the TWIST siRNA also targeted TWIST2 (1.8-fold), albeit at lower levels than TWIST1 (2.5-fold). Thus, it is possible that at least in CAL62 cells effects were due to the combined inhibition of TWIST1 and TWIST2.

TWIST1 expression is responsive to Wnt-1 (31), IGF-I (32), and nuclear factor κ B (NF- κ B) signaling (33). Elements of the Wnt pathway, particularly CTNNB1 (the gene coding β -catenin), were found to be mutated in PDC and ATC (34). Moreover, NF- κ B is activated in human thyroid cancer cells, in particular in ATC (35). Therefore, both the Wnt-1/ β -catenin and NF- κ B pathways are good candidates as mediators of TWIST1 up-regulation in ATC.

Up-regulation of TWIST1 is associated with cellular resistance to anticancer drugs such as cisplatin, taxol, and vincristine in various types of cancers (18, 19, 36). Here, we show that TWIST1 overexpression protected thyroid

cancer cells from cell death induced by cisplatin and staurosporine. This suggests that TWIST1 may be exploited as a molecular marker of the response of thyroid cancer to chemotherapy.

Acknowledgments

We thank G. Vecchio for continuous support. We thank F. Curcio for the P5 4N cells, H. Zitzelsberger for the S11N cells, C. H. Heldin for the SW1736 cells, N. Onoda for the OCUT-2 and ACT-1 cells, and Drs. J. Cameselle-Teijeiro, A. Herrero, and M. Fresno-Forcelledo for providing human ATC samples. We are grateful to Jean Ann Gilder for text editing.

Address all correspondence and requests for reprints to: Giuliana Salvatore, Dipartimento di Studi delle Istituzioni e dei Sistemi Territoriali, Università “Parthenope,” Via Medina 40, 80133 Naples, Italy. E-mail: giuliana.salvatore@uniparthenope.it.

This work was supported by the Associazione Italiana per la Ricerca sul Cancro, the Istituto Superiore di Oncologia, the Italian Ministero della Salute, the Ministero dell’Università e della Ricerca, the European Community Contract FP6-36495, and the Programa Ramón y Cajal–Ministerio de Ciencia e Innovación, Social EU Funds, Universidad de Valladolid, Spain.

Disclosure Summary: The authors have nothing to declare.

References

- Kondo T, Ezzat S, Asa SL 2006 Pathogenetic mechanisms in thyroid follicular-cell neoplasia. *Nat Rev Cancer* 6:292–306
- Fagin JA, Mitsiades N 2008 Molecular pathology of thyroid cancer: diagnostic and clinical implications. *Best Pract Res Clin Endocrinol Metab* 22:955–969
- Smallridge RC, Marlow LA, Copland JA 2009 Anaplastic thyroid cancer: molecular pathogenesis and emerging therapies. *Endocr Relat Cancer* 16:17–44
- Ringel MD 2009 Molecular markers of aggressiveness of thyroid cancer. *Curr Opin Endocrinol Diabetes Obes* 16:361–366
- Nikiforov YE 2004 Genetic alterations involved in the transition from well-differentiated to poorly differentiated and anaplastic thyroid carcinomas. *Endocr Pathol* 15:319–327
- García-Rostán G, Costa AM, Pereira-Castro I, Salvatore G, Hernandez R, Hermsem MJ, Herrero A, Fusco A, Cameselle-Teijeiro J, Santoro M 2005 Mutation of the PIK3CA gene in anaplastic thyroid cancer. *Cancer Res* 65:10199–10207
- Wu G, Mambo E, Guo Z, Hu S, Huang X, Gollin SM, Trink B, Ladenson PW, Sidransky D, Xing M 2005 Uncommon mutation, but common amplifications, of the PIK3CA gene in thyroid tumors. *J Clin Endocrinol Metab* 90:4688–4693
- Malaguarnera R, Vella V, Vigneri R, Frasca F 2007 p53 family proteins in thyroid cancer. *Endocr Relat Cancer* 14:43–60
- Salvatore G, Nappi TC, Salerno P, Jiang Y, Garbi C, Ugolini C, Miccoli P, Basolo F, Castellone MD, Cirafici AM, Melillo RM, Fusco A, Bittner ML, Santoro M 2007 A cell proliferation and chromosomal instability signature in anaplastic thyroid carcinoma. *Cancer Res* 67:10148–10158
- Chen ZF, Behringer RR 1995 Twist is required in head mesenchyme for cranial neural tube morphogenesis. *Genes Dev* 9:686–699
- Thisse B, el Ghouzzi V, Perrin-Schmitt F 1987 The twist gene: isolation of a *Drosophila* zygotic gene necessary for the establishment of dorsoventral pattern. *Nucleic Acids Res* 15:3439–3453
- el Ghouzzi V, Le Merrer M, Perrin-Schmitt F, Lajeunie E, Benit P, Renier D, Bourgeois P, Bolcato-Bellemin AL, Munnich A, Bonaventure J 1997 Mutations of the TWIST gene in the Saethre-Chotzen syndrome. *Nat Genet* 15:42–46
- Maestro R, Dei Tos AP, Hamamori Y, Krasnokutsky S, Sartorelli V, Kedes L, Doglioni C, Beach DH, Hannon GJ 1999 Twist is a potential oncogene that inhibits apoptosis. *Genes Dev* 13:2207–2217
- Puisieux A, Valsesia-Wittmann S, Ansieau S 2006 A twist for survival and cancer progression. *Br J Cancer* 94:13–17
- Valsesia-Wittmann S, Magdeleine M, Dupasquier S, Garin E, Jallas AC, Combaret V, Krause A, Leissner P, Puisieux A 2004 Oncogenic cooperation between H-Twist and N-Myc overrides failsafe programs in cancer cells. *Cancer Cell* 6:625–630
- Yang J, Mani SA, Donaher JL, Ramaswamy S, Itzykson RA, Come C, Savagner P, Gitelman I, Richardson A, Weinberg RA 2004 Twist, a master regulator of morphogenesis, plays an essential role in tumor metastasis. *Cell* 117:927–939
- Kalluri R, Weinberg RA 2009 The basics of epithelial-mesenchymal transition. *J Clin Invest* 119:1420–1428
- Wang X, Ling MT, Guan XY, Tsao SW, Cheung HW, Lee DT, Wong YC 2004 Identification of a novel function of TWIST, a bHLH protein, in the development of acquired taxol resistance in human cancer cells. *Oncogene* 23:474–482
- Li J, Wood 3rd WH, Becker KG, Weeraratna AT, Morin PJ 2007 Gene expression response to cisplatin treatment in drug-sensitive and drug-resistant ovarian cancer cells. *Oncogene* 26:2860–2872
- Ansieau S, Bastid J, Doreau A, Morel AP, Bouchet BP, Thomas C, Fauvet F, Puisieux I, Doglioni C, Piccinin S, Maestro R, Voeltzel T, Selmi A, Valsesia-Wittmann S, Caron de Fromentel C, Puisieux A 2008 Induction of EMT by twist proteins as a collateral effect of tumor-promoting inactivation of premature senescence. *Cancer Cell* 14:79–89
- Schweppe RE, Klopper JP, Korch C, Pugazhenthil U, Benezra M, Knauf JA, Fagin JA, Marlow LA, Copland JA, Smallridge RC, Haugen BR 2008 Deoxyribonucleic acid profiling analysis of 40 human thyroid cancer cell lines reveals cross-contamination resulting in cell line redundancy and misidentification. *J Clin Endocrinol Metab* 93:4331–4341
- Salerno P, De Falco V, Tamburrino A, Nappi TC, Vecchio G, Schweppe RE, Bollag G, Santoro M, Salvatore G 2010 Cytostatic activity of adenosine triphosphate-competitive kinase inhibitors in BRAF mutant thyroid carcinoma cells. *J Clin Endocrinol Metab* 95:450–455
- Curcio F, Ambesi-Impombato FS, Perrella G, Coon HG 1994 Long-term culture and functional characterization of follicular cells from adult normal human thyroids. *Proc Natl Acad Sci USA* 91:9004–9008
- Fusco A, Berlingieri MT, Di Fiore PP, Portella G, Grieco M, Vecchio G 1987 One- and two-step transformations of rat thyroid epithelial cells by retroviral oncogenes. *Mol Cell Biol* 7:3365–3370
- Melillo RM, Castellone MD, Guarino V, De Falco V, Cirafici AM, Salvatore G, Caiazzo F, Basolo F, Giannini R, Kruhoffer M, Orntoft T, Fusco A, Santoro M 2005 The RET/PTC-RAS-BRAF linear signaling cascade mediates the motile and mitogenic phenotype of thyroid cancer cells. *J Clin Invest* 115:1068–1081
- Hedinger C, Williams ED, Sobin LH 1989 The WHO histological classification of thyroid tumors: a commentary on the second edition. *Cancer* 63:908–911
- DeLellis RA, Lloyd R, Heitz PU 2004 WHO classification of tumors: pathology and genetics of tumors of endocrine organs. Lyon, France: IARC Press
- Volante M, Collini P, Nikiforov YE, Sakamoto A, Kakudo K, Katoh R, Lloyd RV, Li Volsi VA, Papotti M, Sobrinho-Simoes M, Bussolati G, Rosai J 2007 Poorly differentiated thyroid carcinoma: the Turin proposal for the use of uniform diagnostic criteria and an algorithmic diagnostic approach. *Am J Surg Pathol* 31:1256–1264
- Demontis S, Rigo C, Piccinin S, Mizzau M, Sonogo M, Fabris M, Brancolini C, Maestro R 2006 Twist is substrate for caspase cleav-

- age and proteasome-mediated degradation. *Cell Death Differ* 13:335–345
30. **Ansieau S, Morel AP, Hinkal G, Bastid J, Puisieux A** 2010 TWISTing an embryonic transcription factor into an oncoprotein. *Oncogene* 29:3173–3184
31. **Reinhold MI, Kapadia RM, Liao Z, Naski MC** 2006 The Wnt-inducible transcription factor TWIST1 inhibits chondrogenesis. *J Biol Chem* 281:1381–1388
32. **Dupont J, Fernandez AM, Glackin CA, Helman L, LeRoith D** 2001 Insulin-like growth factor 1 (IGF-1)-induced twist expression is involved in the anti-apoptotic effects of the IGF-1 receptor. *J Biol Chem* 276:26699–26707
33. **Pham CG, Bubici C, Zazzeroni F, Knabb JR, Papa S, Kuntzen C, Franzoso G** 2007 Upregulation of Twist-1 by NF- κ B blocks cytotoxicity induced by chemotherapeutic drugs. *Mol Cell Biol* 27:3920–3935
34. **Garcia-Rostan G, Tallini G, Herrero A, D'Aquila TG, Carcangiu ML, Rimm DL** 1999 Frequent mutation and nuclear localization of β -catenin in anaplastic thyroid carcinoma. *Cancer Res* 59:1811–1815
35. **Pacifico F, Leonardi A** 2010 Role of NF- κ B in thyroid cancer. *Mol Cell Endocrinol* 321:29–35
36. **Zhang X, Wang Q, Ling MT, Wong YC, Leung SC, Wang X** 2007 Anti-apoptotic role of TWIST and its association with Akt pathway in mediating taxol resistance in nasopharyngeal carcinoma cells. *Int J Cancer* 120:1891–1898



Submit your manuscript to
The Endocrine Society journals for fast turnaround,
rapid publication, and deposits to PubMed.

www.endo-society.org

TWIST1 plays a pleiotropic role in determining the anaplastic thyroid cancer phenotype

Paolo Salerno, Ginesa Garcia-Rostan, Sara Piccinin, Tammaro Claudio Bencivenga, Gennaro Di Maro, Claudio Doglioni, Fulvio Basolo, Roberta Maestro, Alfredo Fusco, Massimo Santoro, Giuliana Salvatore

Supplemental Methods

Cell cultures-Normal thyroid primary S11N cells were provided by H. Zitzelsberger (Department of Radiation Cytogenetics, Neuherberg, Germany) and P5 4N cells were provided by F. Curcio (Università di Udine, Udine, Italia) in 2003. 8505C and CAL62 cells were purchased from DSMZ (Deutsche Sammlung von Mikroorganismen und Zellkulturen GmbH, Braunschweig, Germany) in 2006. SW1736 cells were obtained from N.E. Heldin (University Hospital, Uppsala, Sweden) in 2005. OCUT-2 and ACT-1 cells were provided by N. Onoda (Osaka University of Medicine, Osaka, Japan) in 2005. TPC-1 cells were obtained from M. Nagao (Carcinogenesis Division, National Cancer Center Research Institute, Tokyo, Japan) in 1990. NIM cells were obtained from J. Fagin (Memorial Sloan Kettering Cancer Center, New York, NY) in 1993. BCPAP cells were obtained from N. Fabien (CNRS, Oullins, France) in 1994. 8505C, SW1736 and CAL62 cells were DNA profiled by short tandem repeat analysis in 2009 and shown to be unique and identical to those reported in Schweppe *et al.*, 2008 (1, 2). The BCPAP cell line was genotyped as reported elsewhere Schweppe *et al.*, 2008 (1). The TPC-1 cell line was identified based on the unique presence of the RET/PTC1 rearrangement. S11N cells were grown in RPMI (Invitrogen, Groningen, The Netherlands) containing 20% fetal bovine serum; P5 4N were grown as previously described (3). The thyroid cancer cell lines were grown in Dulbecco's modified Eagle's medium (DMEM) (Invitrogen) containing 10% fetal bovine serum.

The Fischer rat-derived differentiated thyroid follicular cell line PC Cl 3 (hereafter named “PC”) was grown in Coon’s modified Ham F12 medium supplemented with 5% calf serum and a mixture of six hormones (6H): thyrotropin (10mU/ml), hydrocortisone (10nM), insulin (10µg/ml), apo-transferrin (5µg/ml), somatostatin (10ng/ml), and glycyl-histidyl-lysine (10ng/ml) (Sigma-Aldrich, St. Louis, MO). PC adoptively expressing several oncogenes (PC RET/PTC1, PC RET/PTC3, PC v-HRAS, PC-BRAF-V600E, PC-TRK-T1, PC v-RAF, PC v-MOS, PC E1A and PC E1A-v-RAF) have been described previously and cultured in the same medium as PC but without the 6H (4, 5).

Cell culture methods- For cell viability determination, cells were collected by trypsinization, stained for 10 min with 0.4% trypan-blue (Sigma) according to manufacturer’s instructions, and counted in triplicate.

For senescence-Associated-β-galactosidase staining, CAL62 (2×10^5) cells were transfected with TWIST1 siRNA or with scrambled control. Seventy-two h after transfection, the cells were washed twice with PBS, fixed with 2% formaldehyde and 0.2% glutaraldehyde in PBS, and washed twice in PBS. Then, cells were stained overnight in X-gal staining solution [1 mg/ml X-gal, 40 mM citric acid/sodium phosphate (pH 6.0), 5 mM potassium ferricyanide, 5 mM potassium ferrocyanide, 150 mM NaCl, 2 mM MgCl₂] and stained cells were counted. Positive control was represented by normal human diploid fibroblasts IMR-90 treated with Etoposide 20 µM for 24 h.

Cell invasion was examined using a reconstituted extracellular matrix (Matrigel, BD Biosciences, San Jose, CA). The cell suspension (1×10^5 cells per well) was added to the upper chamber of transwell cell culture chambers on a prehydrated polycarbonate membrane filter of 8-µm pore size (Costar, Cambridge, MA) coated with 35 µg of Matrigel (BD Biosciences). The lower chamber was filled with 2.5% medium. After 12-h incubation at 37°C, non-migrating cells on the upper side of the filter were wiped-off. Invading cells were mounted on glass slides

using mounting medium and stained with Hoechst (Sigma). Cell migration was quantified by counting the number of stained nuclei in five individual fields in each Transwell membrane, by fluorescence microscopy, in triplicate.

For wound closure, a wound was induced on the confluent monolayer cells by scraping a gap using a micropipette tip. Photographs were taken at 100 X magnification using phase-contrast microscopy immediately after wound incision and 24 h later. Pixel densities in the wound areas were measured using the Cell^a software (Olympus Biosystem Gmb) and expressed as percentage of wound closure where 100% is the value obtained at 10h for control cells.

For growth in semisolid medium, colony formation ability of CAL62 shLUC mp and CAL62 shTWIST1 mp cells was examined by soft agar assay. Briefly, 7 ml of FBS supplemented medium containing 0.5% noble agar were added to 60-mm cell culture dish and allowed to solidify (base agar). Next, 2×10^4 cells were mixed with 1.5 ml of FBS supplemented medium containing 0.83% noble agar and added to the top of base agar. The cells were then cultured for 14 days at 37°C under 5% carbon dioxide and colonies were counted.

RNA extraction and expression studies - Total RNA was isolated with the RNeasy Kit (Qiagen, Crawley, West Sussex, UK). The quality of the RNAs was verified by the 2100 Bioanalyzer (Agilent Technologies, Waldbronn, Germany); only samples with RNA integrity number (RIN) value > 7 were used for further analysis. One µg of RNA from each sample was reverse-transcribed with the QuantiTect[®] Reverse Transcription (Qiagen). For quantitative RT-PCR, we used the Human ProbeLibray[™] system (Exiqon, Denmark). TWIST1 primer sequences were:

TWIST1 -F: 5'-GGC TCA GCT ACG CCT TCT C-3'

TWIST1 -R: 5'- CCT TCT CTG GAA ACA ATG ACA TCT-3'

PCR reactions were performed in triplicate and fold changes were calculated with the formula:

$2^{-(\text{sample 1 } \Delta\text{Ct} - \text{sample 2 } \Delta\text{Ct})}$, where ΔCt is the difference between the amplification fluorescent

thresholds of the mRNA of interest and the mRNA of RNA polymerase 2 used as an internal

reference. Sample 1 represented each single tumor sample and sample 2 was the average of all (n. 22) normal thyroids.

For microarrays, 10 µg purified total RNA from 3 TWIST1 TPC-1 transfectants (TWIST1 mp1, TWIST1 mp2, TWIST1 C12) and pcDNAmp2 control was transcribed into cDNA using Superscript RT (Invitrogen), in the presence of T7-oligo(dT)₂₄ primer, deoxyribonucleoside triphosphates (dNTPs), and T7 RNA polymerase promoter (Invitrogen). An *in vitro* transcription reaction was then performed to generate biotinylated cRNA which, after fragmentation, was used in a hybridization assay on Affymetrix U133 plus 2.0 GeneChip microarrays, according to manufacturer's protocol (GeneChip 3' IVT Express Kit, Affymetrix). Normalization was performed by global scaling and analysis of differential expression was performed by Microarray Suite software 5.0 (Affymetrix). The final results were imported into Microsoft Excel (Microsoft).

Supplemental Results

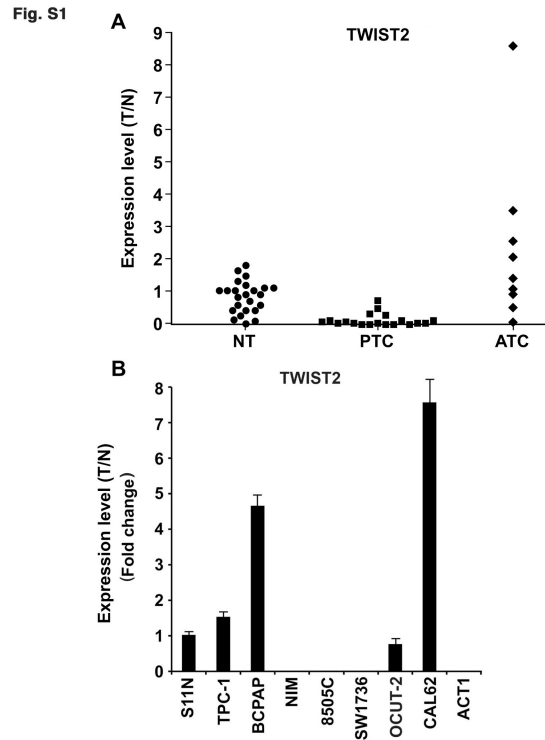


Figure 1: A: Quantitative RT-PCR of TWIST2 mRNA in NT (n=22), PTC (n= 19), and ATC (n=9) snap-frozen tissue samples. The level of TWIST2 expression in each sample was measured by comparing its fluorescence threshold with the average fluorescence threshold of the 22 NT samples. The average results of triplicate samples are plotted. **B:** Quantitative RT-PCR of TWIST2 mRNA in normal human thyroid follicular cells (S11N), PTC (TPC-1, BCPAP and NIM) and ATC (8505C, SW1736, OCUT-2 CAL62, ACT- 1) cell lines. The level of TWIST2 expression in each sample was measured by comparing its fluorescence threshold with the fluorescence threshold of the human thyroid follicular cells (S11N). The average results of triplicate samples \pm SD are plotted.

Fig. S2

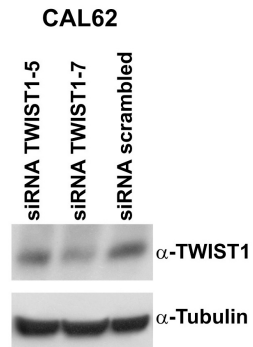


Figure 2: CAL62 were transfected with two different small inhibitor duplex RNA targeting TWIST1 (#5, #7) and the scrambled control. Cells were harvested 48 h after transfection, and analyzed for TWIST1 protein expression. Tubulin was used for normalization.

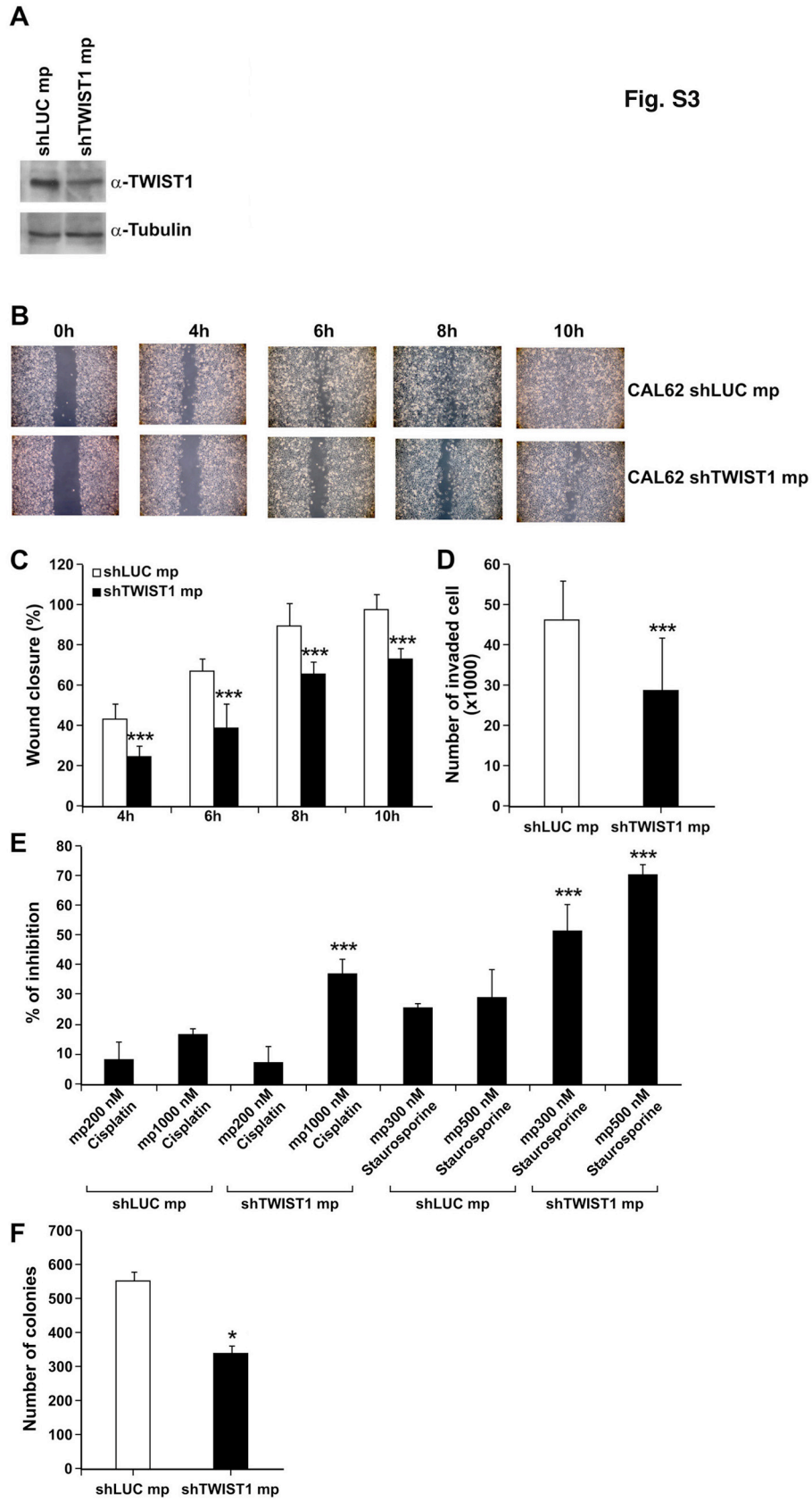


Fig. S3

Figure 3: **A** Expression levels of TWIST1 and Tubulin in CAL62 cells transfected with shLUC or shTWIST1; **B:** A scraped wound was placed on the confluent monolayer of CAL62 transfected with shTWIST1 or shLUC and the cell migration into the wound was monitored at the indicated time points. **C:** Wound closure was measured by calculating pixel densities in the wound area and expressed as percentage of wound closure of triplicate areas \pm SD. **D:** CAL62 transfected with shTWIST1 or shLUC (1×10^5) were seeded in the upper chamber of transwells and incubated for 12 h; the upper surface of the filter was wiped clean and cells on the lower surface were stained and counted. Invasive ability is expressed as number of invaded cells. Values represent the average of triplicate experiments \pm SD. **E:** The cells were treated with increasing doses of Cisplatin or Staurosporine and counted after 24 h. The percentage of viability inhibition is shown: values represent the average of three independent experiments \pm SD. **F:** CAL62 shLUC mp and CAL62 shTWIST1 mp cells were seeded in soft agar. Total number of colonies were counted after 14 days: values represent the average of three independent experiments \pm SD. Asterisks indicate $p < 0.05$ (*), $p < 0.01$ (**) and $p < 0.001$ (***)).

Fig. S4

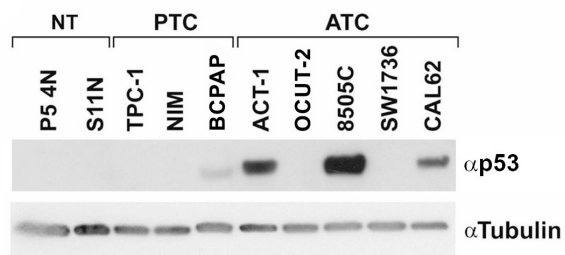


Figure 4: Expression levels of p53 in human thyroid cell lines. Cells were lysed and blotted with the indicated antibodies.

Supplemental References

1. **Schweppe RE, Klopper JP, Korch C, Pugazhenti U, Benezra M, Knauf JA, Fagin JA, Marlow LA, Copland JA, Smallridge RC, Haugen BR** 2008 Deoxyribonucleic acid profiling analysis of 40 human thyroid cancer cell lines reveals cross-contamination resulting in cell line redundancy and misidentification. *J Clin Endocrinol Metab* 93:4331-4341
2. **Salerno P, De Falco V, Tamburrino A, Nappi TC, Vecchio G, Schweppe RE, Bollag G, Santoro M, Salvatore G** 2010 Cytostatic activity of adenosine triphosphate-competitive kinase inhibitors in BRAF mutant thyroid carcinoma cells. *J Clin Endocrinol Metab* 95:450-455
3. **Curcio F, Ambesi-Impiombato FS, Perrella G, Coon HG** 1994 Long-term culture and functional characterization of follicular cells from adult normal human thyroids. *Proc Natl Acad Sci U S A* 91:9004–9008
4. **Fusco A, Berlingieri MT, Di Fiore PP, Portella G, Grieco M, Vecchio G** 1987 One- and two-step transformations of rat thyroid epithelial cells by retroviral oncogenes. *Mol Cell Biol* 7:3365-3370
5. **Melillo RM, Castellone MD, Guarino V, De Falco V, Cirafici AM, Salvatore G, Caiazzo F, Basolo F, Giannini R, Kruhoffer M, Orntoft T, Fusco A, Santoro M** 2005 The RET/PTC-RAS-BRAF linear signaling cascade mediates the motile and mitogenic phenotype of thyroid cancer cells. *J Clin Invest* 115: 1068-1081

Table 1: Clinico-pathological features of anaplastic thyroid carcinoma and TWIST1 expression.

Features	TWIST1 negative (n=21)	TWIST1 positive (n=20)	p-value
Phenotype			
Epithelioid (n=19)	76% (16/21)	15% (3/20)	0.0001
Mixed (n=7)	9% (2/21)	25% (5/20)	
Fusocellular (n=15)	15% (3/21)	60% (12/20)	
Ki67/MIB1 expression			
+++ (n=9)	10% (2/21)	35% (7/20)	0.048
++ (n=16)	33% (7/21)	45% (9/20)	
+ (n=15)	52% (11/21)	20% (4/20)	
Negative (n=1)	5% (1/21)	0% (0/20)	
p53 expression			
+++ (n=14)	19% (4/21)	50% (10/20)	0.030
++ (n=10)	33% (7/21)	15% (3/20)	
+ (n=5)	5% (1/21)	20% (4/20)	
Negative (n=12)	43% (9/21)	15% (3/20)	

+: ≥5–≤25% of positive cells

++: >25–<60% of positive cells

+++ : ≥60% of positive cells

Attached manuscript III

Salvatore G, Salerno P, Cirafici AM, **Bencivenga TC** *et al.* Cytostatic activity of monoclonal antibodies against RET tyrosine kinase receptor in medullary thyroid carcinoma cell lines. Manuscript in preparation.

*Cytostatic activity of novel monoclonal antibodies against RET tyrosine kinase receptor
in medullary thyroid carcinoma cell lines*

Giuliana Salvatore¹, Paolo Salerno², Annamaria Cirafici², Tammaro Claudio Bencivenga², et al.

¹ Dipartimento di Studi delle Istituzioni e dei Sistemi Territoriali, Università "Parthenope", Naples, 80133, Italy.

² Dipartimento di Biologia e Patologia Cellulare e Molecolare c/o Istituto di Endocrinologia ed Oncologia Sperimentale CNR, Università "Federico II", Naples, 80131, Italy.

Abstract

Medullary thyroid carcinoma (MTC), a malignancy of the parafollicular C cells of the thyroid gland, accounts for approximately 5% of all thyroid cancers and presents either sporadically (80% of patients) or in a hereditary pattern. The 10-year overall survival rate in unselected patients with MTC is approximately 75%, but it decreases to 40% or less in patients with locally advanced or metastatic disease. Germline mutations in the RET proto-oncogene occur in virtually all patients with hereditary MTC. Approximately 50% of patients with sporadic MTC have somatic RET mutations. Thus, RET is a potential therapeutic target in MTC. Monoclonal antibodies (mAbs) are important therapeutic agents for cancer. Here, we describe the generation of a panel of mAbs directed against the extracellular portion of RET. The mAbs were characterized by their ability to bind RET wild type and RET mutant proteins by ELISA, dot blot, flow cytometry and immunoprecipitation. The mAbs were grouped on the basis of their epitope by ELISA. Further three mAbs named R10, R50 and R25, recognizing three different regions of the extracellular domain of RET, were selected and tested for their biological effects. R10, R25 and R50 were able to downregulate RET protein in the human medullary thyroid carcinoma cell lines TT and MZ-CRC-1. The downregulation of RET protein was followed by internalization in the early and late endosome as demonstrated by confocal microscopy. This, in turn translate with a cytostatic effects of the mAbs on the growth of NIH3T3 cells transfected with RET mutant proteins, and in the human medullary thyroid carcinoma TT and MZ-CRC-1 cell lines while no effects was seen in cells negative for RET.

INTRODUCTION

Medullary thyroid carcinoma (MTC) arises from parafollicular C cells, comprises ~5% of thyroid cancers, and presents in hereditary (~20% of cases) or sporadic (~80% of MTC cases) forms (Kloos, 2009). The hereditary form of MTC is associated with multiple endocrine neoplasia type 2 (MEN2), including MEN2A, MEN2B, and familial MTC. Germline activating mutations in RET are the cause of inherited forms of MTC and somatic mutations in RET can be found in 30-50% of cases of sporadic MTC. The RET proto-oncogene, codes for a transmembrane receptor that has tyrosine kinase activity. RET is a component of a cell-surface complex that binds glial-derived neurotrophic factor family ligands (GDNF, neurturin, artemin and persephin) in conjunction with a group of coreceptors designated “GDNF-family receptor-a”(GFRa1–4). Somatic RET mutations, particularly M918T, are found in about half of sporadic MTC (Schlumberger, 2008) and correlate with an aggressive disease behavior (Elisei, 2008). MTC-associated mutations activate the RET kinase and convert RET into a dominantly transforming oncogene. Mutated RET in MTC activates several downstream signaling pathways, including the Ras/Raf/Mek/Erk and PI3K (phosphatidylinositol 3-kinase)/Akt/mTor cascades resulting in cancer development and perhaps progression. For MTC limited to the neck, surgery and in some cases external radiation therapy allow for either cure or disease control in the majority of patients. However, for patients with progressive distant metastases chemotherapy regimens have proven largely ineffective, indicating the need for alternative therapies.

One approach that recently has been studied with exciting results is to target the constitutively active RET kinase and/or its key downstream signaling pathways (Wells, 2009; Ye, 2010).

Various RET kinase inhibitors are in clinical trials (Carlomagno, 2011). Vandetanib (ZD6474), an orally bioavailable anilinoquinazoline, potently inhibits the RET kinase (IC₅₀=100 nM). It is also effective against VEGFR2/KDR (IC₅₀=40 nM), EGFR (IC₅₀=500 nM) and VEGFR. Vandetanib, has recently filed for FDA approval in metastatic/locally advanced MTC.

Recently, large-scale genome sequencing revealed a few RET somatic mutations in colon cancer samples (<http://www.sanger.ac.uk/genetics/CGP/cosmic/>). Altered RET expression, rather than structural alterations, has been described in other tumor types, such as neuroblastomas, seminomas, pancreatic and breast carcinomas, myeloid leukemia (Morandi, 2011).

Beside kinase inhibitors, another promising therapeutic approaches to treat cancer is the use of monoclonal antibodies (mAbs). Due to their intrinsic specificity, mAbs represent one of the most promising avenues for the so-called "targeted therapy" of cancer when directed against specific oncogene products. As "targeting drugs," mAbs may have features superior to small-molecule inhibitors. These include very high specificity, generally constant pharmacokinetic properties in different individuals, and the fact that they exert therapeutic effects through a wide spectrum of biological responses. mAbs, interfering with functional cell-surface molecules, such as receptors, can alter different intracellular pathways, thus interfering with the cancer cell biology. Moreover, through interaction with the body's immune system, mAbs can recruit effector functions for

antibody dependent cellular cytotoxicity and complement-dependent cytotoxicity. Many small-molecule agents and mAbs that target growth-factor receptors and their signalling pathways have been developed and subjected to clinical trials.

Here, we report the generation of a panel of novel mAbs against the extracellular portion of RET that could be used for the target therapy of MTC or of other tumors overexpressing RET.

MATERIAL AND METHODS

Generation of mAbs- The extracellular domain of the human RET was expressed as a fusion protein with rabbit IgG Fc in HEK 293T cells. Mice (6-8 weeks old) were immunized four times with the pcDNA3 RET plasmid intradermally (50 µg in 50 µL PBS) with 2-week intervals, and one boost was given with the RET-Fc i.p. (50 µg in 100 µL of PBS) before fusion. Spleens were harvested 84 to 90 hours after the last boost for cell fusion. All animals were maintained in accordance with institutional guidelines. Cell fusions of the splenocytes and the SP2/0 cells were carried out according to the standard fusion protocol. Fourteen days after fusion, the supernatants were harvested and screened for antibody production by ELISA. The selected hybridomas were grown in a CELLINE flask (INTEGRA Biosciences, Chur, Switzerland) and purified on a protein A column (Amersham Biosciences).

ELISA- Screening of hybridomas was done by ELISA on RET-Fc (wild type and mutant) fusion proteins. Briefly, Nunc-Immuno plates (Nalge Nunc International, Rochester, NY) were coated with 2 µg/mL of RET-Fc protein. Plates were incubated overnight at 4°C. Then plates were blocked in blocking buffer (PBS with 25% DMEM, 5% FCS, 25 mmol/L HEPES, 0.5% bovine serum albumin, and 0.1% Azide) for 30 minutes at room temperature, washed twice with washing buffer (PBS with 0.05% Tween 20), and incubated with 100 µL supernatant of hybridoma for 1 hour at room

temperature. After washing, plates were incubated with a horseradish peroxidase–conjugated goat anti-mouse antibody diluted 1:2,000 in blocking buffer. Finally, plates were washed with washing buffer and 100 μ L immunopure tetramethylbenzidine substrate solution (Pierce) was added to each well. The color was allowed to develop for 2 to 5 minutes at room temperature and the reaction stopped by the addition of 50 μ L 2 N solution of sulfuric acid. The plates were read at OD 450 nm using an automated plate reader (Molecular Devices Corp., Sunnyvale, CA).

Isotyping-The isotype of selected mAbs was determined using a mouse immunoglobulin isotyping kit (Roche Applied Science, Indianapolis, IN).

Immunoblotting Analysis- Briefly, mouse fibroblasts and human thyroid carcinoma cells were lysed in a buffer containing 50 mM HEPES (pH 7.5), 1% (vol/vol) Triton X-100, 150 mM NaCl, 5 mM EGTA, 50 mM NaF, 20 mM sodium pyrophosphate, 1 mM sodium vanadate, 2 mM phenylmethylsulfonyl fluoride, and aprotinin at 1 μ g/mL. Lysates were clarified by centrifugation at 10 000 x g for 15 minutes. Protein lysates containing comparable amounts of proteins, estimated by a modified Bradford assay (Bio-Rad, Munich, Germany), were subjected to immunoprecipitation or direct Western blot. Immunocomplexes were detected with the enhanced chemiluminescence kit (Pierce Biotechnology Inc, Rockford, USA). Monoclonal anti- α -tubulin was from Sigma Chemical Co. (St. Louis, MO, USA). Anti-RET is a polyclonal antibody raised against the tyrosine kinase protein fragment of human RET (Carlomagno, 2002). Anti-

phospho905 is a phospho-specific polyclonal antibody that recognizes RET proteins that are phosphorylated at Y905.

Cell cultures- TT cells were purchased from American Type Culture Collection (Manassas, VA). TT cells were derived from the primary tumor of an apparently sporadic MTC (Leong et al. 1981). TT harbor a cysteine 634 to tryptophan (C634W) exon 11 RET mutation as well as a tandem duplication of the mutated RET allele (Huang et al. 2003). The TT cell line, was cultured in RPMI-1640 with 20% fetal calf serum, 2 mM L-glutamine, and 100 units/mL penicillin-streptomycin (GIBCO). MZ-CRC-1 cells were kindly provided by Robert F. Gagel. MZ-CRC-1 were derived from a malignant pleural effusion from a patient with a metastatic MTC. MZ-CRC-1 cells revealed a heterozygous (ATG to ACG) transition in RET exon 16 resulting in the MEN2B-associated substitution of threonine 918 for methionine (M918T). Parental murine NIH3T3 fibroblasts and NIH3T3 cells stably transfected with the RET mutants RET/C634R (MEN 2A), and RET/M918T (MEN 2B)), or wild-type RET are described elsewhere. Cells were cultured in Dulbecco's modified Eagle's medium (DMEM) supplemented with 5% calf serum, 2 mM L-glutamine, and penicillin-streptomycin at 100 units/mL of (GIBCO, Paisley, PA). The TPC-1 cell line, derived from a papillary thyroid carcinoma harboring the RET/PTC1 rearrangement, was cultured in DMEM with 10% fetal calf serum, 2 mM L-glutamine, and penicillin-streptomycin at 100 units/mL).

Growth Curves- Cells (~ 50000/dish) were seeded in 60-mm dishes. The next day, R10, R25 or R50 (40 µg/ml) or vehicle was added to the medium and changed every 2 days. Cells were counted every 2 days.

Immunofluorescence- Cells were treated with R10, R25, or R50 (40 µg/ml) or vehicle at 4°C or at 37°C for different time points. Then cells were fixed in 4% paraformaldehyde and permeabilized with 0.2% Triton X-100 (5 min on ice), and then incubated with α -RET (Carlomagno, 2002) or α -EEA1 (Santa Cruz) or α -LAMP1 (Sigma) for 1 h at RT. Coverslips were washed and incubated with Alexa-488 Goat anti-rabbit (Invitrogen) for 30 min at RT. After 5 min DAPI (4',6-diamidino-2-phenylindole) counterstaining, coverslips were mounted and observed with a Zeiss LSM 510 META confocal microscope (Carl Zeiss, Thornwood, NY).

RESULTS

Generation of new RET mAbs

To obtain mAbs that recognize the extracellular domain of RET we used a DNA immunization protocol followed by protein immunization for the final boost prior to cell fusion. The RET-Fc protein used for immunization and screening was prepared from the medium of transfected HEK293T cells by purification on protein A-Sepharose. Mice were injected intradermally with DNA prepared from the plasmid, pcDNA3-RET. Blood was collected from the mice after multiple injections and the antibody titer was determined by ELISA on plates coated with RET-Fc protein (data not shown). The two mice with the highest titer were sacrificed. Spleen cells from each mouse were fused to myeloma cells following standard procedures (Salvatore, 2002). Supernatants from clones of hybridoma cells were screened using ELISA. To determine the specificity of the antibodies, the screening was done on plates coated with RET wild type-Fc, RET mutant-Fc and CD30-Fc. The latter is a negative control that excludes antibodies reacting with the Fc portion of the fusion. Finally, 52 hybridomas were identified that reacted selectively with RET-Fc and not with CD30-Fc (Figure 1). The isotype of each of the 52 mAb was determined: 33 IgG2a, 9 IgG2b and 10 IgG1 were obtained (Table1).

We then tested the ability of the 52 supernatants ability to bind to the NIH3T3-RET-MEN2A -expressing cell line by flow cytometry. All 52 mAbs bound to NIH3T3-RET-MEN2A cells but did not bind to the parental NIH3T3 negative cells (data not shown).

Epitope mapping of RET mAbs

The extracellular RET domain, contains a signal peptide, four cadherin-like repeats (CLD1-4) and a cysteine-rich domain (CYS). To determine which epitope each mAb recognize we performed a dot blot on proteins encoding full RET extracellular domain (RET ECD), RET cadherin like domain 1-3 (CLD 1-3), RET cadherin like domain 1-2 (CLD 1-2) and as negative controls RET intracellular domain (IC) and non-related proteins BSA and GST. As shown in the Figure 2, mAb R23, R44, R49, R39, R42, R21, R10, R2, R18, R52 and R32 reacted with CLD 1-2; mAb R20, R50 and R1 reacted with CLD3 and mAb R5, R35, R25, 1D9, R8 and R43 reacted with CLD4- cysteine-rich domain.

Three antibodies from different epitope group named R10, R25 and R50, were further selected. We then tested the ability of mAb R10, R25 and R50 to bind to RET directly or to RET GDNF complex by ELISA. As shown in Figure 3, R10 binds preferentially to RET when is complexes with GDNF and GDNFR; in contrast mAb R50 preferentially bind to RET directly, while R25 bind either RET directly or when is complexed with GDNF and GDNFR. As control a commercially available mAbs (AHO1482 and RnD) were used.

Biological effects of RET mAbs

We treated TT cells harbor a cysteine 634 to tryptophan (C634W) exon 11 RET mutation with mAbs R25 and R50 for 6, 12, 24 and 48 hours. Then we lysed the cells and blotted with antibodies against RET and RET phosphorylated at tyrosine 905. As shown in Figure 4 mAb R25 and R50 were able to downregulate RET proteins. Similar results were obtained for R10 in MZ-CRC-1 cell line (data not shown).

RET mAbs induces internalization in RET expressing cells

We treated TT cells and MZ-CRC-1 with 40 ug/ml of RET mAbs R25 and R50 at 4°C and at 37° C for different time points (15 minutes-30 minutes and 6 hours)- and analyzed the cells by confocal microscopy. As shown in Figure 5, at 4°C the mAbs stained the cellular surface, while at 37°C RET was internalized. Furthermore, we showed that RET co-localize intracellularly with the lysosomal marker LAMP1 (lysosome-associated membrane protein 1) and with the early endosome markers (EEA1). Similarly in MZC-RC-1 cells the mAbs R25 and R50 induces RET internalization (Figure 6).

Effects of RET mAbs on cellular growth

Finally, we treated NIH3T3-RET-M918T, NIH3T3, TT and TPC-1 cells treated with 40 µg/ml of R25 and measured cellular growth. As shown in Figure 7, mAb R25 reduced growth rate in the cell lines expressing mutant RET proteins, no effects was seen in

parental or in TPC-1 cells that express only the intracellular portion of RET. Similar results were obtained with mAbs R10 and R50 (data not shown).

Discussion

Oncogenic activation of the RET receptor tyrosine kinase is associated with thyroid cancer (Kondo, 2006). Medullary thyroid carcinoma (MTC) is associated to RET gain-of-function point mutations.

MTC is refractory to conventional chemotherapy and radiotherapy, its treatment relying only on surgery. Unfortunately, postsurgical persistent disease is observed in 70-80% of MTC patients and recurrence rate is between 35 % and 65%. Therefore, there is a need for novel therapeutic approaches for this cancer.

Several chemical inhibitors of oncogenic kinases have been isolated. In most of the cases, such inhibitors are small organic compounds competitive with respect to ATP (Baselga, 2006). The paradigm is imatinib mesylate (STI571, Glivec), a BCR-ABL inhibitor active in chronic myeloid leukemia (CML). Unlike imatinib in CML, kinase inhibitors, when used as single agents, have yielded modest clinical success in patients with solid tumors. Recently, small molecule inhibitors for the RET kinase have also been identified (Carlomagno, 2011).

Scientific exploration of cancer immunotherapy began in the 1950s and the first application relied on polyclonal antibodies. Today, after more than five decades, immunotherapy with monoclonal antibodies continues to offer a promising alternative for cancer treatment. Several antibodies targeting tyrosine kinase receptors (RTKs) in cancer are currently used in clinical practice. Putative mechanisms of mAb-based cancer therapy can be classified into two categories. The first is direct action, which can be further subcategorized into three modes of action. One mode of action is blocking the function of target signalling molecules or receptors. This can occur by blocking ligand binding,

inhibiting cell-cycle progression or DNA repair, inducing the regression of angiogenesis, increasing the internalization of receptors or reducing proteolytic cleavage of receptors. Other modes of direct action are stimulating function, which induces apoptosis, and targeting function. The second mechanism of mAb therapy is indirect action mediated by the immune system. The elimination of tumour cells using mAbs depends on Ig-mediated mechanisms, including complement-dependent cytotoxicity (CDC) and antibody-dependent cellular cytotoxicity (ADCC), to activate immune-effector cells. Thus, the generation of mAbs targeting RET can yield to several advantages compared to kinase inhibitors. Further studies are on going, to validate the efficacy of the mAbs *in vivo* in nude mice.

In conclusion, here we have generated a panel of mAbs that downregulate RET protein, and reduce the growth of thyroid cancer cells positive for RET. The generation of mAbs targeting RET could be beneficial not only for MTC but also for the other human tumors overexpressing RET.

REFERENCES

Baselga J. Targeting tyrosine kinases in cancer: the second wave. *Science*. 2006 26;312(5777):1175-8.

Cabanillas ME, Waguespack SG, Bronstein Y, Williams MD, Feng L, Hernandez M, Lopez A, Sherman SI & Busaidy NL Treatment with tyrosine kinase inhibitors for patients with differentiated thyroid cancer: the M. D. Anderson experience. *J Clin Endocrinol Metab* 95 2588-2595.

Carlomagno F, Vitagliano D, Guida T, Ciardiello F, Tortora G, Vecchio G, Ryan AJ, Fontanini G, Fusco A, Santoro M. ZD6474, an orally available inhibitor of KDR tyrosine kinase activity, efficiently blocks oncogenic RET kinases. *Cancer Res*. 2002 Dec 15;62(24):7284-90.

Carlomagno F, Anaganti S, Guida T, Salvatore G, Troncone G, Wilhelm SM & Santoro M 2006 BAY 43-9006 inhibition of oncogenic RET mutants. *J Natl Cancer Inst* 98 326-334.

Carlomagno F, Santoro M. Thyroid cancer in 2010: a roadmap for targeted therapies. *Nat Rev Endocrinol*. 2011 Feb;7(2):65-7. Review.

Elisei R, Cosci B, Romei C, Bottici V, Renzini G, Molinaro E, Agate L, Vivaldi A, Faviana P, Basolo F, Miccoli P, Berti P, Pacini F, Pinchera A. Prognostic significance of somatic RET oncogene mutations in sporadic medullary thyroid cancer: a 10-year follow-up study. *J Clin Endocrinol Metab*. 2008 Mar;93(3):682-7.

Eng C, Clayton D, Schuffenecker I, Lenoir G, Cote G, Gagel RF, van Amstel HK, Lips CJ, Nishisho I, Takai SI, et al. 1996 The relationship between specific RET proto-oncogene mutations and disease phenotype in multiple endocrine neoplasia type 2. International RET mutation consortium analysis. *JAMA* 276 1575-1579.

Kondo T, Ezzat S, Asa SL. Pathogenetic mechanisms in thyroid follicular-cell neoplasia. *Nat Rev Cancer*. 2006 Apr;6(4):292-306.

Kloos RT, Eng C, Evans DB, Francis GL, Gagel RF, Gharib H, Moley JF, Pacini F, Ringel MD, Schlumberger M, et al. 2009 Medullary thyroid cancer: management guidelines of the American Thyroid Association. *Thyroid* 19 565-612.

Jiménez C, Hu MI, Gagel RF. Management of medullary thyroid carcinoma. *Endocrinol Metab Clin North Am.* 2008 Jun;37(2):481-96.

Lam ET, Ringel MD, Kloos RT, Prior TW, Knopp MV, Liang J, Sammet S, Hall NC,

Wakely PE, Jr., Vasko VV, et al. Phase II clinical trial of sorafenib in metastatic medullary thyroid cancer. *J Clin Oncol* 28 2323-2330.

Morandi A, Plaza-Menacho I, Isacke CM. RET in breast cancer: functional and therapeutic implications. *Trends Mol Med.* 2011 Mar;17(3):149-57.

Nagata S, Salvatore G, Pastan I. DNA immunization followed by a single boost with cells: a protein-free immunization protocol for production of monoclonal antibodies against the native form of membrane proteins. *J Immunol Methods.* 2003 Sep;280(1-2):59-72.

Salvatore G, Nagata S, Billaud M, Santoro M, Vecchio G, Pastan I. Generation and characterization of novel monoclonal antibodies to the Ret receptor tyrosine kinase. *Biochem Biophys Res Commun.* 2002 Jun 21;294(4):813-7.

Schlumberger M, Carlomagno F, Baudin E, Bidart JM, Santoro M. New therapeutic approaches to treat medullary thyroid carcinoma. *Nat Clin Pract Endocrinol Metab.* 2008 Jan;4(1):22-32.

Weiner LM, Surana R, Wang S. Monoclonal antibodies: versatile platforms for cancer immunotherapy. *Nat Rev Immunol.* 2010 May;10(5):317-27.

Wells SA, Jr. & Santoro M 2009 Targeting the RET Pathway in Thyroid Cancer. *Clin Cancer Res* 24 24.

Wells SA Jr, Robinson BG, Gagel RF, Dralle H, Fagin JA, Santoro M, Baudin E, Elisei R, Jarzab B, Vasselli JR, Read J, Langmuir P, Ryan AJ, Schlumberger MJ. Vandetanib in Patients With Locally Advanced or Metastatic Medullary Thyroid Cancer: A Randomized, Double-Blind Phase III Trial. *J Clin Oncol.* 2011 Nov 21.

Ye L, Santarpia L & Gagel RF The evolving field of tyrosine kinase inhibitors in the treatment of endocrine tumors. *Endocr Rev* 31 578-599.

ACKNOWLEDGMENT

We thank M. Billaud for providing RET-Fc proteins and D. Spalletti Cernia for technical assistance. This study was supported by the Associazione Italiana per la Ricerca sul Cancro (AIRC).

Figures legend

Figure 1: Screening of hybridoma supernatants by ELISA.

Supernatants of the 52 Mabs were screened against wild type RET-Fc, mutant RET (C634R)-Fc or CD30-Fc in solution or coated on plate. The 1D9 and 2D6 supernatants were used as control. T6 and T25 are antibody against CD30.

Figure 2: Proteins encoding the RET extracellular domain (RET ECD), RET cadherin like domain 1-3 (CLD 1-3), RET cadherin like domain 1-2 (CLD 1-2) and as negative controls RET intracellular domain (IC) and non-related proteins BSA and GST were coated on nitrocellulose paper and blotted with the indicated supernatants.

Figure 3: ELISA was performed with R10, R25 and R50 or controls on RET protein or on GDNF+GFRA1 or blank control.

Figure 4: NIH3T3-RET/MEN2A cell were treated for 48 hours with 40 $\mu\text{g/ml}$ of R25 Mab. Cell lysates (50 μg) were immunoblotted with anti RET (polyclonal antibody directed to the tyrosine portion of RET) or with anti phospho-RET (tyrosine 905). Anti tubulin stain show equal gel loading.

Figure 5: TT cells were incubated with R25 or R50 at a concentration of 40 $\mu\text{g/ml}$ at the indicated time points. Immunofluorescence was performed with anti RET, anti EEA1 or anti LAMP1.

Figure 6: MZ-CRC-1 cells were incubated with R25 or R50 at a concentration of 40 $\mu\text{g/ml}$ at the indicated time points. Immunofluorescence was performed with anti RET, anti EEA1 or anti LAMP1 antibodies.

Figure 7: The indicated cell lines were treated with 40 $\mu\text{g/ml}$ of R25 mAb at different time points and counted.

Table 1: List of RETmAbs and their isotype.

mAb	Isotype
R1	IgG2a
R2	IgG2b
R3	IgG2a
R4	IgG2a
R5	IgG2b
R6	IgG2a
R7	IgG2b
R8	IgG1
R9	IgG2a
R10	IgG1
R11	IgG2a
R12	IgG2a
R39	IgG1
R40	IgG2a
R42	IgG1
R43	IgG1
R44	IgG2b
R45	IgG1
R46	IgG2b
R47	IgG2a
R48	IgG2a
R49	IgG2b
R50	IgG2a
R51	IgG2a
R52	IgG2a
R53	IgG2a

Fig. 2

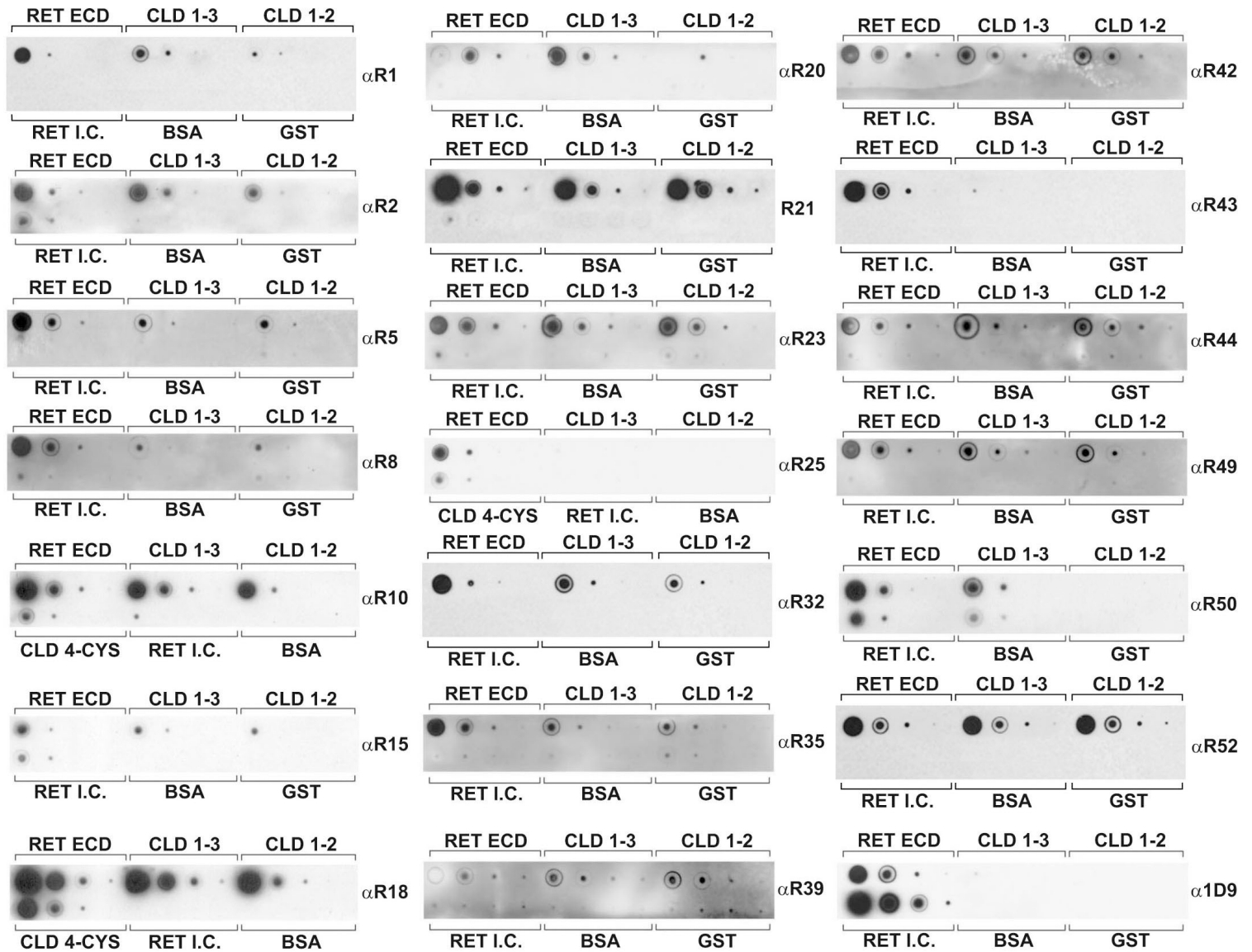


Fig. 3

Binding of mAbs to complexed RET

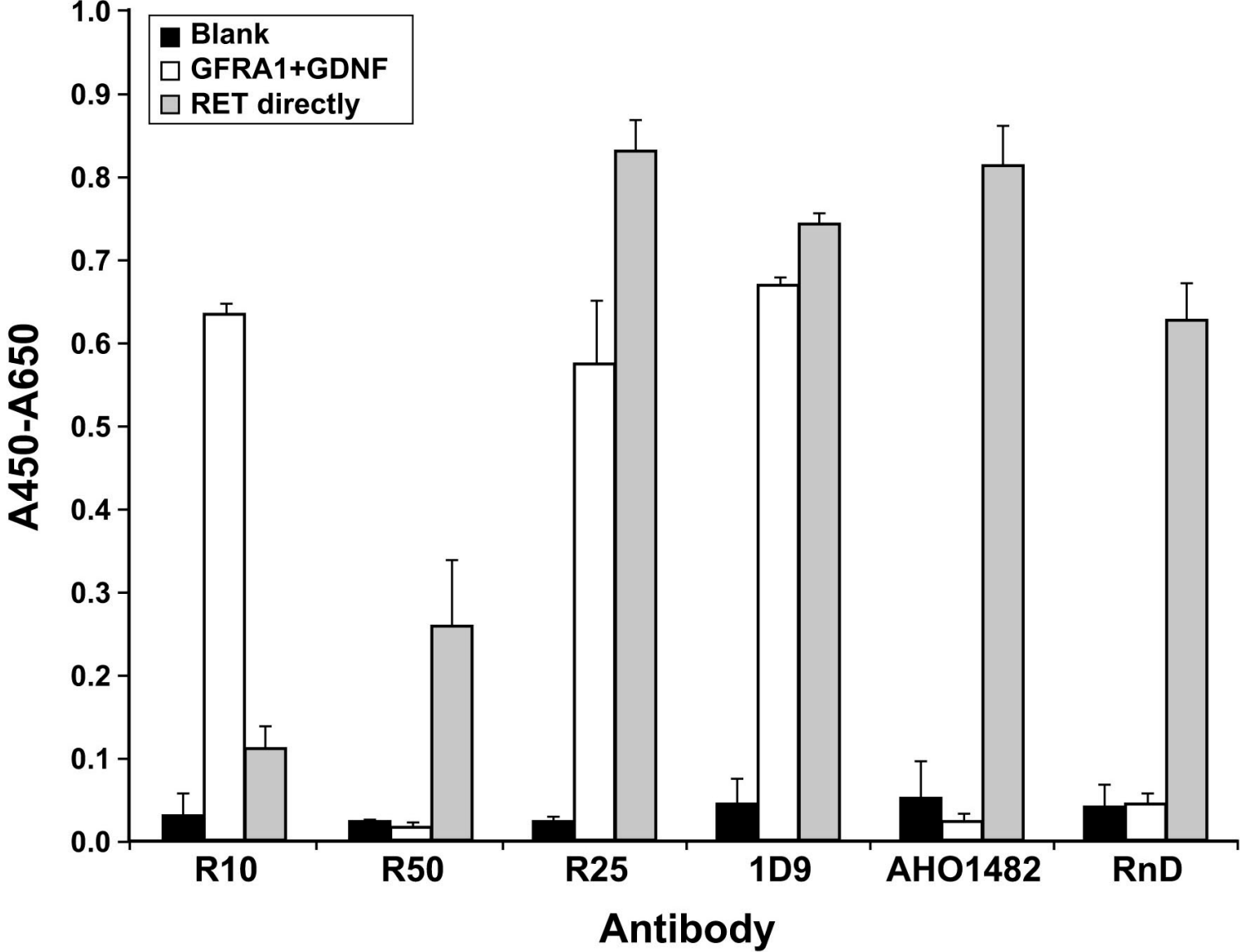


Fig. 4

TT (RET-C634W)

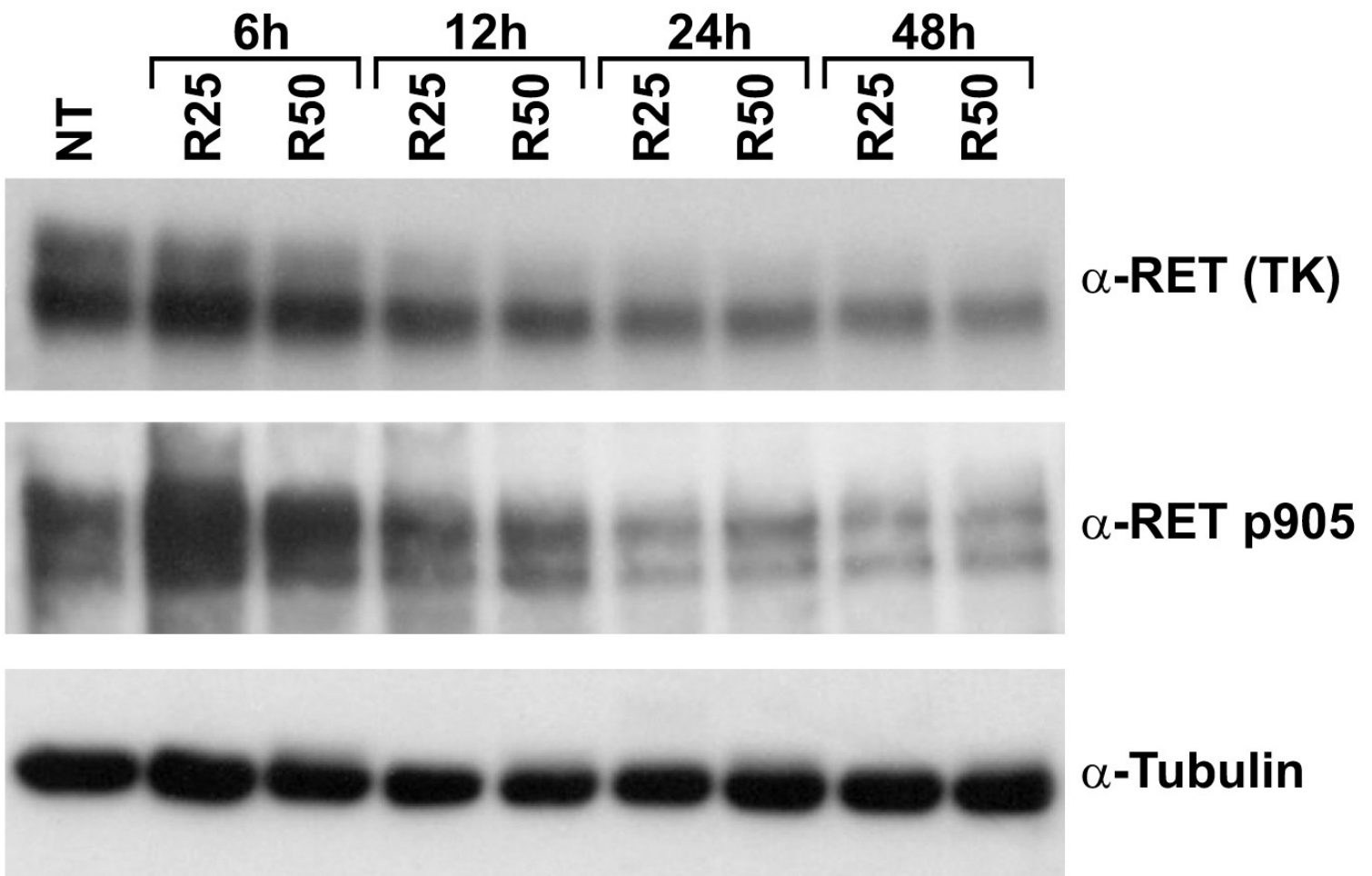


Fig. 5

TT (RET-C634W)

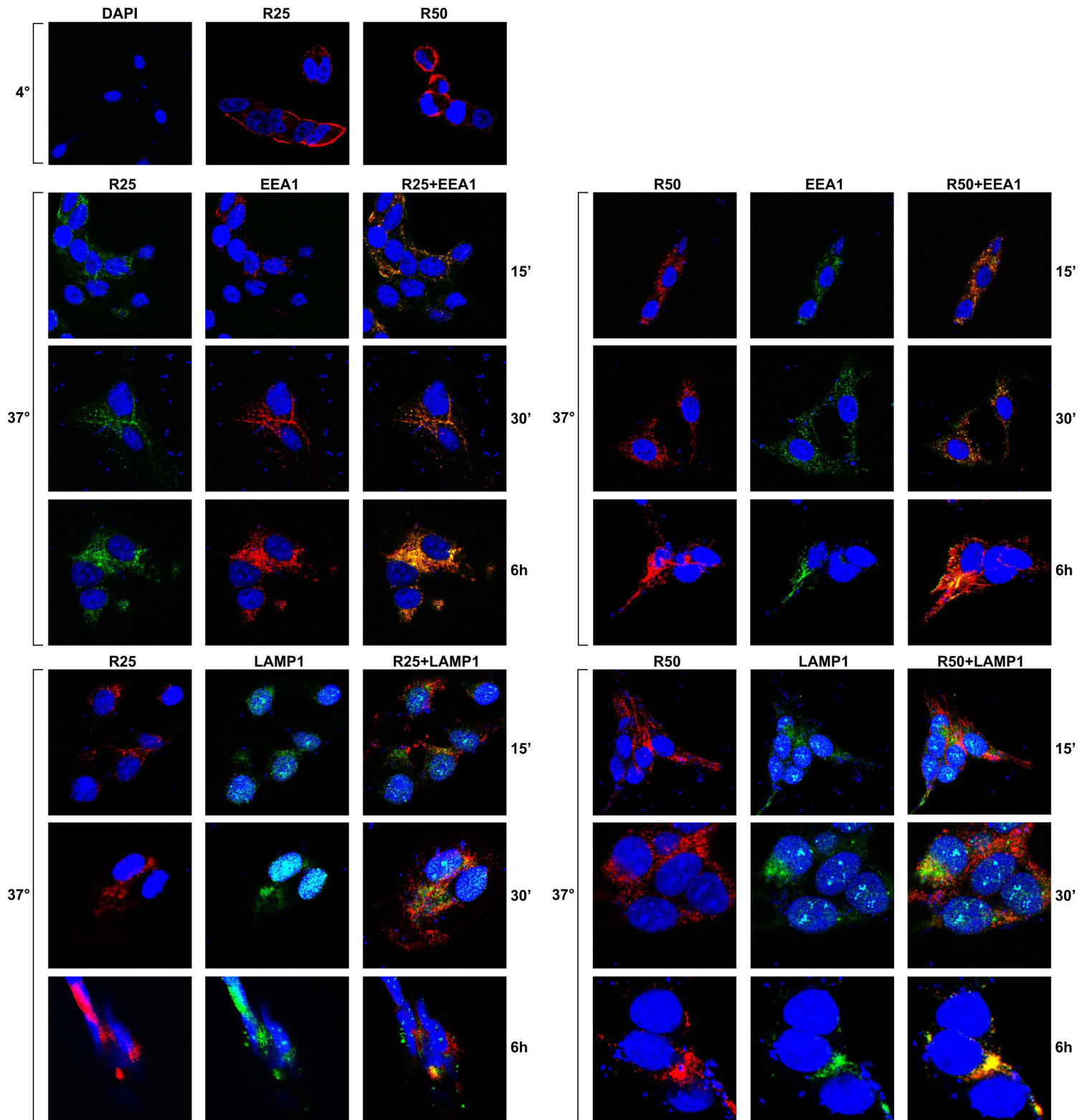


Fig. 6

MZ-CRC-1 (RET-M918T)

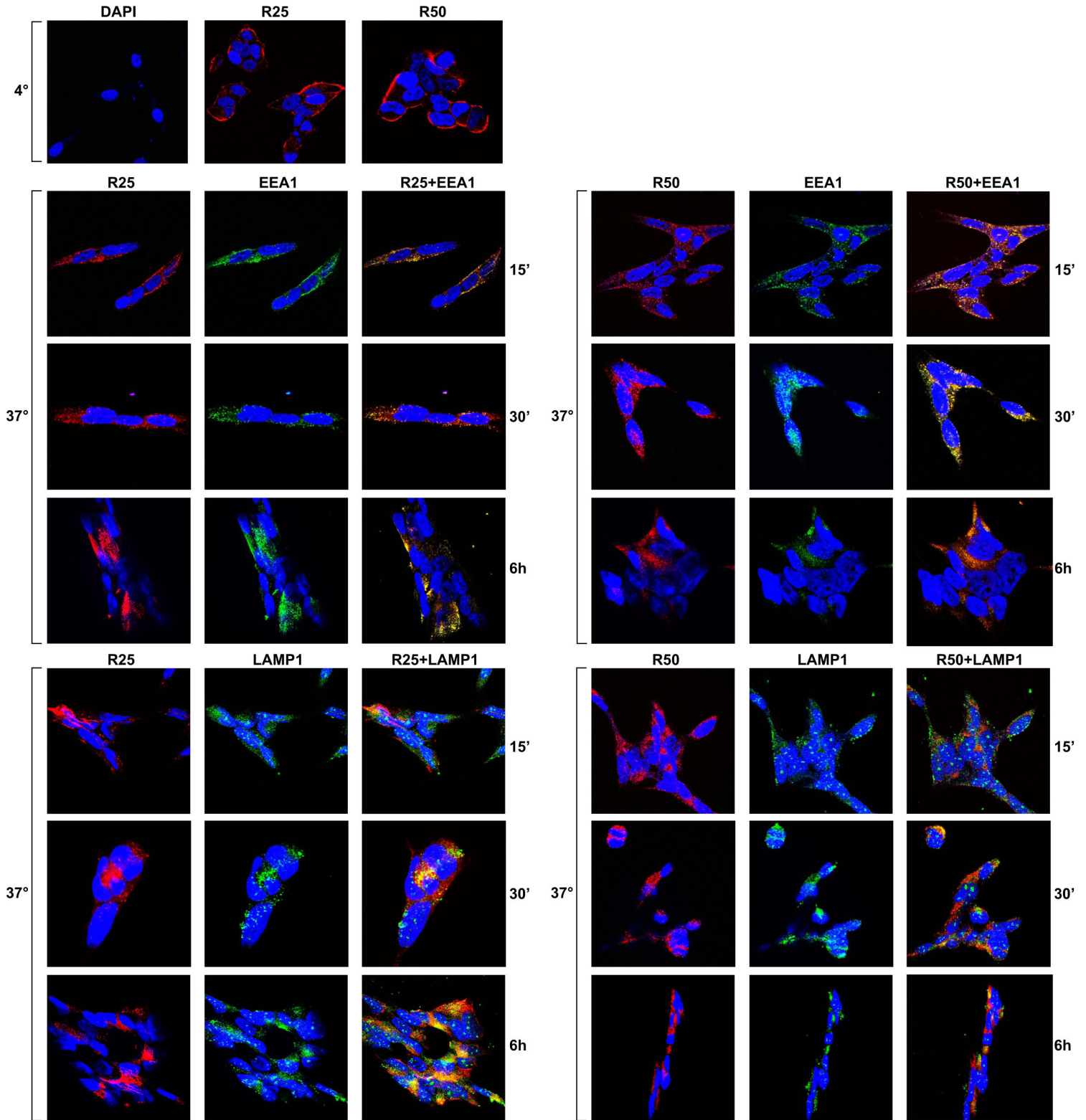


Fig. 7

